Quantum light driven many level systems in the weak and strong coupling limits

Vorgelegt von
M.Sc. Shahabedin Chatraee Azizabadi
geb. in Esfahan

von der Fakultät II – Mathematik und Naturwissenschaften
der Technischen Universität Berlin

zur Erlangung des akademischen Grades

Doktor der Naturwissenschaften
– Dr. rer. nat. –

genehmigte Dissertation

Promotionsausschuss:
Vorsitzender: Prof. Dr. Stephan Reitzenstein
Gutachter: Prof. Dr. Andreas Knorr
Gutachter: Dr. Thomas Koprucki

Tag der wissenschaftlichen Aussprache: 22.11.2017

Berlin 2017

Abstract

We propose a possibility to study the quantum light excitation of atomic systems. To confine our study, we limit the configuration to two and four level emitters as target systems. Source and target are coupled via unidirectional waveguide. We numerically implement the cascaded formalism and use the source-target approach. Herein, we focus on continuous excitation scenarios where the source system is excited by continuous incoherent or coherent pumping. We demonstrate that, to a certain extent, one can control the target system's photon statistics via the source system pumping mechanism. Additionally, different coupling regimes in both cavities can change the output of the target system. In addition, we show that via tuning the cavity's parameters one can produce an exotic type of quasi-probability distributions, a flat Fock state distributions. We also discuss the different obtained photon statistics for different coupling regimes. The used quantum light source, driven by spontaneous emission, can be categorized as a single photon source or two photon source. Therefore, the thesis is divided also according to these types of quantum light sources into two parts:
In the first part of the thesis, after review of the theoretical methods, which are applied in the thesis , we specifically study coupled cavities. The first cavity, pumped incoherently, performs effectively as a single photon source. We consider system-bath interaction in the coupling waveguide, i.e boson-boson interaction, for the photon occurring in the system .We demonstrate that even for a simple scenario , where thermal bath modes couple to the system, the photon statistics of the source is not completely mapped to the target system. This suggest that the environment for such a coupled systems influence the photon statistics of the source while transferring it into the target system. In the case of direct coupling of emitters to the waveguide the influence of the environment, as a dissipator, on the photon statistics can be seen in photon number distribution. Additionally, higher order correlation functions for the target system deviate drastically from the source system and show a mixture of quantum coherent and incoherent dynamics. For the case of indirect coupling of emitters to the waveguide, when the modes of two cavities are coupled, the mediating environment also influences the photon statistics of the target system. This phenomenon manifests itself in the second-order correlation function of the source and target, wherein, while the source behaves in the anti-bunched regime, the target system shows highly bunched pattern.
In the second part of thesis, we study the production of two photons in nonlinear optics. As an example, we propose an optical setup where we can produce entangled pairs of photons through the dynamical Casimir effect(DCE). By applying the laser on a superconducting surface of a metal dielectric we induce a surface plasmon polariton

(SPP). SPP give rise to the enhancement of DCE such as the efficiency of two photon production exceed the common nonlinear optical processes for instance parametric down conversion. We show that the resonant enhancement of the emission of two photons happens when the excitation wavelength coincides with the amplitude of the laser light. Another even more efficient source for the two photon emission is a biexciton excitation of a quantum dot. We provide a formalism for a cascaded biexciton which can be used to show how the source biexciton, pumped coherently or incoherently, influences the target biexciton through a unidirectional waveguide, modeled as a thermal bath.

Zusammenfassung

In dieser Arbeit wird ein Verfahren zur Untersuchung der Anregung von atomaren Systemen mit Quantenlicht vorgeschlagen. Die untersuchten atomaren Zielysteme werden auf Zwei- und Vier-Niveau Systeme begrenzt. Quelle und Ziel sind über einen gerichteten Wellenleiter gekoppelt. Wir implementieren eine numerische Simulation auf Grundlage des kaskadierten Formalismus und des Quelle-Ziel Ansatzes. Wir betrachten kontinuierliche Pump Szeanrien in denen die Quelle kohärent und inkohärent getrieben wird. Wir zeigen, dass die statistischen Eigenschaften des Zielsystems bis zu einem gewissen Grad durch den Pump Mechanismus der Quelle kontrolliert werden kann. Zusätzlich können unterschiedliche Kopplungsregimes in beiden Kavitäten die Abstrahlung des Zielsystems beeinflussen. Zusätzlich zeigen wir, dass in einem speziellen Parameterbereich eine exotische Quasi-Wahrscheinlichkeitsverteilung, eine flache Fock-Zustandsverteilung, generiert werden kann. Auch werden die unterschiedlichen Photonenstatistiken für unterschiedliche Kopplungsregimes diskutiert. Die verwendete quanten Lichtquelle, getrieben durch spontane Emission, kann als einzel oder zwei Photonenquelle kategorisiert werden. Deshalb wird die vorliegende Arbeit nach diesen Typen von Quantenlichtquellen aufgeteilt in zwei Teile:
Im ersten Teil der Arbeit, nach Einführung der theoretischen Methoden, welche indieser Arbeit verwendet werden, untersuchen wir gekoppelte Kavitäten. Die erste Kavität, welche inkohärent gepumpt wird, wirkt effektiv wie eine einzel Photonenquelle. Wir betrachten System-Bad Wechselwirkung in dem Kopplungswellenleiter, d.h. Boson-Boson-Wechselwirkung, für das im System auftretenden Photon. Wir zeigen, dass auch für ein einfaches Szenario mit einem thermischen Bad, die Photonstatistik der Quelle nicht vollständig auf das Zielsystem übertragen wird. Dies deutet darauf hin, dass das Bad für solche gekoppelten Systeme die Photonstatistik der Quelle beeinlusst bei gleichzeitiger Übertragung auf das Zielsystem. Im Falle von direkter Kopplung der Emittern an den Wellenleiter kann der Einfluss des Bades, als Dissipator, auf die Photonstatistik in der Photonenzahlverteilung gesehen werden. Darüber hinaus weichen Korrelationsfunktionen höherer Ordnung für das Zielsystem drastisch vom Quellsystem ab und zeigen eine Mischung aus quantenkohärenter und inkohärenter Dynamik. Auch für den Fall der indirekten Kopplung der Emittern an den Wellenleiter, wenn die Moden der zwei Kavitäten gekoppelt sind, beeinflusst das Bad die Photonenstatistik des Zielsystems. Dieses Phänomen manifestiert sich in der Korrelationsfunktion zweiter Ordnung von Quelle und Ziel: während sich die Quelle antibunching aufweist ist die Statistik im Zielsystem gebuncht.
Im zweiten Teil der Arbeit untersuchen wir die Produktion von zwei Photonen in nichtlinearer Optik. Als Beispiel schlagen wir einen optischen Aufbau vor, in dem verschränkte Photonen Paare durch den dynamischen Casimir-Effekt (DCE)

hergestellt werden können. Trifft ein Laser auf eine supraleitende Oberfläche eines Metalldielektrikums so werden Oberflächenplasmon-Polaritonen erzeugt. Diese Oberflächenplasmon-Polaritonen verstärken den DCE, so wird die Effizienz der Erzeugung von verschränkten Photon Paaren die üblichen nichtlinearen optischen Prozesse wie etwa parametrischen Fluoreszenz übersteigen. Wir zeigen, dass die Resonanzverstärkung der Emission von zwei Photonen dann erfolgt, wenn die Anregungswellenlänge mit der Wellenlänge des Laserlichts zusammenfällt. Wir führen einen Formalismus für ein kaskadiertes Biexziton ein, mit dem untersucht werden kann, wie die Biexzitonquelle, sowohl kohärent als auch inkohärent gepumpt, das Zielbiexziton durch einen unidirektionalen Wellenleiter beeinflusst.

Contents

List of Figures

List of Tables

1 Introduction

1.1 Excitation by quantum light: motivation and question

Production of quantum light is not a new trend and the subject has been studied along the fruition of quantum optics since its establishment. However, the inquiry about quantum light has stayed focused on understanding its properties [1, 2] and improving its production scheme [3]. Quantum light sources are realized for many different material platforms in semiconductor, atom and molecular systems [4, 5, 6, 7, 8] which can be implemented for the production of quantum light. They can be applied as a testbed for nonlinear quantum dynamics [9] which includes quantum ghost imaging, two-photon-spectroscopy [10, 11, 12] and quantum light spectroscopy [13, 14].
Typically, there are two types of quantum light sources: single-photon and two-photons emitters. Different prototypes of single-photon emitters based on semiconductor nanostructures are manufactured [15, 16, 17] and implemented in quantum cryptography protocols [18, 19, 20] and quantum sensing [21]. Polarization-entangled photon sources [22] are another class of quantum light sources. They can be electrically driven and triggered on demand [23]. However, the traditional way to produce two entangled photon comes from nonlinear optical processes [24, 25].

This rich variety of quantum light sources follows by excitation proposals. For example, single photon excitation can purify non-classical states of light and suppresses additional fluctuations [26]. This process allows for Hilbert-state addressing [27]. One the other hand, entangled photon pairs are applied for ultrafast double-quantum-coherence spectroscopy of excitations with entangled photons [28]. Also, they can be used for the quantum gates which are based on entanglement swapping protocols [29].

It was rather in the recent years that researchers have started to pay attention to use these nonclassical light sources to radiate them on other quantum systems [30]. They can vary from simple harmonic oscillators to fully quantized cQED systems. The treatment for the aforesaid problem was unknown as the tenable formalism for such interactions was unclear. However Kobolove et al attempt, supposedly in an indirect way, can be seen as a starting point [31], the first real effort to attack this problem was done by Gardiner where he implemented and modified input-output methods [32, 33] and quantum noise theory to tackle the problem of coupled quantum systems [34]. At the same time, but in a separate study, Carmichael [35] formulated a theory that, with a contribution to both researchers, has been called the cascaded

formalism. This formalism distincts the source and the target of quantum excitation to such degree that the source influences the target but is not influenced back. The more rigorous treatments of such a problem have been enunciated in Gardiners book [36].

In the very recent study by Carreno et al, the excitation with quantum light has been treated extensively. They have introduced new mapping from Hilbert space of quantum light to present the accessible part of physical Fock states. This is due to the fact that a pure Fock state is difficult to generate, specifically in the steady-state scheme and by charting the Hilbert space of the system (by its observables) one can detect the obtainable part of quantum states. They have also inspected the excitation of a two-level system (TLS) with different types of light sources [27, 37].
Herein, as a completion to the previous efforts to understand the influence of quantum excitation, we propose different sets of questions to be answered. The first goal of this research is to exploit the possible influence of the quantum light on the properties of the target system. On the other hand, we investigate the control of rudimentary part of target systems photon statistics by the source. We want to see how one can control a quantum system with another quantum system. Finally, we examine the effect of environment on the coupled systems as an inquiry for better understanding of open quantum system dynamics.

1.2 Structure of thesis

In this thesis, we start from the theoretical background in chapter 2. The quantization of electromagnetic field, quantum dynamical pictures and the theory of open quantum systems are fundamentally discussed.

In chapter 3 the method of the cascaded formalism ,to describe the physical model of the coupled quantum systems, is conceptually introduced. We then provide a direct derivation of master equation to obtain the density matrix of the combined systems. In chapter 4 the main ideas behind the statical and dynamical Casimier effect (DCE) are presented. A brief overview of the state of the art of experimental realization of DCE is also given.
In chapter 5 we apply the formalism, obtained in chapter 3, for the specific setup: coupling between two optical cavities. Then we derive the final version of the corresponding master equation and evaluate it numerically. The results for different configuration is illustrated and discussed in this chapter. In Chapter 6, we overview a nonlinear optical process, spontaneous parametric down conversion (SPDC), which is traditionally a source for two entangled photons. Then, we present a setup based on DCE that can fabricate two entangled photon emission. In chapter 7, after introducing biexcitons as a source for two entangled photon production , we give a full mathematical procedure for obtaining Lindblad and Redfield master equations of cascaded biexcitons. This formalism initiates a foundation for the future study of such systems.

Chapter 8 recaps this manuscript, summarize it and gives an outlook.

2 Theoretical framework

In this chapter, we will introduce the theoretical backgrounds which are essential knowledge for the rest of the thesis. However, these topics are from different field of modern physics, they have a common aspect. They go beyond the exciting theory or framework towards a more explicit view that one can apply to explain unsolved physical questions. For further inquiries about this topics, we address the readers to the corresponding standard books in each subject [38, 39, 40, 41, 42, 43, 44].
Starting from the quantization of electromagnetic field, we quantize the Maxwell equations for a vacuum cube. This part will be necessary for the investigation of the quantum aspects of light which later will be consider in the study of (the dynamical) Casimir effect. Additionally, the environment surrounding our quantum systems investigated in this thesis are considered to be in a vacuum state. Therewith we overview different dynamical pictures resp. three representations in quantum mechanics: These three pictures are isomorphic, in the sense that they give the same expectation values for the desired observables of the system. They are important because in the derivation of optical master equation in chapters 3,5 and 7 we often transfer our differential equations from one representation to another , which helps us to obtain a simpler version of these particular equations. Finally, we briefly introduce the main ideas behind open quantum system formalism. This formalism is relevant for the cases, in which there is a cooperation between a quantum system and its surrounding. As the aim of this dissertation is to cascade two quantum systems via an environment, this outstanding framework is essential for the realization of their complex dynamics.

2.1 Quantization of electromagnetic field

The Maxwell-Faraday equation and Ampere's circuital law in vacuum ($c = 1/\sqrt{\mu_0 \varepsilon_0}$) are written as

$$\nabla \times \vec{E} = -\frac{1}{c}\frac{\partial \vec{B}}{\partial t} \tag{2.1.1a}$$

$$\nabla \times \vec{B} = \frac{1}{c}\frac{\partial \vec{E}}{\partial t}. \tag{2.1.1b}$$

Further, the Gauss law for magnetic and electrical field in vacuum is given by

$$\nabla \cdot \vec{E} = 0 \tag{2.1.2a}$$

$$\nabla \cdot \vec{B} = 0. \tag{2.1.2b}$$

There are two types of potentials in electromagnetic field and both of them are functions of position and time.The derivation of potential gives (electric or magnetic) fields and is associated with energy. In addition fields are associated with forces in classical electromagnetism [45]. On the other hand, Gauge invariance principal suggests that there are many different potentials which can generate the same fields. We then define the most general transformation which leaves the fields $\vec{E}$ and $\vec{B}$ unchanged. Therefore one can define two potential functions: a magnetic vector potential $\vec{A}$ and a electric scalar potential Φ which is a directionless value and consequently only depends on its location. These two potentials are related to the electric and magnetic fields via

$$\vec{B} = \nabla \times \vec{A} \tag{2.1.3a}$$

$$\vec{E} = \nabla\Phi - \frac{\partial \vec{A}}{\partial t}. \tag{2.1.3b}$$

One should keep in mind that the ability to do this transformation is the result of Helmholtz theorem [46]. According to the invariant principle [47] , we are free to choose the simplest gauge. For a electric scalar potential we assume that it goes to zero in the limit of large distances

$$\iiint_V d^3r(\nabla\Phi)^2 = 0 \Longrightarrow \nabla\Phi = 0. \tag{2.1.4}$$

Further, we employ the Coulomb gauge demanding the magnetic vector potential to be free of any divergence

$$\nabla \cdot \vec{A} = 0. \tag{2.1.5}$$

By plugging Eq.(2.1.4) into Eq.(2.1.3b) the electric field can be written as $E = -\partial A/\partial t$. Thus, from Eq.(2.1.1b) in combination with Eq.(2.1.5) one can derive the wave equation for vacuum field

$$\frac{\partial^2 A}{\partial t^2} - c^2\nabla^2 A = 0. \tag{2.1.6}$$

If we choose a cubic cavity with edge length L, the solution of the wave equation should have the form of a Fourier's series:

$$\vec{A} = \sum_{\vec{k}} \vec{A}_k \exp(i\vec{k}\vec{r} - i\omega t). \tag{2.1.7}$$

Substituting this ansatz to Eq.(2.1.6) we will reach the following solution

$$\vec{A} = \sum_{k_x,k_y,k_z} \vec{A}_k \exp i(k_x x + k_y y + k_z z - \omega t) \tag{2.1.8}$$

where $k_x = 2\pi v_x/L,\ k_y = 2\pi v_y/L,\ k_z = 2\pi v_z/L$ are the components of the wavevector. with $v_x, v_y, v_z = \pm 1, \pm 2, ...$ The Fourier amplitude $\vec{A}_k$ is time independent. The

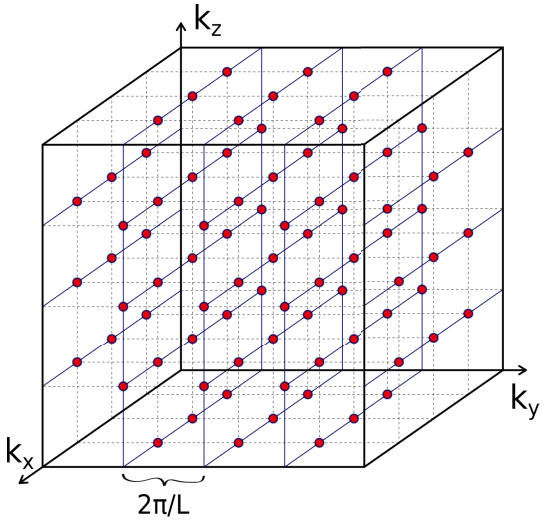

Figure 2.1.1: The possible wavevectors k for the cubic cavity with the side size$L$

time evolution of the vector $\vec{A}$ is stored in $\exp(\omega t)$. The first part of exponential is a spatial function which gives us a lattice of points in the three dimensional space with a lattice constant $2\pi/L$. The allowed wavevectors k for a cavity are illustrated in Fig.2.1.1.
Thus, we can write corresponding solution for electric field and magnetic field according to the vector potential $\vec{A}$

$$\vec{E} = -\frac{\partial A}{\partial t} = \sum_{\vec{k}} i\omega(\vec{A}_k \exp(i\vec{k}\vec{r} - i\vec{\omega}t) + c_L \tag{2.1.9a}$$

$$\vec{B} = \vec{\nabla} \times \vec{A} = \sum_{\vec{k}} i(\vec{k} \times \vec{A}_k) \exp(i\vec{k}\vec{r} - i\omega t) + c_L \tag{2.1.9b}$$

where c_L is a constant depending on the length L of the cavity. It can be argued that the electromagnetic field can be resembled to an infinite number of (independent) harmonic oscillators [48]. In this system the electromagnetic field can be excited in discrete modes of the cavity, however, the results of that system are mostly independent of the size and nature of cavity and can be used for arbitrary optical cases. In fact, this is the reason behind the definition of the constant c_L.
It is prominent, that in classical physics we just consider the real part of the Fourier amplitude $\vec{A}_k$, thus in order to have a real quantity, not a complex one, we define the general form of $\vec{A}$

$$\vec{A}(\vec{r}, t) = \sum_{\vec{k}} (\vec{A}_k \exp(-i\omega_k t + i\vec{k}\vec{r}) + \vec{A}_k^* \exp(-i\omega_k t + i\vec{k}\vec{r})). \tag{2.1.10}$$

Substituting $\vec{A}$ into Eq. (2.1.9a) and Eq. (2.1.9b) we obtain explicit expressions for

the electric and magnetic fields given by

$$\vec{E}(r,t) = -\frac{\partial \vec{A}}{\partial t} = \sum_{\vec{k}} i\omega(\vec{A}_k \exp(-i\omega_k t + i\vec{k}\vec{r}) - \vec{A}_k^* \exp(-i\omega_k t + i\vec{k}\vec{r})) \tag{2.1.11a}$$

$$\vec{B}(\vec{r},t) = \vec{\nabla} \times \vec{A} = \sum_{\vec{k}} i((\vec{k} \times \vec{A}_k) \exp(-i\omega_k t + i\vec{k}\vec{r}) - (\vec{k} \times \vec{A}_k) \exp(-i\omega_k t + i\vec{k}\vec{r})). \tag{2.1.11b}$$

We note that the spatial parts of Eqs. (2.1.11a) and (2.1.11b), which are only time dependent, are similar to the eigenfunctions of the wave equation and are called normal modes. Thus, one can rewrite vector potential equation in the form of modes function $\vec{u}_k(r) = L^{-3/2}\hat{e}^\lambda \exp(i\vec{k}\vec{r})$(the polarization vector $\hat{e}^\lambda$ is perpendicular to $\vec{k}$) and normalized amplitudes a_k as follows

$$\vec{A}(\vec{r},t) = \sum_{\vec{k}} (\frac{\hbar}{2\omega_k \varepsilon_0})^{1/2} (a_k \vec{u}_k(r) \exp(-i\omega_k t) + a_k^* \vec{u}_k^*(r) \exp(i\omega_k t)). \tag{2.1.12}$$

One should notice that a_k and a_k^* are complex numbers in the framework of classical electromagnetism. The quantization procedure starts from the fact that the Hamiltonian of the electromagnetic field can be written as

$$H = \frac{1}{2} \int \int \int (\varepsilon_0 E^2 + \mu_0 B^2) dr. \tag{2.1.13}$$

By plugging Eq. (2.1.11a) and Eq. (2.1.11b) into Eq.(2.1.13) of one can reformulate the Hamiltonian as

$$H = \frac{1}{2} \int \int \int (\varepsilon_0 (\partial_t \vec{A})^2 + \frac{1}{\mu_0} (\nabla \times \vec{A})^2) dr. \tag{2.1.14}$$

We have already mentioned that the electromagnetic field can be modeled as a set of harmonic oscillators. Before the quantization procedure, we define the position and momentum operators

$$q_k = \sqrt{\frac{\hbar}{2\omega}} \ (a_k \exp(-i\omega_k t) + a_k^* \exp(i\omega_k t)) \tag{2.1.15a}$$

$$p_k = -i\sqrt{\frac{\hbar\omega}{2}} \ (a_k \exp(-i\omega_k t) - a_k^* \exp(i\omega_k t)). \tag{2.1.15b}$$

By substituting the definition of $\vec{A}$ in Eq. (2.1.14) and considering q_k and p_k we can rewrite the Hamiltonian for k harmonic oscillators as

$$H = \sum_k (\frac{p_k^2}{2} + \frac{\omega_k^2}{2} q_k^2). \tag{2.1.16}$$

For the quantization of the electromagnetic field, the first step is to quantize harmonic oscillator and by this knowledge we can establish the quantum state of electromagnetic field.
It can be shown that the spatial dependence of the electromagnetic field are preserved in quantization [49]. This is the point where we can start to replace the vector potential $\vec{A}$ by an operator $\hat{A}$. Also, the cavity is considered to be a region of space without any boundaries. The wave, in this case, is a progressive wave compared to the classical standing wave . In general, at each point of space, the simple harmonic oscillator is replaced by quantum harmonic oscillator. Thus for the quantization, we need to substitute the complex numbers a_k and a_k^* by the complex operators $\hat{a}$, $\hat{a}^\dagger$ and insert the time evolution to each of them. Then we can write the operator as follows

$$\hat{A}(\vec{r},t) = \sum_k (\frac{\hbar}{2\omega_k \varepsilon_0})^{1/2} (\hat{a}_k(t)\vec{u}_k(r) + \hat{a}_k^\dagger(t)\vec{u}_k^*(r)). \tag{2.1.17}$$

The Hermitian operators $\hat{a}_k$and $\hat{a}_k^\dagger$ follows the scalar products rule

$$[\hat{a}_m, \hat{a}_n^\dagger] = \delta_{mn} \quad , [\hat{a}_m, \hat{a}_n] = 0 \quad , [\hat{a}_m^\dagger, \hat{a}_n^\dagger] = 0. \tag{2.1.18}$$

The dynamical behavior of the electric-field amplitudes may then be described by an ensemble of independent harmonic oscillators obeying the above commutation relations. The quantum states of each mode may now be discussed independently of each other. The state in each mode may be described by a state vector ψ_k of the Hilbert space appropriate to that mode. The states of the entire field are then defined in the tensor product space of the Hilbert spaces for all of the modes. Assuming for the magnetic field that $B = \mu_0 H$, the Hamiltonian of the free magnetic field is given by

$$H = \frac{1}{2}\int (\varepsilon_0 E^2 + \mu_0 H^2) dr = \sum_k \hbar\omega_k (\hat{a}_k^\dagger \hat{a}_k + \frac{1}{2}). \tag{2.1.19}$$

This relation is well known from the quantum harmonic oscillator, where $n_k = a_k^\dagger a_k$ is the number operator. As a matter of fact, $\hat{n}$ stands for quantum particle mode occupation. So we can write the Hamiltonian as

$$H = \sum_k \hbar\omega (\hat{n}_k + \frac{1}{2}). \tag{2.1.20}$$

This represents the sum of the number of photons in each mode multiplied by the energy of a photon in that mode, plus $\frac{1}{2}\hbar\omega_k$ representing the energy fluctuations in each mode. Of course the Fock states are not the only states of light but if one can produce quantum light in the experiment these states are the best tools to describe the quantum features of the light field. Other state of light like coherent states or squeezed states expose the important aspect of light and can be reviewed in the relevant literature [50, 49, 51].

2.2 Dynamical pictures

While the different pictures of quantum mechanics have distinct formalism, these representations are isomorphic in the evaluation of the state of quantum system. In other word, one obtains similar predictions for the observables in each of these pictures. Their difference comes from the time evolution of the basis that constitute the Hilbert space of the system. This is apparently the difference between fixed and moving frames or active and passive transformations [52]. Fundamentally, any observation in the framework of quantum mechanics should be unrelated how we choose to represent the state vector ψ_s of an arbitrary system. Therefore, any new dynamical picture or representation of quantum mechanics must satisfy the following two rudimentary criteria:

1. The eigenspectrum of an arbitrary operator in a quantum system must stay the same if we move to another dynamical representation.

2. The probabilistic amplitude of any measurement $\langle n \,|\psi\rangle$ must be identical.

Now by keeping these two rules of thumb in mind , we can introduce three representations that shall be applied in the succeeding chapters. In the following, the subscripts S , H and I stand for Schrödinger , Heisenberg and interaction pictures.

Schrödinger picture:

In this picture the observables of the system, $\hat{O}_S$, stay time independent, $\hat{O}_S \neq \hat{O}_S(t)$. In this picture, the Schrödinger equation changes the states , basis for the Hilbert space, of the system with time while the operators of the system stay time independent. The only operator which can be time-dependent is the Hamiltonian of the system $\hat{H}_S$. So in this picture basis evolve and we have a passive transformation

$$\frac{d}{dt}|\psi_S(t)\rangle = -\frac{i}{\hbar}\hat{H}_S|\psi_S\rangle. \tag{2.2.1}$$

Consequently, the time evolution of operators is carried by the state vector

$$\left\langle \hat{O}_S \right\rangle (t) = \left\langle \psi_S(t) \,|\, \hat{O}_S \,|\psi_S(t)\right\rangle. \tag{2.2.2}$$

Additionally, by using Eq. (2.2.1) and Eq. (2.2.2) one can prove the so called Ehrenfest theorem [53]

$$\frac{d}{dt}\left\langle \hat{O}_S \right\rangle = \frac{i}{\hbar}\left\langle \left[\hat{H}_S, \hat{O}_S\right]\right\rangle + \left\langle \frac{\partial \hat{O}_S}{\partial t} \right\rangle. \tag{2.2.3}$$

On the other hand, we can represent a state as a Taylor series, polynomial in time

$$\psi_S(t) = \psi_S(0) + t\dot{\psi}_S(0) + \frac{t^2}{2}\ddot{\psi}_S(0) + ... = (1 + \frac{t}{i\hbar}\hat{H}_S + t^2\frac{1}{2(i\hbar^2)}\hat{H}_S^2 + ...)\psi_S(0)$$
$$= \sum_{n=0}^{\infty} t^n \frac{1}{n!(i\hbar)^n}\hat{H}_S^n\psi_S(0) = \sum_{n=0}^{\infty}\frac{1}{n!}(-\frac{i}{\hbar}\hat{H}_S t)^n\psi_S(0). \tag{2.2.4}$$

This time series can be approximated as an exponential function and we can reformulate the Eq. (2.2.4) in the form of

$$\psi_S(t) = e^{-iH_S t/\hbar}\psi_S(0) = U_S(t)\psi_S(0) \tag{2.2.5}$$

where U_S is an unitary operator which shifts the states of the system in time. One should keep in mind, that the definition of U_S is in alignment with the exponential map between vector space of self-adjoint operators and the group of unitary operators. The Hamiltonian of the system is indeed a self-adjoint operator, $H_S \in L_S$, and there is an exponential map for the Hamiltonian which is a unitery operator [54].
The representation of time-evolution operator also can be driven from the solution of Schrödinger equation by replacing $\psi_S(t)$ with $U_S(t)\psi_S(0)$ in that equation. The result will be the same exponential formalism. U_S can also be defined in Dirac notation as a time-evolution operator which acts on the ket at time $t_0 = 0$ to produce a ket at some other time t

$$|\psi_S(t)\rangle = U_S|\psi_S(0)\rangle. \tag{2.2.6}$$

Further, the unitary operator U_S has also time reversal property $U_S(t) = U_S^\dagger(-t)$. Thus, we can go backward on the time scale of the system

$$U_S^\dagger(t)|\psi_S(t)\rangle = |\psi_S(0)\rangle \tag{2.2.7a}$$
$$\langle\psi_S(t)| = \langle\psi_S(0)|U_S^\dagger(t). \tag{2.2.7b}$$

Since the time-dependent Hamiltonian commutes in different time scales we can rewrite the operator U_S in terms of an integral

$$U_S = \exp\left(-\frac{i}{\hbar}\int_0^t H_S(t')dt'\right). \tag{2.2.8}$$

Heisenberg picture:

In Heisenberg picture, the quantum states are time independent while the quantum operators evolve with time, $\hat{O} = \hat{O}(t)$. We know that the expectation value is obtained from Eq. 2.2.2. Since, $|\psi_S(t)\rangle = U_S|\psi_S(0)\rangle$and $\langle\psi_S(t)| = \langle\psi_S(0)|U_S^*(t)$ we can reformulate the expectation value for the system operator $\hat{O}_H$ as

$$\left\langle \hat{O}_S \right\rangle (t) = \left\langle \psi_S(0) \mid U_S^*(t)\hat{O}_S U_S(t) \mid \psi_S(0) \right\rangle = \left\langle \psi_H \mid e^{i\hat{H}_S t/\hbar}\hat{O}_S e^{-i\hat{H}_S t/\hbar} \mid \psi_H \right\rangle. \tag{2.2.9}$$

Therefore, we can find a relation between Schrödinger and Heisenberg representations of an operator

$$\hat{O}_H = U_S^\dagger(t)\hat{O}_S U_S(t) = e^{i\hat{H}_S t/\hbar}\hat{O}_S e^{-i\hat{H}_S t/\hbar}. \tag{2.2.10}$$

We may verify the operations time-dependence through differentiation

$$\begin{aligned}
\frac{d\hat{O}_H}{dt} &= \frac{i}{\hbar}\hat{H}_S e^{i\hat{H}_S t/\hbar}\hat{O}_S e^{-i\hat{H}_S t/\hbar} - \frac{i}{\hbar}e^{i\hat{H}_S t/\hbar}\hat{O}_S H_S e^{-i\hat{H}_S t/\hbar} + \frac{\partial\hat{O}_S}{\partial t} \\
&= \frac{i}{\hbar}e^{i\hat{H}_S t/\hbar}(\hat{H}_S\hat{O}_H - \hat{O}_H\hat{H}_S)e^{-iH_S t/\hbar} + e^{iH_S t/\hbar}(\frac{\partial\hat{O}_S}{\partial t})e^{-iH_S t/\hbar} \qquad (2.2.11) \\
&= \frac{i}{\hbar}(\hat{H}_S\hat{O}_H - \hat{O}_H\hat{H}_S) + \left(\frac{\partial\hat{O}_H}{\partial t}\right) \\
\Rightarrow \frac{d\hat{O}_H}{dt} &= \frac{i}{\hbar}\left[\hat{H}_S, \hat{O}_H\right] + (\frac{\partial\hat{O}_H}{\partial t}). \qquad (2.2.12)
\end{aligned}$$

This is what in the literature is often called the Heisenberg equation.

The interaction(Dirac) picture:

The interaction picture constitutes a framework in which both the quantum states and the operators are time dependent. This presentation is a matter of interest for the cases wherein the total Hamiltonian of the system can be separate to a time independent and a time dependent parts, $H = H_0 + H_{int}(t)$. We call the time independent part free Hamiltonian and the time dependent part interaction Hamiltonian. In this sense, the state vectors evolve via the interaction(perturbative) part of the Hamiltonian and the operators due to the free part.
In the interaction picture, the state vectors are again defined as transformations of the Schrodinger states. These state vectors are converted only by the free part of the Hamiltonian

$$|\psi_I(t)\rangle = e^{i\hat{H}_{0,S}t/\hbar}|\psi_S(t)\rangle = e^{i\hat{H}_{0,S}t/\hbar}e^{-i\hat{H}_S t/\hbar}|\psi_S(0)\rangle. \tag{2.2.13}$$

And the Dirac operators are transformed similarly to the Heisenberg operators by the free part of Hamiltonian

$$\hat{O}_I(t) = e^{i\hat{H}_{0,S}t/\hbar}\hat{O}_S e^{-i\hat{H}_{0,S}t/\hbar}. \tag{2.2.14}$$

So it follows that for the independent Hamiltonian we can write

$$\hat{H}_{0,I}(t) = e^{iH_{0,S}t/\hbar}\hat{H}_{0,S}e^{-i\hat{H}_{0,S}t/\hbar}. \tag{2.2.15}$$

As a matter of fact, the operators commute with differentiable functions of themselves. This also follows from $\hat{H}_{0,S}$ commuting with itself in the Eq. 2.2.4. So one has a relation between the Hamiltonian in the Schrödinger and the interaction pictures

$$\hat{H}_{0,I}(t) = \hat{H}_{0,S}. \tag{2.2.16}$$

The interacting part also can be defined similarly

$$\hat{V}_I(t) = e^{i\hat{H}_{0,s}t/\hbar}\hat{V}_S e^{-i\hat{H}_{0,S}t/\hbar}. \tag{2.2.17}$$

In interaction picture, the evolution of the states is obtained from

$$\frac{d}{dt}|\psi_I(t)\rangle = \frac{i}{\hbar}\hat{H}_{0,S}e^{i\hat{H}_{0,S}t/\hbar}|\psi_S(t)\rangle + e^{iH_{0,S}t/\hbar}\frac{d}{dt}|\psi_S(t)\rangle. \tag{2.2.18}$$

This can be proven easily from Schrödinger equation

$$\begin{aligned}\frac{d}{dt}|\psi_S(t)\rangle &= -\frac{i}{\hbar}\hat{H}_S|\psi_S(t)\rangle \\ &= \frac{i}{\hbar}\hat{H}_{0,S}|\psi_I(t)\rangle + e^{i\hat{H}_{0,S}t/\hbar}(-\frac{i}{\hbar}\hat{H}_S|\psi_S(t)\rangle).\end{aligned} \tag{2.2.19}$$

But we know that $\hat{H}_S = \hat{H}_{0,S} + \hat{V}_S$ holds, so that Eq. 2.2.19 can be written as

$$\frac{d}{dt}|\psi_S(t)\rangle = \frac{i}{\hbar}\hat{H}_{0,S}|\psi_I(t)\rangle - \frac{i}{\hbar}\hat{H}_{0,S}e^{i\hat{H}_{0,S}t/\hbar}|\psi_S(t)\rangle - \frac{i}{\hbar}e^{i\hat{H}_{0,S}t/\hbar}\hat{V}_S|\psi_S(t)\rangle. \tag{2.2.20}$$

The first two terms vanish and and together with Eq. (2.2.13) we get

$$\begin{aligned}\frac{d}{dt}|\psi_S(t)\rangle &= e^{i\hat{H}_{0,S}t/\hbar}(\frac{1}{i\hbar}\hat{V}_S e^{i\hat{H}_{0,S}t/\hbar}|\psi_I(t)\rangle) \\ &= \frac{1}{ih}e^{i\hat{H}_{0,S}t/\hbar}\hat{V}_S e^{-i\hat{H}_{0,S}t/\hbar}|\psi_I(t)\rangle\frac{d}{dt}|\psi_I(t)\rangle = \frac{1}{ih}\hat{V}_I(t)|\psi_I(t)\rangle\end{aligned} \tag{2.2.21}$$

This shows that the state vectors in the Dirac picture evolve in time according to the interaction term only. Also, it can be shown that the operators in the Dirac picture evolve in time only according to the free Hamiltonian [55]

$$\frac{d\hat{O}_I}{dt} = \frac{i}{\hbar}\left[\hat{H}_{0,I}, \hat{O}_I\right] + (\frac{\partial\hat{O}_I}{\partial t}). \tag{2.2.22}$$

One should consider that the Hermitian conjugate of the Schrödinger equation is a consequence of Hamiltonian hermiticity. So we have a conjugate of the time-dependent Schrodinger equation as

$$-i\hbar\frac{\partial}{\partial t}\langle\psi| = H\langle\psi|. \tag{2.2.23}$$

We know that bounded operators in Hilbert space follow the conjugate property $\langle\psi\,|H\psi\rangle = \langle H^\dagger\psi\,|\psi\rangle$ and in general $\langle\psi\,|A^\dagger\varphi\rangle = \langle A\psi\,|\varphi\rangle$. Further, we know that H is Hermitian so $H = H^\dagger$. One implication of the Dirac picture is the perturbation theory which , in the realm of quantum optics, has various applications, for instance Jaynes-Cumming model that we will use latter in this thesis.

2.3 Open quantum systems

The isolated quantum system is in the center of study in the conventional quantum mechanics, where one needs to just concentrate on the systems properties. This isolation can be seen as an assumption that deviates from the reality, wherein the system and the environment are coupled and affect each other. The reason for the absence of rigorous development of theory for open quantum systems rests in the fact that the conventional one, for a while, had a successful prediction for the representative cases in the early days of the development of quantum mechanics. In addition, considering all degrees of freedom of the environment is in fact a difficult task to handle [56].

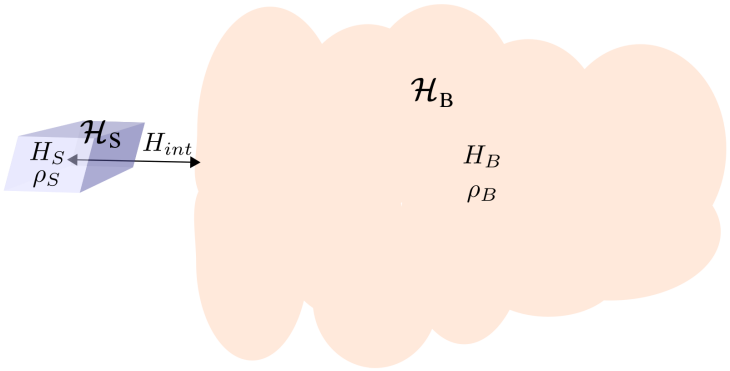

Figure 2.3.1: The interaction between a quantum system and bath. The composite Hilbert space consist of the tensor product between the Hilbert space of the system $\mathcal{H}_s$ and the Hilbert space of bath $\mathcal{H}_B$.

Thus, the cornerstone of the theory of open quantum system is to first study the dynamics of the system together with environment(bath). Then we average the dynamical properties of environment and finally reduce the whole system-bath dynamics by tracing the general density matrix over the environment variable to just systems density matrix. Physically, this means that we consider the influence of the average properties of the environment on the system [41]. The time evolution, in this case, can be understood as a dynamical map T which transfers the density matrix in its initial condition $\rho(0)$ to the density matrix at time t, $T : \rho(0) \to \rho(t)$. One should notice that the density matrix is a mixture of pure states in its initial condition and remain mixed when it is mapped to another point of the dynamical phase space. Here, the density matrix is defined in a usual way as [57]

$$\rho(t) = |\psi(t)\rangle\langle\psi(t)| = \sum_n p_n |\psi_n(t)\rangle\langle\psi_n(t)|. \tag{2.3.1}$$

Where $\psi(t)$ stands for pure state and $|\psi_n(t)\rangle$ is the ensemble of pure states. Each ψ_n has a probability p_n. Of course, the general evolution of the density matrix can be obtained from the Von Neumann equation for pure or mixed state description of

quantum systems

$$\frac{\partial \rho(t)}{\partial t} = -i\,[H(t), \rho(t)]. \tag{2.3.2}$$

As a matter of fact, the environment also can be seen as another system which is much larger than the system under study. The combination of the system and the environment (bath), $S + B$ however, is presumed to be a closed system; e.g., no other external environment, $\bar{B}$ contains the arrangement of $S + B$. Then the Hilbert space of the combined systems takes the form

$$\mathcal{H} = \mathcal{H}_{sys} \otimes \mathcal{H}_B. \tag{2.3.3}$$

Each Hilbert space has a separate basis which can be shown as $\{|\psi_n\rangle_s\}$ and $\{|\psi_m\rangle_B\}$. Consequently, the basis for the combined Hilbert space $\mathcal{H}$, $\{|\psi_r\rangle_G\}$ can be described via the tensor product between theses basis

$$\{|\psi_r\rangle_G\} = \{|\psi_n\rangle_s \otimes |\psi_m\rangle_B\}\,. \tag{2.3.4}$$

The concept that the reduced density operator contains all the necessary information about the system is a matter of importance. This is done by tracing out all the degrees of freedom of the bath or in a formal language as $\rho_s(t) = tr_B\rho(t)$ where $\rho_s(t)$ has a smaller dimension than $\rho(t)$ and easier perhaps to compute. Now one can show that for any observable of the system, $\rho_s(t)$ suffices to give a suitable answer [58, 59]. In the most universal case, we can write the Hamiltonian of the system and the bath as

$$H = H_s + H_B + H_I. \tag{2.3.5}$$

The first two Hamiltonians, are the free part of Hamiltonian, $H_0 = H_s + H_B$. Therefore, it is the H_I which has a time dependence. It was discussed in Sec.2.2 that, by moving to the interaction picture this part will be important . The general representation of the coupling between the source and target is shown in Fig.2.3.1 and is written

$$\tilde{H}_I(t) = e^{i(H_S+H_B)t} H_I e^{-i(H_S+H_B)t}. \tag{2.3.6}$$

By keeping in mind that the combination $S + B$ is closed, we can rewrite the Von Neumann equation for such a combination as follows

$$\frac{\partial \rho(t)}{\partial t} = -i[\tilde{H}_I(t), \rho(t)]. \tag{2.3.7}$$

The Eq. (2.3.7) is a first order differential equation and has a solution

$$\rho(t) = \rho(0) - i \int_0^t ds[\tilde{H}_I(s), \rho(s)]. \tag{2.3.8}$$

In an iterating procedure, by substituting the solution back into the differential equation (2.3.7), one gets a result with the products of $\tilde{H}_I$

$$\frac{\partial \rho}{\partial t} = -i[\tilde{H}_I(t), \rho(0)] - \int_o^t ds[\tilde{H}_I(t), [\tilde{H}_I(s), \rho(s)]. \tag{2.3.9}$$

This is, of course, the equation for the general density matrix but we are interested in the reduced density matrix so the tracing over the environment is necessary. By doing so, from Eq. (2.3.9) we can write

$$\frac{\partial \rho_S(t)}{\partial t} = -itr_B[\tilde{H}_I(t), \rho(0)] - \int_0^t ds\, tr_B[\tilde{H}_I(t), [\tilde{H}_I(s), \rho(s)]]. \tag{2.3.10}$$

Finally, by transferring the term $-itr_B[\tilde{H}_I(t), \rho(0)]$ from the interaction Hamiltonian to the system Hamiltonian, equivalently putting it zero in the current picture, one can write

$$\frac{\partial \rho_S(t)}{\partial t} = -\int_0^t ds\, tr_B[\tilde{H}_I(t), [\tilde{H}_I(s), \rho(s)]]. \tag{2.3.11}$$

We have not made any assumption (of course except assuming combination of system and bath is closed) so the Eq. (2.3.11) is still exact though very difficult to solved. From this point, we will make some assumptions that make the solution of Eq. (2.3.11) easier. One should bear in mind that for an open quantum system dynamics, there are three different timescales that will be in the center of following approximations. The first one is the system's time scale τ_s, the second one is τ_B which is the bath timescale and finally τ_I which is the interaction timescale.

Born approximation

Before introducing the Born approximation we shall introduce an initial condition which is related to this approximation. We set the initial density operator as $\rho(0) = \rho_S(0) \otimes \rho_B(0)$ which states that in the time $\tau_s = \tau_B = 0$, there is no interaction between system and bath and they can be factorized from each other. The essence of the Born approximation is of the extension of above assumption where we assume that the density operators stay factorized for $t > 0$ as well

$$\rho(t) \approx \rho_S(t)\rho_B. \tag{2.3.12}$$

The more fruitful explanation for the Born approximation is that we only consider the first back action from the bath on the system and the second order terms will not be considered. This approximation fundamentally relies on the fact that the environment is considered to be sufficiently larger than the system that its states are not influenced by the system. This implies that the interaction Hamiltonian H_I is considerably weak. By such an approximation one can rewrite the Eq. (2.3.11) as

$$\frac{\partial \rho_S(t)}{\partial t} = -\int_0^t ds\, tr_B[\tilde{H}_I(t), [\tilde{H}_I(s), \rho_S(s)\rho_B]]. \tag{2.3.13}$$

Markov approximation

The Markov approximation, as it is clear from its name, comes from the Markovian chain in statistical mechanics. It indicates the fact that the only information that we need to predict the future of the systems is the current state of them. Putting it differently, there is no need to rely on the past trail of the system and all the information necessary for prediction of its future is already contained in the present state. In the case of open quantum systems, this implies that the memory of environment is much shorter than of the system, i.e., environment is big enough that will not remember the past behavior of the system. This allows us to assign the present time to the time scale of the system: $\rho_S(s) \to \rho_S(t)$. The memory effect elimination can be reflected on dynamical map formalism. Assuming the family of dynamical map $\{T(t)\}$ and two different times $t_1, t_2 > 0$ we have

$$T(t_1)T(t_2) = T(t_1 + t_2). \tag{2.3.14}$$

This is exactly semi-group property that turn dynamical map to dynamical semi-group. The functional equation Eq. (2.3.14) has a family of solution as

$$T(t) = e^{\mathcal{L}t}. \tag{2.3.15}$$

From that property one can derive general Markovian master equation

$$\frac{d\rho_S}{dt} = \mathcal{L}\rho_S \tag{2.3.16}$$

where $\mathcal{L}$ is a generator that should be explicitly defined. This is the stage that the so called Lindblad theorem was proposed for the definition of this generator [60, 61, 62].

Furthermore, by considering that the system and the environment are disjoint, we can extend the limitation of the time integral to infinity in Eq. (2.3.13) and use the variable transformation $\tau = t - s$ to obtain

$$\frac{\partial\rho_S(t)}{\partial t} = -\int_0^\infty d\tau\, tr_B[\tilde{H}_I(t), [\tilde{H}_I(t-\tau), \rho_S(t)\rho_B]]. \tag{2.3.17}$$

Without specification about a particular system, still we can get further and have more definite form for the master equation. This is generally done by reformulating the interaction Hamiltonian into the summation where bath correlation functions are separated from system operators. This form specifically can be written in the interaction picture as

$$H_I(t) = \sum_i S_i(t) \otimes B_i(t). \tag{2.3.18}$$

As it is clear that in the interaction picture these operators are time dependent. The relation between these operators in Schrodinger and interaction pictures can be expressed as:

$$S_i(t) = e^{iH_S t} S_i e^{-iH_S t} \tag{2.3.19a}$$

$$B_i(t) = e^{iH_B t} B_i e^{-iH_B t}. \tag{2.3.19b}$$

Secular approximation

Secular approximation stands for the omission of the fast oscillating terms. As we mentioned above in the Eq. (2.3.19a) and Eq. (2.3.19b) , the exponential terms are considered in the master equation and will have two different time scales for t and s. The corresponding frequencies to these time scales are ω and ω'. In this case the timescale of the system can be written as

$$\tau_s = \frac{1}{(\omega - \omega')} \qquad for \qquad \omega - \omega' \neq 0. \tag{2.3.20}$$

Thus, the essence of the secular approximation is that the time evolution of the system-bath interaction is slower that time evolution of the system, $\tau_s << \tau_I$. Where τ_I represents the interaction timescale which also can be seen as relaxation time. Hence, as we are interested on relaxation of system, the fast oscillating terms are estimated to be zero. It is worthwhile to notice that the secular approximation is not necessary an indication for Markov approximation. In other word, it does not suggest that the bath timescale is much faster than the relaxation timescale, $\tau_B << \tau_I$.

Finally, the secular approximation also holds for non-Markovin dynamics, wherein, τ_S should be smaller than non-Markovian timescale.

3 Cascaded formalism

Herein, we present a formalism developed for coupled quantum systems. As a matter of fact, a very convenient method to simulate quantum excitation experiments is the quantum cascade formalism developed concurrently by Gardiner [34] and Carmichael [35]. The quantum cascade approach allows a self-consistent mapping of the sources quantum excitation onto a second-system, via the quantum Langevin [34] or quantum stochastic Schrödinger equations [36, 63]. The concept for such a formalism is a continuation of the theory of open quantum systems discussed in Chapter.2. Firstly, we introduce the input-output method which was developed by Gardiner et al [36]. We will see that this method is the step stone for the equation of motion for cascaded systems. We then move forward, and treat coupled quantum system in such a way that the properties of the source can be studied first and then it can be used to shine it on the target system. This concept of source and target initiates the core notion for the cascaded formalism. Finally, we discus different methods to derive a master equation which determines the density matrix of composite systems. This obtained density matrix is used to study the dynamics of source and target systems.

3.1 Input-output method

The first general formulation of in-out operators is developed in the realm of quantum field theory. This is done by introducing reduction formula where input-output transition amplitudes determine S-matrix elements [64]. However, the initial effort to specifically tackle the problem of input-output of damped quantum systems was established by Gardiner and Collet [32, 33]. This method later was applied for derivation of the cascaded formalism. Thus, it is important to have an overview about it. The essence of input-output formulation is that one can think of the bath as a field or equivalently as a set of harmonic oscillators.
The first step is to define the general Hamiltonian of the system and bath

$$H_G = H_s + H_B + H_{int}. \tag{3.1.1}$$

We take the Hamiltonian of the system unspecified. On the other hand one can write down H_B and H_{int} as

$$H_B = \hbar \int_0^{+\infty} d\omega\, \omega\, b^\dagger(\omega)\, b(\omega) \tag{3.1.2a}$$

$$H_{int} = i\hbar \int_0^{+\infty} d\omega \kappa(\omega)[b^\dagger(\omega)\, e^{-i\omega t} + b(\omega) e^{i\omega t}][c e^{-i\Omega t} - c^\dagger e^{i\Omega t}]. \tag{3.1.2b}$$

where c is an arbitrary system operator without further specification, $b(\omega)$ is the annihilation bosonic operator of the bath with canonical commutation relation $[b(\omega), b^\dagger(\omega')] = \delta(\omega - \omega')$. There are some assumptions that make these Hamiltonians rather simplified. The first and foremost is the rotating wave approximation where we assume that the time dependent terms of $b^\dagger(\omega)c^\dagger e^{i(\omega+\Omega)t}$ are oscillating so fast that its integral vanishes over long times. The second one is the near resonant approximation where the only significant terms are the ones related to resonance time dependency of $b^\dagger(\omega)ce^{i(\omega-\Omega)t}$ whose exponent becomes zero, basically time independent, on resonance. Thus, only these terms remain in interaction Hamiltonian.
After above procedure, the resultant interaction Hamiltonian H_{int} is according to the rotating wave and near resonance approximations. Now we can derive the Langevin equations of motion starting from the Heisenberg equation of motion for the bath operators and also an arbitrary system operator that we want to find the dynamics of. Taking into account that the coupling strength κ is time independent the equations of motion for $b(\omega)$ and a reads

$$\dot{b}(\omega, t) = -i\omega\, b(\omega, t) + \kappa(\omega)c \tag{3.1.3a}$$

$$\dot{a}(t) = -\frac{i}{\hbar}[a(t), H_{sys}] + \int d\omega\, \kappa(\omega)\{b^\dagger(\omega, t)[a(t), c(t)] - [a(t), c^\dagger(t)]b(\omega, t)\}. \tag{3.1.3b}$$

Formally integrating these differential equations we obtain an explicit function for the dynamics of bath operator $b(\omega)$ as

$$b(\omega, t) = e^{-i\omega(t-t_0)}b_0(\omega, t_0) + \kappa(\omega)\int_{t_0}^{t} dt' c(t')e^{-i\omega(t-t')} \tag{3.1.4}$$

where $b_0(\omega, t_0)$ is an initial condition for b.

It can be shown that the initial condition $b_0(\omega, t_0)$ satisfies the same commutation relation as b $[b_0(\omega, t_0), b_0^\dagger(\omega', t_0)] = \delta(\omega - \omega')$. This relation has a simple proof which is missing in the quantum noise book [36] and can be proven as an exercise as following

Knowing that

$$\Big[b(\omega, t), b^\dagger(\omega', t)\Big] = b(\omega, t)b^\dagger(\omega', t) - b^\dagger(\omega', t)b(\omega, t) = \delta(\omega - \omega') \tag{3.1.5}$$

and

$$b(\omega, t) = e^{-i\omega(t-t_0)}b_0(\omega) + \kappa(\omega)\int_{t_0}^{t} \mathrm{d}t'\, e^{-i\omega(t-t_0)}c(t') \tag{3.1.6}$$

it follows that

$$\begin{aligned}\Big[b(\omega, t), b^\dagger(\omega', t)\Big] = {} & e^{-i(\omega-\omega')(t-t_0)}\Big[b_0(\omega), b_0^\dagger(\omega')\Big] + \kappa(\omega)\int_{t_0}^{t} \mathrm{d}t'\, e^{-i(\omega-\omega')(t-t_0)}\Big[b_0(\omega), c^\dagger(t')\Big] \\ & + \kappa^*(\omega')\int_{t_0}^{t} \mathrm{d}t' e^{-i(\omega-\omega')(t-t_0)}\Big[c(t'), b_0^\dagger(\omega)\Big] \\ & + \kappa(\omega)\kappa^*(\omega')\int_{t_0}^{t} \mathrm{d}t_1 \int_{t_0}^{t} \mathrm{d}t_2\, e^{-i(\omega-\omega')(t-t_0)}\Big[c(t_1)c^\dagger(t_2)\Big]\end{aligned} \tag{3.1.7}$$

So by putting t to t_0 we obtain

$$\Big[b(\omega,t), b^\dagger(\omega',t)\Big] \xrightarrow{t\to t_0} \Big[b_0(\omega), b_0^\dagger(\omega')\Big]. \tag{3.1.8}$$

Which is exactly what we wanted to prove. Substituting the solution for the $b(\omega,t)$ into Eq. (3.1.3b), we obtain

$$\dot{a}(t) = -\frac{i}{\hbar}[a(t), H_{sys}] + \int d\omega\kappa(\omega)\{e^{i\omega(t-t_0)}b_0^\dagger(\omega,t_0)[a(t),c] - [a(t),c^\dagger]e^{-i\omega(t-t_0)}b_0(\omega,t_0)\}+$$
$$\int d\omega[\kappa(\omega)]^2\int_{t_0}^{t} dt'\{e^{i\omega(t-t')}c^\dagger(t')[a,c] - [a,c^\dagger]e^{-i\omega(t-t')}c(t')\}. \tag{3.1.9}$$

The Eq. (3.1.9) however in its exact form is difficult to solve. At this stage we apply an approximation that simplifies this equation and results in an attentive version that can be used further. This is in alignment with Markov approximation where the thermal bath modes have the same coupling ratio, the bath is considered as a field or a set of harmonic oscillators that couple to the system with the same coupling constant. This is called a flat bath spectrum [33]. Formally, this can be stated as a relation for the coupling ratio

$$\kappa(\omega) = \sqrt{\frac{\gamma}{2\pi}}. \tag{3.1.10}$$

Additionally, two integration identities are useful

$$\int_{-\infty}^{+\infty} d\omega\, e^{-i\omega(t-t')} = 2\pi\delta(t-t') \tag{3.1.11a}$$
$$\int_{t_0}^{t} c(t')\delta(t-t')dt' = \frac{1}{2}c(t). \tag{3.1.11b}$$

We can redefine the frequency integral in Eq. (3.1.9) as an input field

$$b_{in}(t) = \frac{1}{\sqrt{2\pi}}\int d\omega\, e^{-i\omega(t-t_0)}b_0(\omega). \tag{3.1.12}$$

The commutation relation between the input operator $b_{in}(t)$ and its conjugate $b_{in}^\dagger(t')$ is

$$[b_{in}(t), b_{in}^\dagger(t')] = \delta(t-t'). \tag{3.1.13}$$

Thus, by applying Eq. (3.1.10) - Eq. (3.1.12) in the Eq. (3.1.9), this equation can be written in the simplified form

$$\dot{a}(t) = -\frac{i}{\hbar}[a(t), H_{sys}] - [a(t), c^\dagger(t)]\big\{\frac{\gamma}{2}c(t) + \sqrt{\gamma}b_{in}(t)\big\} + \big\{\frac{\gamma}{2}c^\dagger(t) + \sqrt{\gamma}b_{in}^\dagger(t)\big\}[a(t), c(t)]. \tag{3.1.14}$$

One should notice that the overall operators $\frac{1}{2}\gamma c(t)+\sqrt{\gamma}b_{in}(t)$ and $\frac{1}{2}\gamma\, c^{\dagger}(t)+\sqrt{\gamma}b_{in}^{\dagger}(t)$ commute with all system operators. As an additional exercise which is absent in the related literatures, We can prove that

$$\frac{1}{\sqrt{2\pi}}\int d\omega\, b(\omega,t) = b_{in}(t) + \frac{\sqrt{\gamma}}{2}c(t). \tag{3.1.15}$$

The proof of that relation is absent in the related literature and we will provide it here. Inserting the definition of the $b(\omega,t)$ in Eq. (3.1.4) into the integral $\int d\omega b(\omega,t)$ one will gets

$$\begin{aligned}\int d\omega b(\omega,t) &= \int d\omega e^{-i\omega(t-t_0)}b_0(\omega,t_0) + \int d\omega\kappa(\omega)\int_{t_0}^{t} dt' c(t')e^{-i\omega(t-t')} \\ &= \sqrt{2\pi}b_{in}(t) + \sqrt{\frac{\gamma}{2\pi}}\int_{t_0}^{t} dt' c(t')\int d\omega e^{-i\omega(t-t')}\end{aligned} \tag{3.1.16}$$

where we used the Eq. (3.1.12) for the first sum and Eq. (3.1.10) for the second sum on the right hand side. By applying the Eq. (3.1.11a) first we arrive at

$$\int d\omega b(\omega,t) = \sqrt{2\pi}b_{in}(t) + \sqrt{2\pi\gamma}\int_{t_0}^{t} dt' c(t')\delta(t-t'). \tag{3.1.17}$$

Finally we use Eq. (3.1.11b) for the time integral and obtain the desired relation.

Now if we consider that some time passed, $t_1 > t$ and the system is already influenced by the input field, it starts to radiate an output field. In this situation, one can solve the differential Eq. 3.1.3a for different initial conditions and find the solution for the output field as

$$b(\omega,t) = e^{-i\omega(t-t_1)}b_1(\omega,t_1) - \kappa(\omega)\int_{t}^{t_1} dt' c(t')e^{-i\omega(t-t')}. \tag{3.1.18}$$

The equation of motion is written also by considering the output field as

$$\dot{a}(t) = -\frac{i}{\hbar}[a(t),H_{sys}] - [a(t),c^{\dagger}(t)]\big\{\frac{\gamma}{2}c(t) - \sqrt{\gamma}b_{out}(t)\big\} - \big\{\frac{\gamma}{2}c^{\dagger}(t) - \sqrt{\gamma}b_{out}^{\dagger}(t)\big\}[a(t),c(t)]. \tag{3.1.19}$$

Where b_{out} is defined analogously as b_{in}

$$b_{out}(t) = \frac{1}{\sqrt{2\pi}}\int d\omega\, e^{-i\omega(t-t_1)}b_1(\omega,t_1). \tag{3.1.20}$$

One should bear in mind that the Eq. (3.1.19) is a time reversal equation of the original Langevin equation.
Similarly the relation in Eq. (3.1.15) is reproducible for b_{out}

$$\frac{1}{\sqrt{2\pi}}\int d\omega\, b(\omega,t) = b_{out}(t) - \frac{\sqrt{\gamma}}{2}c(t). \tag{3.1.21}$$

These substitute relations give rise to the final association between b_{in} and b_{out}:

$$b_{out}(t) - b_{in}(t) = \sqrt{\gamma}c(t) \tag{3.1.22}$$

This is the boundary condition which relates the input and the output fields. Considering the time reversal equation, we will arrive at the concept of causality. Herein, the term causality means that first the present input field has an influence on the system's future, and then the present dynamics of the system influence the future of the output field. We may well see that in our formalism if we solve the Langevin equation for an arbitrary system operator $a(t)$ where the b_{in} is also a function of t. Thus, for $t' > t$ the $b_{in}(t')$ will not influence $a(t)$. This can be expressed through the mathematical formulation of quantum mechanics

$$[a(t), b_{in}(t')] = 0 \quad , \quad t' > t. \tag{3.1.23}$$

Similar argument applies for the time reversal equation where there is no influence from the $b_{out}(t')$ on the system operator at the time $t' < t$

$$[a(t), b_{out}(t')] = 0 \qquad t' < t. \tag{3.1.24}$$

By using the step function $\Theta(\Delta t)$ we can express the causality in a compact form

$$[a(t), b_{in}(t')] = -\Theta(t - t')\sqrt{\gamma}[a(t), c(t')] \tag{3.1.25a}$$
$$[a(t), b_{out}(t')] = \Theta(t' - t)\sqrt{\gamma}[a(t), c(t')] \tag{3.1.25b}$$

where $\Theta(\Delta t)$ is expressed as

$$\Theta(\Delta t) = \begin{cases} 1 & \Delta t > 0 \\ 1/2 & \Delta t = 0 \\ 0 & \Delta t < 0. \end{cases} \tag{3.1.26}$$

This is also a manifesto for the calculation of the output field without using the time reversal equation. Firstly, we calculate $a(t)$ by using Eq. (3.1.14) then we can apply Eq. (3.1.25a) and Eq. (3.1.25b). This gives an easier way of solution for the output field.

3.2 Equation of motion for cascaded source and target

The input output model applies essentially for one system interacting with input and output noise. Consequently, this model can be seen as a building block of the dissipation of two systems interacting with each other via a common bath. As a matter of fact, considering that there is no limit to the number of cascaded systems [34], one can build up a network of systems where the system k is the output of system and its output is used to feed the $k + 1$ system. The general schematic for both scenarios is shown in the Fig. 3.2.1 and Fig. 3.2.2.

Traditionally, any coupled system can be divided into a source and a target. Then one can study the properties of each separately and observe the influence of the source on the target. At first glance it seems obvious that one can determine the correlation functions of the source and then use them to drive the target system. However, the possibility to go through all correlation functions, as the treating of these functions analytically is too complex, is restricted.

Also these functions are time-dependent and can not be set as an initial condition for the dynamics of the target system. Thus, a cascaded formalism is necessary where we are free from dealing with the correlation functions of the source and target separately. The down-side of this formalism is that it excludes back actions from the target to the source. This formalism distinguishes the source and the target quantum excitations such that the source influences the target but not the other way around. This is the cornerstone of cascaded formalism, that the unidirectionality excludes the possibility to be applied for feedback actions in quantum feedback schemes.

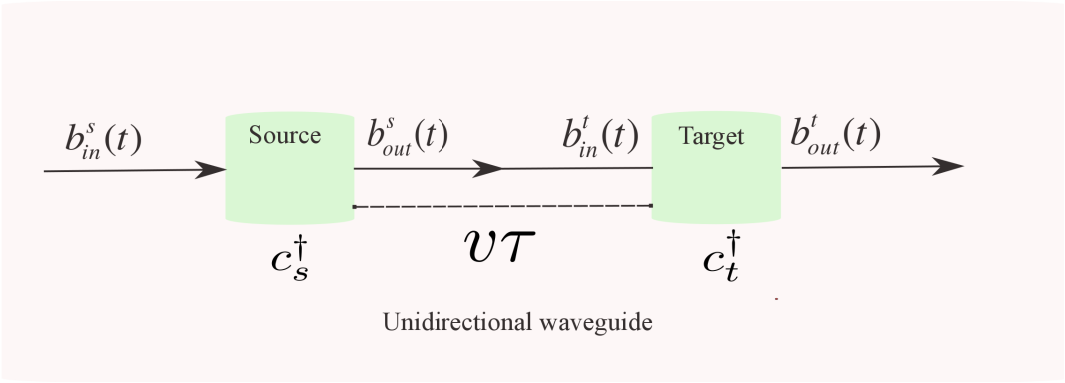

Figure 3.2.1: The unidirectional coupling between an arbitrary source and target. The time delay between the coupled systems is represented by τ.

We assume that the quantum system consists of two subsystems. Adapting the input-output method we see $b^s_{in}(t)$ to drive the first system (source) and then the first system produces $b^s_{out}(t)$. The latter field travels from the first system to the second system in a time τ. Then it becomes the input for the second system (target) $b^t_{in}(t)$. With respect to the subsystems, one can define the Hamiltonian of the entire system $H_{sys} = H_s + H_t$. Then, we have two Langevin equations for an arbitrary operator of the source and target

$$\dot{a}_s = -\frac{i}{\hbar}[a_s, H_s] - [a_s, c_s^\dagger]\{\frac{\gamma_s}{2}c_s + \sqrt{\gamma_s}b^s_{in}(t)\} + \{\frac{\gamma_s}{2}c_s^\dagger + \sqrt{\gamma_s}b^{\dagger s}_{in}(t)\}[a_s, c_s] \quad (3.2.1a)$$

$$\dot{a}_t = -\frac{i}{\hbar}[a_t, H_t] - [a_t, c_t^\dagger]\{\frac{\gamma_t}{2}c_t + \sqrt{\gamma_t}b^t_{in}(t)\} + \{\frac{\gamma_t}{2}c_t^\dagger + \sqrt{\gamma_t}b^{\dagger t}_{in}(t)\}[a_t, c_t]. \quad (3.2.1b)$$

From the input-output method we can relate the input to the first system, output form the first system and input to the second system as follows

$$b^s_{out}(t) = b^s_{in}(t) + \sqrt{\gamma_s}c_s(t). \quad (3.2.2)$$

Introducing the time delay τ we obtain

$$b^t_{in}(t) = b^s_{out}(t-\tau) = b^s_{in}(t-\tau) + \sqrt{\gamma_s}c_s(t-\tau). \tag{3.2.3}$$

And also for the output of the combined systems, output from the target system, one can use the same procedure

$$b_{out}(t) = b^t_{out}(t) = b^t_{in}(t) + \sqrt{\gamma_t}c_t(t) = b^s_{in}(t-\tau) + \sqrt{\gamma_s}c_s(t-\tau) + \sqrt{\gamma_t}c_t(t). \tag{3.2.4}$$

By relating the inputs and outputs of the source and target, we can define an operator

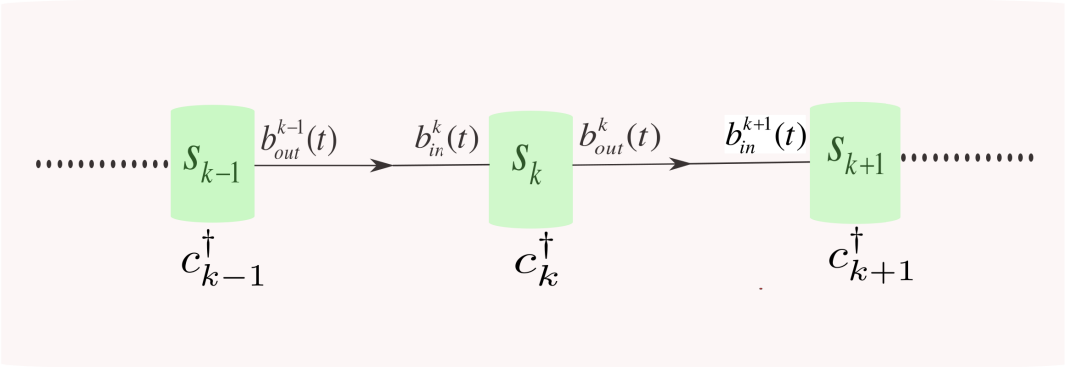

Figure 3.2.2: The assembly of the cascaded network of the systems. The output of each system becomes the input for the next system.

which represents either the source or the target

$$\begin{aligned}\dot{a} = -\frac{i}{\hbar}[a, H_{sys}] &- [a, c^\dagger_s]\{\frac{\gamma_s}{2}c_s + \sqrt{\gamma_s}b^s_{in}(t)\} + \{\frac{\gamma_s}{2}c^\dagger_s + \sqrt{\gamma_s}b^{\dagger s}_{in}(t)\}[a, c_s] \\ &- [a, c^\dagger_t]\{\frac{\gamma_t}{2}c_t + \sqrt{\gamma_s\gamma_t}c_s(t-\tau) + \sqrt{\gamma_t}b^t_{in}(t-\tau)\} \\ &+ \{\frac{\gamma_t}{2}c^\dagger_t + \sqrt{\gamma_s\gamma_t}c^\dagger_s(t-\tau) + \sqrt{\gamma_t}b^{\dagger t}_{in}(t-\tau)\}[a, c_t].\end{aligned} \tag{3.2.5}$$

One should notice that the equation of motion, in its general form, is a function of two different time t and $t-\tau$. For the sake of unidirectionality, τ must have a random positive value. By redefining the arbitrary operator of the second system as $\bar{a}(t) \equiv a(t+\tau)$, describing why we put time delay to zero, we can rewrite the Eq. (3.2.5) as

$$\begin{aligned}\dot{a} = -\frac{i}{\hbar}[a, H_{sys}] &- [a, c^\dagger_s]\{\frac{\gamma_s}{2}c_s + \sqrt{\gamma_s}b^s_{in}(t)\} + \{\frac{\gamma_s}{2}c^\dagger_s + \sqrt{\gamma_s}b^{\dagger s}_{in}(t)\}[a, c_s] \\ &- [a, c^\dagger_t]\{\frac{\gamma_t}{2}c_t + \sqrt{\gamma_t}b^t_{in}(t)\} + \{\frac{\gamma_t}{2}c^\dagger_t + \sqrt{\gamma_t}b^{\dagger t}_{in}(t)\}[a, c_t] \\ &- [a, c^\dagger_t]\sqrt{\gamma_s\gamma_t}c_s + \sqrt{\gamma_s\gamma_t}c^\dagger_s[a, c_t].\end{aligned} \tag{3.2.6}$$

As it can be seen, we obtain a one time equation of motion for the arbitrary operators of the both system. This method is equivalent to assign $\tau \to 0$ in Eq. (3.2.5). The

above procedure is applicable for any part of the quantum cascade network. For instance, consider system s_{k-1} and s_k in Fig. 3.2.2 as source and target, then for the subsystem k with operator c_k we can reformulate the Eq. (3.2.6) as

$$\begin{aligned}\dot{a} = -\frac{i}{\hbar}[a, H_{sys}] &- [a, c_{k-1}^\dagger]\{\frac{\gamma_{k-1}}{2}c_{k-1} + \sqrt{\gamma_{k-1}}b_{in}^{k-1}(t)\} + \{\frac{\gamma_{k-1}}{2}c_{k-1}^\dagger + \sqrt{\gamma_{k-1}}b_{in}^{\dagger k-1}(t)\}[a, c_{k-1}] \\ &- [a, c_k^\dagger]\{\frac{\gamma_k}{2}c_k + \sqrt{\gamma_k}b_{in}^{k}(t)\} + \{\frac{\gamma_k}{2}c_k^\dagger + \sqrt{\gamma_k}b_{in}^{\dagger k}(t)\}[a, c_k] \\ &- [a, c_k^\dagger]\sqrt{\gamma_{k-1}\gamma_k}c_{k-1} + \sqrt{\gamma_{k-1}\gamma_k}c_{k-1}^\dagger[a, c_k]. \end{aligned} \tag{3.2.7}$$

Where a stands for either a_{k-1} or a_k and the Hamiltonian of the system is defined as $H_{sys} = H_{k-1} + H_k$.

3.3 Master equation approach

There are two ways to derive the master equation for such a cascaded system. The first one is in the realm of quantum trajectory theory, by converting the Langevin equation into an Ito integro-differential equation as it was provided by Gardiner et al [65]. The second method is to derive the master equation directly by defining the coupling Hamiltonian between the source and target and taking the conventional procedure of derivation of optical master equation [66]. The first approach is also discussed properly in [36] where the steps from the equation of motion to the master equation are introduced.
Here we present a general scheme for the second way of derivation.

First we define the general Hamiltonian of the system: $H = H_{sys} + H_c$. The system part of the Hamiltonian will defined later for each separate case. The bosonic bath creation operator is set to be $b^\dagger$. Also, the source and target creation operators are $a_s^\dagger$ and $a_t^\dagger$. The main concern here is to find the coupling part of the Hamiltonian which can be used to derive the coupling part of the master equation. We want to understand the connection between two systems and the influence of environment on that communication.
Thus the coupling Hamiltonian is defined as

$$H_c = H_s + H_t + H_B + H_{int}. \tag{3.3.1}$$

Where the corresponding definition for each Hamiltonian reads

$$H_B = \hbar \int d\omega \omega \, b_\omega^\dagger b_\omega. \tag{3.3.2}$$

And in relation to the coupling ratio of the system and bath, the interaction Hamiltonian takes a similar form to Eq. (3.1.2b)

$$H_{int} = \hbar \int d\omega \, [g_s(\omega)(a_s^\dagger b_\omega + h.c) + g_t(\omega)(a_t^\dagger b_\omega e^{i\omega\tau} + h.c)]. \tag{3.3.3}$$

The time delay here is defined as τ and is the same as in the input-output method discussed in the beginning of this chapter.
For now we shall set the Hamiltonians of the source and target arbitrary. The further specification of these Hamiltonians will be discussed for each case study in the following chapters. So the coupling Hamiltonian is written explicitly as

$$H_c = \hbar\omega_s a_s^\dagger a_s + \hbar\omega_t a_t^\dagger a_t + \hbar\int d\omega\,\omega\, b_\omega^\dagger b_\omega + \hbar\int d\omega[g_s(\omega)(a_s^\dagger b_\omega + h.c) + g_t(\omega)(a_t^\dagger b_\omega e^{i\omega\tau} + h.c)]. \tag{3.3.4}$$

By switching into the interaction picture we can rewrite the coupling Hamiltonian in the form of

$$\frac{H_c}{\hbar} = \int d\omega\, g_s(\omega)(a_s^\dagger e^{i\omega_s t} b_\omega e^{-i\omega t} + h.c) + \int d\omega\, g_t(\omega)(a_t^\dagger e^{i\omega_t t} b_\omega e^{-i\omega t} e^{i\omega\tau} + h.c). \tag{3.3.5}$$

The general procedure is to reformulate the coupling Hamiltonian in a more compact form by defining new operators in such way that the terms related to the system, either source or target, and the terms related to the bath are disjoint. The operator for frequency integrals reads

$$\Gamma_i(t) = \int d\omega\, g_i(\omega) e^{-i\omega t} b_\omega e^{i\omega\tau} \quad , \quad (i = s, t). \tag{3.3.6}$$

Where the time delay τ is zero for $i = s$. As it can be seen, we compressed the frequency integral into one operator. The reason for that will become clear later. Thus, the coupling Hamiltonian can be written as

$$\frac{H_c}{\hbar} = a_s^\dagger e^{i\omega_s t}\Gamma_s(t) + a_s e^{-i\omega_s t}\Gamma_s^\dagger(t) + a_t^\dagger e^{i\omega_t t}\Gamma_t(t) + a_t e^{-i\omega_t t}\Gamma_t^\dagger(t). \tag{3.3.7}$$

The conventional way is to insert this Hamiltonian into the general form of master equation is

$$\frac{\partial\rho}{\partial t} = -\frac{1}{\hbar^2}\int ds\, tr_B\{\underbrace{[H_c(t), [H_c(s), \rho(s)\rho_B]]}_{*}\}. \tag{3.3.8}$$

Where the Born approximation implies that $\rho_{tot} \approx \rho(t) \otimes \rho_B$. The reason behind the separation of frequency integral is clear. In the master equation the time integral and frequency integral can be computed separately. The commutation part can be written as

$$\begin{aligned} * = [H_c(t), [H_c(s)\rho(s) - \rho(s)H_c(s)]] = H_c(t)H_c(s)\rho(s) - H_c(t)\rho(s)H_c(s) - \\ H_c(s)\rho(s)H_c(t) + \rho(s)H_c(s)H_c(t). \end{aligned} \tag{3.3.9}$$

However, this is the straightforward approach to gain the expanded version of master equation, one can use another, yet more strenuous way to derive the final version

First approach: $\kappa(\omega) = \kappa(0)$	Second approach: $\kappa(\omega)$
Born	Born
Markov: $\int_0^t ...dt \longrightarrow \int_{-\infty}^{+\infty} ...dt$	Time delay between two systems: τ
$\langle b_\omega(t) b_\omega^\dagger(t')\rangle = \delta(t-t')$	$\langle b_\omega(0) b_{\omega'}^\dagger(0)\rangle = \delta(\omega-\omega')$
bidirectional	unidirectional

Table 3.3.1: Regarding to the coupling ration between the bath and systems, there are two distinct ways to derive a master equation .

of master equation from the Eq.(3.3.8). To do so, first we define also new operators for the source and target operators. This allows us to reformulate the coupling Hamiltonian to the summation formula

$$f_1 = a_s^\dagger e^{i\omega_s t}, f_2 = a_s e^{-i\omega_s t}, f_3 = a_t^\dagger e^{i\omega_t t}, f_4 = a_t e^{-i\omega_t t}. \tag{3.3.10}$$

Now the coupling Hamiltonian can be written as summation

$$\frac{H_c}{\hbar} = \sum_l f_l \Gamma_l = -\frac{1}{\hbar^2} \sum_{l,k} \int_0^t ds\, tr_B\{[f_l(t)\Gamma_l(t), [f_k(s)\Gamma_k(t), \rho_s \rho_B]]\}. \tag{3.3.11}$$

And the cyclic property of trace leads to

$$\begin{aligned} \frac{\partial \rho}{\partial t} = -\frac{1}{\hbar^2} \sum_{l,k} \int_0^t ds \{ &[f_l(t) f_k(s) \rho(s) - f_k(s) \rho(s) f_l(t)] \langle \Gamma_l(t) \Gamma_k(s)\rangle_B + \\ &[\rho(s) f_k(s) f_l(t) - f_l(t) \rho(s) f_k(s)] \langle \Gamma_k(s) \Gamma_l(t)\rangle_B . \end{aligned} \tag{3.3.12}$$

From this point there will be only further mathematical manipulations to derive the final version of master equation.

The way we are considering the coupling ration of bath and the systems also determines the derivation process of the master equation. Whether we take $\kappa(\omega)$ constant or frequency depended, changes the order of approximation and what we can assume in this process. This two approaches are shown in the table 3.3.1.
The above process to derive a master equation is applicable to each part of the quantum cascaded network. A more detailed derivation will be presented in forthcoming chapters where we are dealing with cascaded two and four level systems.

3.4 conclusion

We have provided an overview for the input-output method and how it can be used to arrive at cascaded formalism. Some additional proofs for the conventional method also are given. Then, we presented a direct procedure to derive a master equation for the cascaded setup. This method is straightforward and easy to implement in comparison to the conventional procedure, wherein, one uses the equation of motion to derive a master equation.

For the direct derivation of master equation , two different views can be implemented. It is customary in literature that the coupling ratio of two systems to the wave guide, $\kappa_i(\omega)$ is frequency dependent. Then, one should add an additional assumption, namely unidirectionality of coupling. However, in this thesis we take another manifesto. We apply what is so called first Markov approximation in which the coupling ratio is frequency independent $\kappa_i(\omega) = \kappa$. To this end, three is no need for additional unidirectionality assumption. In fact, the terms corresponding to the back action in Eq. (3.3.12) will be out of the time integral limits and can be omitted.

4 Casimir effect

This chapter deals with one of the main result of the quantization of the electromagnetic field, namely, vacuum fluctuation. To be more precise, we give an overview for the macroscopic phenomena named Casimir effect in its static and dynamic forms. This concept is necessary for chapter 6 wherein we propose an experimentally accessible setup to imitate the dynamical Casimir effect and produce pairs of photons. The whole setup can be regarded as a source for the quantum excitation via non-classical light. Here, the microscopic consequences of vacuum fluctuation like Lamb shift and spectral lines width, etc are not described but can be found in the standard quantum optics books [67, 68, 69]. Firstly, we describe the zero point energy and vacuum fluctuation as an extension to the quantization of electromagnetic field. Then we describe the suggested setup by Casimir [70] where the Casimir force can be observed. We also present the main idea behind the dynamical version of the Caimir effect and shortly refer to the experimental setups which are proposed for observing this effect.

4.1 Zero point energy and Casimir effect

What is the vacuum energy? This notion suggests that a vacuum in space, without any external field involved, still has some ground energy. The influences of this energy fluctuation surprisingly can be observed through (statical or dynamical) Casimir effect. Casimir effect and force are macroscopic consequences of vacuum energy density.

As a result of the uncertainty principle, every physical system in quantum mechanics should have a lowest possible energy otherwise the uncertainty principle will be violated [71]. One should note that for the ground state of quantum harmonic oscillator we have a relation

$$\hat{a}_k|\psi_0\rangle = 0, \quad \forall k. \tag{4.1.1}$$

Where the $\hat{a}_k$ are the ladder operator in the mode k. The ψ_0 is the ground state of the Hamiltonian defined in Eq. (2.1.19). By substituting this into the Schrödinger equation we can find the zero point energy as

$$E_0 = \frac{1}{2}\hbar\omega. \tag{4.1.2}$$

The quantum electromagnetic field in a vacuum can be represented by an infinite number of quantum harmonic oscillators and the zero energy state by the tensor product of the ground states of all modes, k. This can be written as:

$$\psi_0 = \psi_{k1} \otimes \psi_{k2} \otimes ..... \tag{4.1.3}$$

Thus, we can find the ground state energy of that field from the Hamiltonian operator as

$$E_0 = \langle \psi_0 | H | \psi_0 \rangle = \frac{1}{2} \sum_k \hbar \omega_k = \langle H_{vac} \rangle. \tag{4.1.4}$$

One can see that the above series is divergent for infinite k number

$$\frac{1}{2} \sum_k \hbar \omega_k \to \infty. \tag{4.1.5}$$

But this should not bother us in the experimental perspective as in the framework of quantum mechanics only differences of energies are measurable so that the vacuum energy is impossible to measure. However, for the theoretical importance, there are some renormalization procedure that treat this problem [72, 73]. For instance, in the relatively recent publication by Hizhnyakov et al , an argument is presented about the possibility to counterbalance the energy density of the vacuum by the negative gravitational energy of Plank scale quantum fluctuation [74].
Additionally, the expectation value of electric field is zero, however, the expectation value of E^2 is written as

$$\left\langle a_k^\dagger a_k \middle| E^2 \middle| a_k^\dagger a_k \right\rangle = \frac{\hbar \omega_k}{\varepsilon_0 V} (n_k + \frac{1}{2}). \tag{4.1.6}$$

This result already shows that an arbitrary vacuum field has non-zero intensity which is called vacuum fluctuation.

To derive the value of the zero energy, first we assume that the cavity has large dimensions so we can have a continuum approximation for the allowed values of k. Furthermore, we assume that the density of the modes is $\rho(k) = 2V/\pi^3$ (factor 2 for the two possible polarizations channel). Then the zero point energy density is written as [75, 68]

$$E_0 = \frac{2}{V} \sum_{k=1}^{k_c} \frac{1}{2} \hbar \omega_k \approx \frac{2}{V} \frac{1}{8} \int \frac{1}{2} \hbar \omega(k) \rho(k) d^3k. \tag{4.1.7}$$

The sum is over all positive k and multiplied by the number of possible polarizations as it was mentioned in section 2.1. Additionally, each wave-vector k has three components in the Euclidean space. The integral is the approximation of the sum over the positive octant (hence the factor 1/8 is induced). Substituting $\omega(k) = kc$ and $d^3k = 4\pi\, k^2 dk$ in Eq. (4.1.7) we obtain

$$E_0 = \frac{2}{V}\frac{2V}{\pi^3}\frac{4\pi}{8}\int_{k=0}^{k_c}\frac{1}{2}\hbar k^3 c\, dk = \frac{c\hbar}{2\pi^2}\int_{k=0}^{k_c} k^3 dk = \frac{\hbar c k_c^4}{8\pi^2}. \tag{4.1.8}$$

The cutoff wave-vector set to be $k_c = \omega_c/c$ [76]. One can notice the factor k_c^4 in Eq. (4.1.8) which indicates that the energy density is mainly in the high-frequency and equivalently in the short-wavelength modes. With a minimum wavelength $\lambda_c = 2\pi/k_c = 0.4 \times 10^{-6}$m, for the visible light spectrum, Eq. (4.1.8) yields a zero-point energy density of $23\mathrm{J/m}^3$.

One way to calculate the zero point energy is to consider a gravitational energy package. We have the plank constants for length $l_p = \sqrt{\hbar G/c^3} = 1.61 \times 10^{-35}$m, time $t_p = l_p/c = 5.39 \times 10^{-44}$ sec and energy

$$E_p = \sqrt{\frac{hc^5}{G}} = 1.22 \times 10^{19}\mathrm{GeV}. \tag{4.1.9}$$

Of course it is impossible to extract any of the zero-point energy, since it is the minimum possible energy of the field, and so our inability to perceive that large energy density is not incompatible with its existence. .
Indeed, since all experiments in the domain of physics detect only energy differences, and not absolute energies, it is often suggested that the troublesome zero-point energy of the field should simply be omitted.
One might even think that this energy is only a constant background to every experimental situation, and that, as such, it has no observable consequences. In contrast to this view, one of the main consequences of vacuum energy theory is the concept of Casimir force and effect. To observe this effect two requirements should be fulfilled. The first is the presence of vacuum fluctuation. Second we need to implement some sort of boundaries(for instant plates) that contain and separate the vacuum electromagnetic field in some part of space. The Casimir force is a direct measurable result of vacuum energy and can be observed as a force between two uncharged conducting plates. Here, we outline the derivation of Casimir force from the zero energy of vacuum. In order to have some view about the magnitude of the zero point energy, we can calculate the zero point energy in a cubic cavity with the $L \times L \times L$ size and from that obtain the existent force. There is also a plate placed close to one of the walls of the cavity. This simple setup is shown in Fig.4.1.1 Now, one can calculate the zero point energy at each point of the system. The net energy will be the difference between the energy on the two sides of the plate

$$\delta E = E_p + E_{L-p} - E_L \tag{4.1.10}$$

where each energy can be calculated according to the Eq. (4.1.7). By mentioning the main assumptions, we skip the explicit derivation of δE . It is assume that the field modes have a frequency smaller than some cutoff ω_c. Also we use the Euler-Maclaurin formula for an infinite number of modes and finalize the derivation in equation [77]

$$\delta E = -\frac{\hbar c \pi^2 L^2}{720 a^3}. \tag{4.1.11}$$

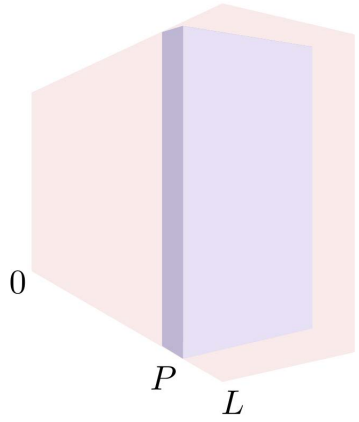

Figure 4.1.1: Sufficiently, large cavity, with a plate implemented inside, in distance P near the end of one side

Then the force at any point is the derivative of δE with respect to a, the distance between the plates

$$F(a) = -\frac{\partial \delta E}{\partial a} = -\frac{\hbar c \pi^2 L^2}{240 a^4}. \tag{4.1.12}$$

This force is very small but in a recent experiment it was finally observed [78, 79, 80] and it is a direct result of vacuum modes mismatch in space [75].

4.2 Dynamical Casimir effect

The essence of the dynamical Casimir effect is the amplification of vacuum fluctuation by time dependence of some parameters in the system. In general the time dependence corresponds to a change in the boundary conditions of the field. These changes in boundary conditions result in a new state in which virtual particles come to existence. The virtual photons created by such a procedure are often called Casimir light. This time dependent boundary conditions can be caused by fast moving mirrors or time dependent material properties. The time dependence of energy in this case can be modeled by adding the interaction Hamiltonian H_{int} to the Hamiltonian of the field H_0

$$H = H_0 + H_{int} = \sum_k \hbar \omega_k (\hat{a}_k^\dagger \hat{a}_k + \frac{1}{2}) + H_{int}. \tag{4.2.1}$$

The interaction Hamiltonian can then be approximated by an expansion of first

order and second order relations between the operators of the field $\hat{a}_k$ and system $\hat{b}_k$

$$H_{int} = f_1(\hat{a}_k\hat{a}_k^\dagger, \hat{b}_m\hat{b}_m^\dagger) + f_2(\hat{a}_k\hat{b}_m^\dagger, \hat{a}_k\hat{b}_m). \tag{4.2.2}$$

The second order function f_2 is responsible for the time dependence of eigenfrequencies [81]. They can cause the amplification of initial fluctuations if there are any. Thus, if we assume that there is a zero point fluctuation of the vacuum from the perspective of quantum physics, then these terms increase zero point fluctuations and possibly produce photons. The number of produced photons can be obtain from the following relation [82, 83]

$$n = \left\langle \hat{a}^\dagger\hat{a} \right\rangle = W\frac{R}{T}. \tag{4.2.3}$$

The terms W , R and T are determined by the solution of the quantum harmonic oscillator equation. T is considered as energy transmission and R is considered a reflection of the energy $\hbar\omega(t)$ for a potential well with frequency $\omega(t)$ between oscillators. The equation of motion for quantum harmonic oscillators is written as

$$\ddot{\zeta} = -\omega^2(t)\zeta. \tag{4.2.4}$$

Assuming after a time $\tau < t$ the frequency will be constant $\omega(t) = \omega_\tau$, one can find the solution for Eq. (4.2.4)as

$$\zeta(t > \tau) = \frac{1}{\sqrt{\omega_\tau}}[Ae^{-i\omega_\tau t} + A^* e^{i\omega_\tau t}]. \tag{4.2.5}$$

By knowing that solution one can determine the parameters T and R as

$$T = \frac{1}{|A|^2} \tag{4.2.6a}$$

$$R = |\frac{A^*}{A}|^2. \tag{4.2.6b}$$

In addition, the coefficient W is a function of initial thermal state and it takes the form

$$W = \coth(\frac{\hbar\omega_{int}}{2k_B\theta}). \tag{4.2.7}$$

The maximum possible photon creation can be obtain from the limitation imposed by Fresnel formula for R and the characteristic dimension of the cavity L . The time scale of the dynamical process should be fast enough that to be comparable with the period of the field oscillation [84]. Thus the maximum photon production is written as

$$n_{max} \simeq (\frac{\Delta L}{L})^2 \simeq (\frac{v}{c})^2 \tag{4.2.8}$$

where ΔL is responsible for a variation of the length and v is the velocity of the boundary compared to the velocity of light. Thus, for a rather high probability of photon production one needs to have a relativistic velocity of the boundary which makes the dynamical Casimir effect a relativistic process. There is also a solution to the Eq. (4.2.3) by considering a periodic function for frequency change as

$$\omega(t) = \omega_0[1 + 2gcos(2\omega_0 t)] \tag{4.2.9}$$

where $|g| \ll 1$ so the photon number can be obtained from

$$n = \sinh^2(\omega_0 g t). \tag{4.2.10}$$

The important parameter that verifies the possibility of photon production is the frequency variation amplitude [85, 86]

$$\Delta\omega = 2g\omega_0 \tag{4.2.11}$$

wherein, ω_0 is the frequency of created light. The frequency $2\omega_0$, the frequency of the mirror vibration, is the main challenge, as one needs a very high value for this frequency to observe the dynamical Casimir effect. However, the energy is conserved in such a process as the amount of energy that is used for moving of plate will be converted to photons. The amount of the energy and complexity of the process is not available in current technology. As the conduction layer of electrons reflects the electromagnetic field, most of energy gets lost in moving the body of the mirror.
One suggestion to overcome the mechanical difficulties in movement of the mirrors is to vibrate the mirror instead of moving it [87, 88], for example by acoustic waves [89]. This suggestion is also problematic[90]. For instant, to observe one or two photons in such a vibrating cavity is impossible as the high frequency, at least in the GHz range, of vibration diminishes the Q factor of the cavity [91]. Additionally, vibration inherently is moving an object with small amplitude and that results in a small oscillation speed which makes the Casimir light production hard to achieve [92]. Thus, there is no available technique to achieve the dynamical Casimir effect through mechanically moving objects. Search Results Nevertheless, one of the main reason that make Casimir light special, is the possibility to extract light from mechanical movement, the connection between the mechanical objects and quantum electromagnetic field.

To this end, there is only one known possible way to make a realistic set up to create Casimir light. Namely, one can imitate the oscillation of a mirror by making the optical properties of the boundary time dependent. As an example, there is a proposed scheme called motion-induced radiation or MIR experiment where we have a creation of particles, in this case plasma, by laser light shined on a semiconductor [93]. The moving plasma is assumed to behave similarly to the moving mirror and we can produce Casimir light. Similar to that experiment, there are processes which are often called parametric dynamical Casimir effect [81]. In Chapter 6, as an example for two photon generation by a nonlinear optical process, we propose a set up to produce two entangled photons from the parametric dynamical Casimir effect.

5 Cascaded systems 1: excitation via incoherently pumped TLS

Herein, we investigate the excitation of emitters inside a cavity by a specific single photon source. The physical system consists of two microcavities with two-level atoms inside them. The cavity itself consists of two parallel high Q mirrors. The mirrors reflect back the emitted photons from the TLS(s). In contrast to the emission in free space with a continuum of modes, TLS emit into a spectrum of discrete modes. In the current study, we consider a continues wave driving mechanism and exclude the pulse dynamics. The entire combined system is implemented inside a photonic waveguide which is chosen to be unidirectional. The unidirectionality of the waveguide is a requirement for the applicability of a cascaded formalism described in Chapter 3.
We consider two different scenarios for the coupling of the target emitters to the waveguide. First we consider a direct coupling of the target system's emitters, where the emitters are excited directly through the output of the source cavity. Secondly, we assume indirect coupling of the target system's emitters, where they are excited through the target cavity mode which is coupled to the source cavity mode via the waveguide. A simple schematic of these two scenarios is depicted in Fig.5.1.1. We are interested in the steady-state properties of the system, such as the photon statistics of cascaded cavities that can be measured in any future experimental setups in this limit. Besides, as a scheme to control the quantum system, it is a matter of relevance to manipulate the output of the second cavity in the steady-state boundary. By governing the steady-state density matrix ρ_s of a quantum system, hypothetically from a master equation, one can have sufficient information about the behavior of the system in this limit. In this chapter, we start with the investigation of the photon statistics of the source system for a range of different incoherent pumping strengths. Then we provide a formalism for cascaded cavities. We show that, in the direct coupling scenario, we can access to new photon statistics. Finally, we investigate the indirect coupling case and introduce a platform for the quantum statistical control of the target cavity.
Part of this chapter has been published recently in Physical Review A [94] and also part of it is in preparation for submission.

For notational convenience from now on, we omit the symbol($\hat{}$) because there is no more source of potential confusion between operator like and vector like objects.

5.1 Quantum statistics of incoherently pumped TLS

Although, we limit ourselves to only one type of quantum light source, still, it is interesting to examine its quantum dynamical behavior. Specifically, as we have direct control of the incoherent pumping, we want to see how the photon statistics of such a source evolves due to changes in pump strength. On the other hand, it is important to discern the behavior of the source cavity when it is in the weak or moderate coupling regimes. Additionally, to frame the formalism of the cascaded system, we need to explore the quantum dynamics of the source cavity.
Borrowing the concept of source and target in previous studies [33, 30, 32, 30], the first cavity is a source cavity driven by incoherent light. Inside this cavity, there is an archetypal two-level atom included. The incoherent pump interacts with the cavity mode via the electric dipole. The role of excitation of the two-level atom inside the source cavity is the production of anti-bunched, fully quantized light. This is the typical Jaynes-Cummings system that has been always a subject of interest in cavity QED. Through incoherent pumping mechanism, one can conveniently control the photon statistics of the output field. By adjusting the incoherent pumping, one can achieve coherent, thermal or quantum light as an output. One should bear in mind that by pumping incoherently, we are able to observe the performance of the source as a function of the pump strength. Following the tradition, the full dynamics of the source cavity can be obtained through the master equation formalism. For the incoherently driven source cavity, we substitute the noise term (here coupling term to the waveguide) Γ_s with Γ_p which represents the incoherent pumping strength. For the source cavity, the conventional Jaynes-Cumming Hamiltonian is applied here. Giving the fully quantized treatment and applying the rotating wave approximation, we have the following interaction Hamiltonian in the rotating frame

$$H_s = \hbar g_s(a_s^\dagger \sigma_s^- + \sigma_s^+ a_s) \tag{5.1.1}$$

where a_s ($a_s^\dagger$) is the corresponding annihilation (creation) operator with the commutation relation $[a_s, a_s^\dagger] = 1$. The cavity is coupled with the coupling strength g_s to a TLS.
For a perfect resonance between cavity mode and emitter, the cavity detuning Hamiltonian $H_{\Delta c}$ is zero. On the other hand, in the off-resonant regime, the cavity detuning reads $H_{\Delta c} = \Delta_c a^\dagger a$ where $\Delta_c = \omega_c - \omega_{field}$ and one should it to the system Hamiltonian. In this case, the system Hamiltonian will be $H_S = H_{JC} + H_{\Delta C}$. The full master equation for the source cavity with a two-level system inside reads

$$\begin{aligned}\frac{\partial}{\partial t}\rho\,|_s &= -i\,[H_s, \rho] + \Gamma_s^P(2\sigma_s^+\rho\sigma_s^- - \sigma_s^-\sigma_s^+\rho - \rho\sigma_s^-\sigma_s^+) \\ &\quad + \kappa_s(2a\rho a^\dagger - a^\dagger a\rho - \rho a^\dagger a) + \Gamma_r^s(2\sigma_s^-\rho\sigma_s^+ - \sigma_s^+\sigma_s^-\rho - \rho\sigma_s^+\sigma_s^-)\end{aligned} \tag{5.1.2}$$

where Γ_s^Pstands for incoherent pumping strength, κ_s cavity dissipation rate and Γ_r^s represents the radiative decay of emitter. For different boundary conditions, there

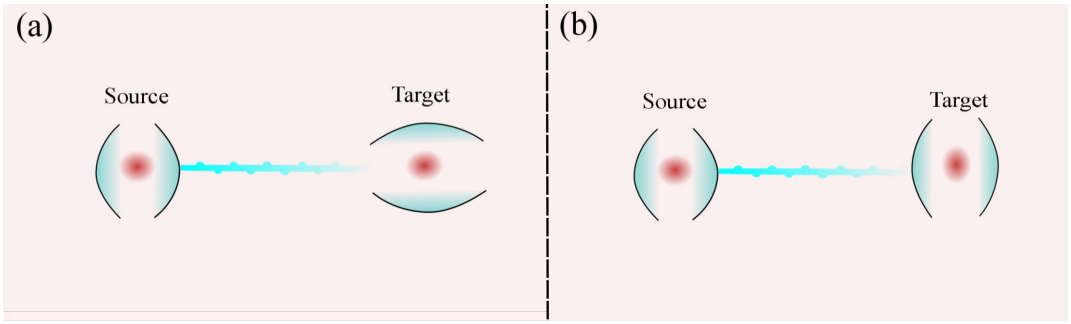

Figure 5.1.1: Simple schematic of two systems coupled unidirectionally via a waveguide(pink rectangle). (a) The direct coupling of emitters in target cavity to the output of the source cavity. (b) The indirect coupling of emitters in target cavity to the output of the source cavity, coupling between cavity's modes. The unidirectionallity allows for transport of excitation from a source system to target system but not vice versa. The waveguide is considered to be a thermal bath described by boson creation and annihilation operators $b^{\dagger}(\omega), b(\omega)$ in our formalism.

are analytical and numerical solutions to Eq. (5.1.2) that gives the density operator ρ or for a steady-state solution ρ_s. To inspect the dynamic of our quantum system rigorously, first, we analyze the Fock state distribution and Wigner function. As a matter of fact, these Fock states constitute the Hilbert space for further observables of the system so it is important to see how these state functions are distributed. The Fock state distribution can easily be obtained from the relation

$$P(n) = \langle n \left| \rho_s \right| n \rangle \,. \tag{5.1.3}$$

Furthermore, the Wigner quasiprobability distribution can help us to recognize the transition between classical and quantum states of light. It is a quantum counterpart of phase space distribution in the classical world which is represented in complex space. It has been shown that for a density matrix ρ, a consistent analytical solution for P representation and Wigner function Wcan be achieved and later can be written as [95]

$$W(\alpha) = 2Tr\left[\hat{D}(-\alpha)\rho\hat{D}(\alpha)\exp(i\pi\, a_s^{\dagger}a_s)\right] \tag{5.1.4}$$

where α is the complex field amplitude and the displacement operator $\hat{D}$ corresponds to the generation of coherent state from vacuum state $|0\rangle$ which can be written as $\hat{D}(\alpha) = \exp(\alpha a_s^{\dagger} - \alpha^* a_s)$. In some literature the exponential part of Eq. (5.1.4) is referred to as parity operator $\hat{P} = \exp(i\pi\, a_s^{\dagger}a_s)$ [96, 97]. The higher peak in the Wigner function shows the higher probability of excitation of vacuum state,$|0\rangle$. By procurement of ρ_s one can compute two quasiprobability distributions, Fock and Wigner that we cited in the previous chapter. Such a result is shown in Fig. 5.1.2

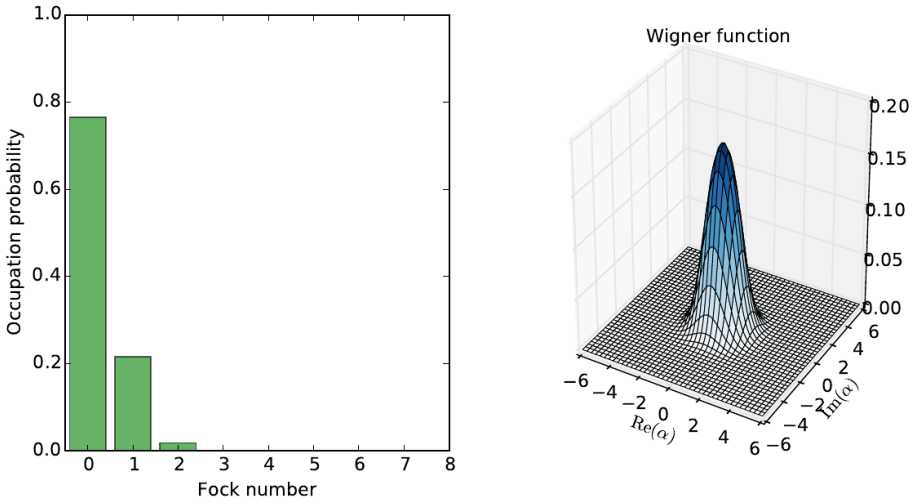

Figure 5.1.2: Fock state distribution and Wigner function for the moderate inter-cavity coupling regime of the source cavity. The incoherent pumping strength is fixed at incoherent pumping strength $\Gamma_s^P = 0.05$

for moderate intra-cavity coupling regime of the source. For the moderate coupling regime, the incoherently pumped source shows a higher probability of producing a photon at weak pump strengths Fig. 5.1.2 (a).

To show the dynamics of the source cavity, the spectrum and the two-time correlation function of the source for a fixed incoherent pump strength are computed. The two-time correlation function of the source cavity mode can be described as $\langle a_s(t+\tau)a_s(t)\rangle$. Given a correlation function for the source cavity in a steady-state limit, $\langle a_s(\tau)a_s(0)\rangle$, one can subsequently define the power spectrum as

$$S(\omega) = Re[\int_0^\infty \left\langle a_s^\dagger(\tau)a_s(0)\right\rangle e^{i\omega\tau}d\tau]. \tag{5.1.5}$$

This correlation function and its corresponding power spectrum for different values of g_t is represented in Fig.5.1.3. The well-known Mollow triplet can be seen in the strong intra-cavity coupling regime. When the intra-cavity coupling g_s decreases the interaction of the cavity field with matter is not strong enough to dress the states of the atom.Consequently, the satellites of triplet resolves to the central line. This behavior is typical signature of the Jaynes-Cummings model. The two-time correlation function of the source cavity indicates that the source system reaches the steady-state regime. Thus, to approximate that the system is stationary is validated by this result.

5.2 Direct coupling to the target emitter(s)

In the open quantum systems scheme, each cavity in this arrangement can be perceived

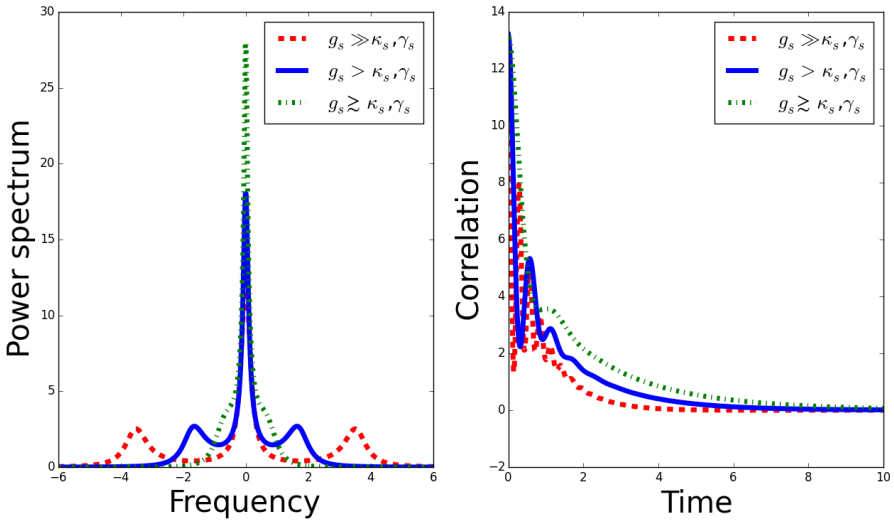

Figure 5.1.3: Power spectrum and two-time correlation functions of the output field from the source cavity for different cavity coupling strength g_s. The time considered here is τ in Eq. (5.1.5). By decreasing the coupling strength, the behavior of power spectrum develops from Mollow triplets to a central line spectrum. The parameters are $\kappa_s = 0.1$ ps^{-1} , $\gamma_s = 0.02$ ps^{-1} , $g_s = 6$ ps^{-1}(red) , $g_s = 3$ ps^{-1}(blue) and $g_s = 1.5$ ps^{-1}(green) . The incoherently pumping strength is fixed at $\Gamma_s^P = 5$ ps^{-1}.

as a system and the unidirectional waveguide plays the role of environment or bath. Thus, the dynamics of the system can be formalized as a source-target pairing or cascaded source and target [35]. From analyzing the source of quantum light, one can move forward and add the target cavity to the entire open quantum system. Coupled to the source cavity, the target cavity can then have different configurations. Mutually, both target and source are assumed to be two-sided cavities where one can have input and output fields in two directions.

One generic assumption for such a system is that the source cavity will not be influenced by the target system so the coupling is unidirectional. In practice, this is feasible by the implementation of a unidirectional waveguide, wherein the output field from the source reaches the target without allowing any reflection, a topological photonic structure. Additionally, we assume for TLS(s) in both cavities to be in perfect resonant with one mode of the cavities: only one mode of the cavities is in resonate with the energy levels of the TLS(s).

Traditionally, in the realm of asteady-state apparatus, three physical parameters determine the coupling regime of the cavity. These parameters are the cavity coupling strength g_i, cavity dissipation rate κ_i and atomic decay rate γ_i. The relation between these parameters shows whether photon creation is reversible or not. If we have $C_i = g_i^2/\kappa_i\gamma_r^i \gg 1$, with the cooperativity, C_i, and $i = s, t$ corresponds to the source

and target cavities respectively, then the spontaneous emission and absorption process of a photon in the cavity is reversible, the atom-cavity coupling is stronger than dissipation rates, and thus we are in the strong coupling regime. In contrast, when $C_i = g_i^2/\kappa_i\gamma_r^i \ll 1$ the atom-cavity coupling is weaker than the dissipation rates and the weak coupling regime rules the dynamics of the cavity.
Throughout this thesis, we encounter two cavities and thus the influential dynamical parameters are doubled. The main difficulty for such a study lies in the fact that there are many parameters, which are the elements of the dynamics of the source or target, that can influence the outcome of the coupled system. Herein we assume that

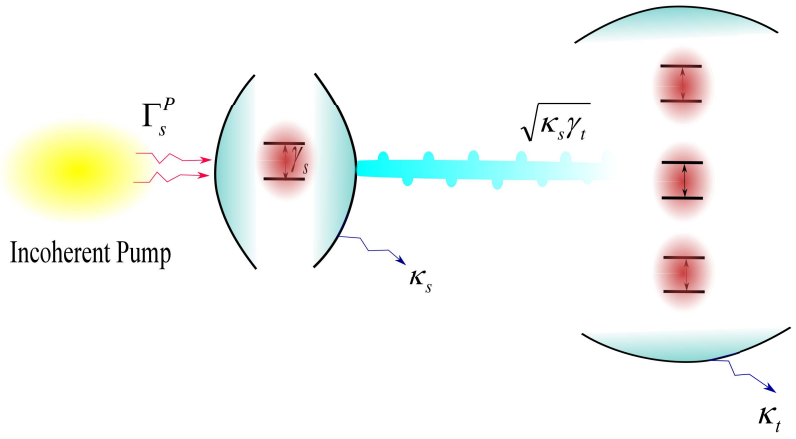

Figure 5.2.1: Different configurations for the target cavity excitation. The source cavity with aTLS inside is pumped incoherently wuth rate Γ_s^P. The source and the target cavity are implemented in the unidirectional waveguide. The main physical parameters of both source and target cavities are presented.

the source and target cavities stay in the weak and moderate intra-cavity coupling regimes. This is due to the fact that, an incoherently pumped cavity with a TLS has more quantum mechanical features in these regimes [98]. This assumption is also in line with the physicality of the target cavity, as exciting a long-lived target is unlikely [27].
Each coupling regime, whether weak, moderate or strong, generates different effects. In a weak coupling regime, we have the modification of the atomic energy levels whereas in the stronger coupling regimes there is a constant exchange of energy between atoms and cavity fields. To observe larger nonlinear influence of the cascaded quantum system , we consider various TLS configurations inside the target cavity as three scenarios.

An essential assumption for the source-target cavity setups is the absence of direct interaction between TLSs. The simplified schematic of such configurations is represented in Fig. 5.2.1. This system is very different from the usual cascaded cavity, because here the target emitters are directly coupled to the waveguide. Therefore, the only function of the target cavity is to enhance interactions between the light mode and the target emitters. By exciting the two-level system in the source cavity, we transform the harmonic ladder of energy into the Jaynes-Cumming type and subsequently produce the desired quantum light. For the target cavity arrangements with many TLSs, one should notice that the only way that these two-level systems communicate is through cavity modes and no direct interaction between them is considered here. This gives the cavity modes the role of mediator that we discuss later in the following section. These setups can also be seen as a way to directly control the dynamics of a quantum system with another quantum system. In the absence of feedback, there are two ways of control. Firstly, by changing the incoherent pumping strength of the source which changes the output field of the source cavity. This output field can be seen as an input for the target system and causally changes the behavior of the target system. Secondly, one can adjust the physical parameters of both cavities and observe the changes in the output photon statistics of the entire combined system.

5.3 Quantum cascade model: Master equation

To investigate the influence of the output light from the source cavity on the target cavity we need to understand the dynamics of cascaded quantum systems.

We will consider systems, as illustrated in Fig. 5.2.1 , where an incoherently pumped source cavity containing a two level system (TLS) as emitter will serve as the source of nonclassical light. This emitted light will be fed via a unidirectional waveguide into the emitters contained in a second cavity. All cavities and emitters are subject to incoherent decay processes. i.e. a source quantum system with Hamiltonian H_s coupled via a thermal bath, H_c to the target quantum system H_t. The basis of our analysis will be a Hamiltonian formulation of the problem, from which we derive a master equation in the Born-Markov limit [27, 33, 32, 30]. The full Hamiltonian reads

$$H = H_0 + H_s + H_c + H_t \tag{5.3.1}$$

where H_0 represents the free evolution dynamics of all quantities which belong to the total system. At this point, we take the H_s and H_t in general form and do not specify them. Instead, we focus on the coupling Hamiltonian H_c to derive the coupling part of general master equation. It can be represented as

$$H_{\rm c} = \hbar \int d\omega \omega b^\dagger(\omega) b(\omega) + \hbar \int d\omega \Big[K^s(\omega) J_s^\dagger b(\omega) + K^t(\omega) J_t^\dagger b(\omega) e^{i\omega\tau} + h.c. \Big]. \tag{5.3.2}$$

The waveguide consists of a continuum of modes, where each mode with frequency ω has an annihilation (creation) operator $b(\omega)$ ($b^\dagger(\omega)$). In a rotating frame which corresponds to H_0, and by applying the rotating wave approximation H_c in it's compact form is

$$\frac{H_{\rm c}}{\hbar} = \int d\omega \; b(\omega) \Big[K_\omega^s J_s^\dagger(t) + K_\omega^t J^\dagger(t,\tau) \Big] + \text{H.c.}, \tag{5.3.3}$$

where τ stands for a finite time delay between the target and source system and J_s, J_t describe a general operator or a superposition in the source and target system, that will be defined in the following subsection explicitly. We are using the second approach presented in chapter 3 in the Table.3.3.1. The term $K_\omega^{s/t}$ is the coupling ratio of the source or target system to the connecting waveguide. Following the second approach in Table.3.1, we assume that $K_\omega^{s/t}$ is independent of the frequency in the narrow bandwidth limit (very narrow connection between system and bath) $K_\omega^{s/t} \equiv K_0^{s/t}$.
For the derivation of the master equation of the quantum cascaded system, we employ the canonical method in the Born-Markov limit. The Born approximation allow us to factorize the density matrix of the whole setup to system and bath part resulting in: $\chi_{\rm tot}(t) = \rho(t)\rho_B(0)$, where ρ_B is the time independent density operator of the bath. By assuming that the coupling reservoir is in equilibrium and in a thermal state we obtain [56, 66]

$$\left.\frac{d\rho}{dt}\right|_c = -\frac{1}{\hbar^2} \int_0^t ds \text{Tr}_B \left\{ [H_{\rm c}(t), [H_{\rm c}(s), \rho(t)\rho_B]] \right\}. \tag{5.3.4}$$

Following the derivation method of the master equation discussed in chapter 3 for a damped quantum system, we transfer the coupling Hamiltonian in Eq. (5.3.4) to the summation formula

$$H_c/\hbar = \sum_{l=1}^{M} \sum_{k=1}^{N} f_{l,k}(t) \Gamma_{l,k}(t) \tag{5.3.5}$$

where M and N depend on the number of emitters in the target system. $f_{l,k}(t)$ represent the source and target time dependent bosonic operator and $\Gamma_{l,k}(t)$ is a compact form for the bath operator. Now substituting Eq. (5.3.5) into the Eq. (5.3.4), one can reformulate it as

$$\frac{\partial \rho}{\partial t} = -\frac{1}{\hbar^2} \sum_{l,k} \int_0^t ds \, Tr_B \left\{ f_l(t)\Gamma_l(t), [f_k(s)\Gamma_k(t), \rho(t)\rho_B] \right\} . \tag{5.3.6}$$

By applying the cyclic property of trace two important terms in the master equation appear. These are the bath correlation functions and can be described as

$$\langle \Gamma_l(t)\Gamma_k(s)\rangle_B = tr_B\left[B\Gamma_l(t)\Gamma_k(s)\right] \tag{5.3.7a}$$
$$\langle \Gamma_k(s)\Gamma_l(t)\rangle_B = tr_B\left[B\Gamma_k(s)\Gamma_l(t)\right]. \tag{5.3.7b}$$

One can assume the thermal bath to be flat , to be in vacuum state, and consider only bath contributions proportional to $\langle b(\omega)b^\dagger(\omega)\rangle$.
Following the usual procedure, but keeping track of all couplings, here, tr_B is the trace over all bath modes. Inserting Eq. (5.3.7)(a-b) into Eq. (5.3.6) and using the cyclic property of the trace, we get several terms with different combinations of system- and bath-operators. Assuming a time independent bath in the vacuum state allows to neglect terms with $b(\omega)^2$ and $b^\dagger(\omega)^2$ (the secular approximation), as well as terms, where $b(\omega)$ acts first on the density matrix. Also, in chapter 3, we have shown that for the bath operators one can obtain canonical commutator relations as $[b(\omega), b^\dagger(\omega')] = \delta(\omega-\omega')$. By applying these conditions, the double commutators can be evaluated.Thus we will have the series of relations

$$\left\langle \Gamma_{k,l}, \Gamma_{k,l}\right\rangle_B = \left\langle \Gamma^\dagger_{k,l}, \Gamma^\dagger_{k,l}\right\rangle_B = 0. \tag{5.3.8}$$

This originates from the time causality that we stated in chapter 3. So the only parts of Eq. (5.3.6) that remains will include the noise relations $\left\langle \Gamma_{k,l}, \Gamma^\dagger_{k,l}\right\rangle_B$ and can be written in the explicit recipe. By recognizing these assumptions and tracing out the bath degrees of freedom, one gets the following master equation

$$\begin{aligned}
\left.\frac{d\rho}{dt}\right|_c &= -2\pi \sum_{i=s,t} (K_0^i)^2 \int_0^t ds\delta(s-t) \\
&\times \left[J_i^\dagger(t)J_i(s)\rho(s) - J_i(t)\rho(s)J_i^\dagger(s) - J_i(s)\rho(s)J_i^\dagger(s) + \rho(s)J_i^\dagger(s)J_i(t)\right] \\
&- 2\pi K_0^s K_0^t \int_0^t ds\delta(s-(t-\tau)) \\
&\times \left[J_t^\dagger(t)J_s(s)\rho(s) - J_t(t)\rho(s)J_s^\dagger(s) - J_s(s)\rho(s)J_t^\dagger(t) + \rho(s)J_s^\dagger(s)J_t(t)\right] \\
&- 2\pi K_0^s K_0^t \int_0^t ds\delta(s-(t+\tau)) \\
&\times \left[J_s^\dagger(t)J_t(s)\rho(s) - J_s(t)\rho(s)J_t^\dagger(s) - J_t(s)\rho(s)J_s^\dagger(s) + \rho(s)J_t^\dagger(s)J_s(t)\right].
\end{aligned} \tag{5.3.9}$$

We take into account that $\int_0^t ds\delta(t-s)h(s) = h(t)/2$ and that $s \le t$. Also by the first Markov approximation we have $K_0^i = \sqrt{\gamma_i/(2\pi)}$, where γ_i are the decay rate of the subsystems that couple source and target. The Markovian process is based

on the decay of bath properties and Eq. (5.3.5)(a-b) can be estimated as a delta distribution $\delta(t-s)$. This is based on that the time scales of the system are slower than that corresponding to the noise terms [36]. The emerging time delay in the interaction is characteristic of the cascaded system, as the term with $\delta(t-s+\tau')$ does not contribute, excluding the backaction of the target on the source. Thus, one coupling contribution between target and source vanishes. The full master equation in the Born-Markov limit reads

$$\begin{aligned}\frac{d\rho}{dt} &= \frac{1}{i\hbar}[H_s + H_t, \rho] \\ &\quad + \sum_{i=s,t} \frac{\gamma_i}{2}\left(2J_i(t)\rho(t)J_i^\dagger(t) - \{J_i^\dagger(t)J_i(t), \rho(t)\}\right) \\ &\quad - \sqrt{\gamma_s\gamma_t}\left(J_t^\dagger(t)J_s(t_D)\rho(t_D) - J_t(t)\rho(t_D)J_s^\dagger(t_D)\right) \\ &\quad - \sqrt{\gamma_s\gamma_t}\left(\rho(t_D)J_s^\dagger(t_D)J_t(t) - J_s(t_D)\rho(t_D)J_t^\dagger(t)\right), \end{aligned} \tag{5.3.10}$$

with $t_D = t - \tau$ indicating that the terms with time beyond the limitation of integral vanish. Furthermore, in the current setup, the delay τ is small compared to the time integral limitation. Thus, one can set $\tau = 0$ without violating the Markovian approximation. Transforming back from the rotating frame, the coupling part of the master equation reads

$$\begin{aligned}\frac{d\rho}{dt} &= \frac{1}{i\hbar}[H_0 + H_s + H_t, \rho] \\ &\quad + \sum_{i=s,t} \frac{\gamma_i}{2}\left(2J_i\,\rho J_i^\dagger - \{J_i^\dagger J_i\,, \rho\}\right) \\ &\quad - \sqrt{\gamma_s\gamma_t}\left([J_t^\dagger, J_s\rho] + [\rho J_s^\dagger, J_t\,]\right). \end{aligned} \tag{5.3.11}$$

The first term describes the coupling from the source cavity and the target emitters into the waveguide, where no excitation is exchanged. The second term describes the interaction exchanging excitation, which, due to our assumptions, may only take place from the source to the target. Given this result, we can investigate different kinds of systems and study the particular features of a quantum cascaded driving. The coupling coefficients γ_s and γ_t contain the integrals over the bath modes, and become time independent in the Markovian limit.

5.3.1 Full master equation: Derivation of source-target coupling

So far we have derived a general master equation for the coupling of the source system to the target system. As an example, the specific setup illustrated in Fig. 5.2.1 is considered. Now, in order to investigate the dynamics of this setup we derive a full master equation. Starting from the source system, a single emitter in the cavity, we have the Jaynes-Cummings model in the interaction picture as it is described in Eq. (5.1.1).

In this setup we have three emitters in a cavity as a target system. Thus, one can describe the Hamiltonian of the target system in the interaction picture by the Tavis-Cummings Hamiltonian of the cavity which contains N TLSs

$$H_{\mathrm{t}} = \hbar \sum_{j=1}^{N} g_{j,t} \left(a_t^{\dagger} \sigma_{j,t}^{-} + \sigma_{j,t}^{+} a_t \right), \tag{5.3.12}$$

where $N = 3$ for three emitters.
For the free part of the Hamiltonian, one can write H_0 in a compact form for the source and target together

$$H_0 = \hbar\omega_0 \sum_{i=s,t} a_i^{\dagger} a_i + \hbar\omega_e (\sigma_s^{+}\sigma_s^{-} + \sum_{i=1}^{N=3} \sigma_{t,i}^{+}\sigma_{t,i}^{-}). \tag{5.3.13}$$

The first term is the free energy of the cavity mode, where ω_0 is the resonance frequency of the source cavity and a_i ($a_i^{\dagger}$) is the corresponding annihilation (creation) operator with the commutation relation $[a_i, a_i^{\dagger}] = 1$.The second term is the free energy of the TLS, which is in resonance with the cavity mode and is described by the spin flip matrices σ_s^{+} (σ_s^{-}). They obey the commutation relation $[\sigma_s^{-}, \sigma_s^{+}] = 2\sigma_z$, where σ_z is the third Pauli matrix. As we assume the cavity mode to be at the atomic resonance $\omega_e = \omega_0$. In the following, we will assume, that all emitters are in resonance with the source cavity and that all couplings are equal $g_{i,t} = g_t$ for all i. In the first step, H_s and H_t transfers are transformed into the interaction picture using the unitary transformation $U = \exp(i\xi t)$ with

$$\xi = \omega_0 (a_s^{\dagger} a_s + \sigma_s^{+}\sigma_s^{-} + a_t^{\dagger} a_t + \sum_j \sigma_{j,t}^{+}\sigma_{j,t}^{-}) + \sum_j \int d\omega \omega b_j^{\dagger}(\omega) b_j(\omega). \tag{5.3.14}$$

This removes all the terms not describing any interaction.
Following the formalism in section 5.3, now we are able to define explicitly the operator J_s,J_t. The coupling operator of the source system to the bath is assigned to be $J_s = a_s$. Also, the coupling operator of the target system is $J_{i,t} = \sigma_{i,t}$. This definition indicates that there is no superposition between target emitters and they are directly and separately connected to the source system.

To describe additional incoherent processes such as the radiative decay of the emitters, further terms are needed. This is done via Lindblad terms. For this, we define the Lindblad operator as follows. For the incoherent pumping mechanism of the source cavity we have [99, 100]

$$\mathcal{L}[\sqrt{\Gamma_s^P}\sigma_s^{+}]\rho := \Gamma_s^P \left(2\sigma_s^{+}\rho\sigma_s^{-} - \{\sigma_s^{-}\sigma_s^{+}, \rho\} \right). \tag{5.3.15}$$

Additionally, for the source and target, we have atomic radiative decay which can be presented as

$$\mathcal{L}[\sqrt{\gamma_\beta}\sigma_\beta^{-}]\rho := \Gamma_r^\beta \left(2\sigma_\beta^{-}\rho\sigma_\beta^{+} - \{\sigma_\beta^{+}\sigma_\beta^{-}, \rho\} \right). \tag{5.3.16}$$

Where $\beta = s, t$. Finally the Lindblad operator for cavity dissipation rate reads

$$\mathcal{L}[\sqrt{\kappa_\beta}a_\beta]\rho := \kappa_\beta \left(2a_\beta \rho a_\beta^\dagger - \{a_\beta^\dagger a_\beta, \rho\}\right). \tag{5.3.17}$$

As it has been mentioned previously, the formalism for such a system follows from the theory of open quantum systems. We extend the previous master equation for the source cavity and include Liouvillian superoperator responsible for the coupling contributions to the environment and target system dynamics. Thus, the full master equation is a summation of three superoperators

$$\frac{d\rho}{dt} = L\rho = (L_s + L_c + L_t)\rho. \tag{5.3.18}$$

Where $L_s$is similar to the Eq. (5.1.2) except that we transfer the cavity dissipation part of L_s to the environment coupling superoperator. The formalism for two superoperators L_c, L_tvaries for different target systems. With this, the total master equation becomes

$$\begin{aligned}\frac{d\rho}{dt} &= \frac{1}{i\hbar}[H_0 + H_s + H_t, \rho] \\ &+ \mathcal{L}[\sqrt{\Gamma_s^P}\sigma_s^+]\rho + \mathcal{L}[\sqrt{\gamma_s}\sigma_s^-]\rho + \mathcal{L}[\sqrt{\kappa_s}a_s]\rho \\ &+ \mathcal{L}[\sqrt{\kappa_t}a_t]\rho + \sum_{i=1,2,3}\mathcal{L}[\sqrt{\gamma_t}\sigma_{t,i}^-]\rho \\ &- \sqrt{\kappa_s\gamma_t}\sum_{i=1,2,3}\left([\sigma_{t,i}^+, a_s\rho] + [\rho a_s^\dagger, \sigma_{t,i}]\right).\end{aligned} \tag{5.3.19}$$

In this final master equation, the first term is the Hamiltonian evolution of source and target. The second term gives the incoherent pumping with Γ_p, then the radiative decay of the source emitters, the decay of source and target cavity, the decay of the target emitters and the interaction between source cavity and target emitters follow subsequently. To characterize the cascaded driving, we choose first a specific system and then propose the photon-photon correlation functions as a measure for coherence in the system.

5.3.2 Cascaded system – influence on the target

In the following subsection, we consider the source cavity to produce a certain light statistics as its output, which will be fed into the target emitters as input. We will characterize source and target by the cooperativity C_β, which indicates whether the photon spontaneous emission is reversible in each cavity: In case of $C_\beta \gg 1$, the photon number shows long lived oscillations, while for $C_\beta \ll 1$, dissipation dominates the dynamics of the cavity mode.

Furthermore, we will focus on the cases of one to three emitters in the target cavity. The reason for possible additivity between emitter's atomic operators is coming from the fact that there is no direct coupling between them. In the presence of coupling

between emitters, the additivity in Eq. (5.3.19) fails and each term should be treated separately in the master equation formalism. The current formalism is also applicable for such a case. There is no available analytical solution for Eq. (5.3.19) such that the system of equations of motion can be constructed assertively. As a consequence, we implemented a numerical procedure, fourth-order Runge-Kutta algorithm for different values of Γ_s^P, to obtain the general density matrix ρ of the cascaded system.
The density matrix ρ is calculated in the composite Hilbert space of $\mathcal{H}$ with the basis

$$\langle e_s, p_s, e_t, p_t|\rho|e'_s, p'_s, e'_t, p'_t\rangle \tag{5.3.20}$$

where e_i are emitter states and p_i are photon manifold of source and target $i = s, t$. Similar to the target system analysis, one can obtain the steady state solution for the entire cascaded system. Subsequently, by assigning zero to the left-hand side of Eq. (5.3.19) and solving it results in a steady-state density matrix ρ_s. Besides Γ_s^P,all other physical parameters are fixed throughout sec 5.1. We set a cut-off for the fock states which constitutes the composite Hilbert space. Because of this photon manifold cut-off $p_i < N_i$, the expectation values of the considered observables do not change if we increase N_i. For the current setup we assign $p_i \leq N_i = 10$.

parameter	value (ps^{-1})
g_s	0.1
g_t	0.1
γ_s	0.02
γ_t	0.5
κ_s	0.1(0.4 for $C_s = 1.2$)
κ_t	0.005

Table 5.3.1: Parameters used for the cascaded setup throughout the section.

After showing the photon statistics for the bare source cavity in section 5.1, we will now show how the statistics of the target cavity may be influenced by the source and focus on the cases of one, two and three emitters. We consider their numbers of emitters in the parameter regime of interest and we see that only multiple emitters allow to produce quantum nonlinearities.
The output of the coupled cavities is depleted by the cavity loss of the target cavity. We consider two regimes for the intra-cavity coupling for both cavities. As it was mentioned above, these regimes can be distinguished by the cooperativity C_i. However, the physical parameters are not the same for both cavities, still, we can achieve the preferred cooperativity for them. First, we set the intra-cavity coupling strength of source and target equal:$g_s = g_t = 0.1$GHz. Note that the noise term in Eq. (5.3.19) for the target cavity, with rate γ_t, is responsible for the atomic decay rate of the TLSs, whereas, the TLSs are directly coupled to the bath. Another channel of decay is through cavity dissipation factor where the target cavity loses photon to the bath. Together with the intra-cavity coupling strength one can reformulate the cooperativity

as $C_t = g_t/\kappa_t\Gamma_t$. As an initial condition, we set $\Gamma_t = 0.5GHz$. Hence, κ_t should be chosen small enough, in fact much smaller than κ_s, that the coupling of the target cavity stays at a moderate level. Since quantum effects are more likely to be observed for C close to unity [98], we will study two cases. First, a weak intra-cavity coupling regime for the source and moderate regime for the target. Second, we assume that both cavities are in the moderate regime. Reciprocal values for the coopretivity are shown in table 5.3.1. $C_s = 5, C_t = 4$.The set of parameters in table 5.3.2 corresponds to these cases.

Scenario	Cooperativity	Inrra-cavity coupling regime
Case.1	$C_s = 1.2$ $C_t = 4$	Weak Moderate
Case.2	$C_s = 5$ $C_t = 4$	Moderate Moderate

Table 5.3.2: Two distinct cases for inter-cavity coupling regime of source and target.

As an important observable for the response of the target system, we can find the steady-state expectation value of the cavity photon number

$$\langle n \rangle = \left\langle a_i^\dagger a_i \right\rangle = Tr(\rho_s a_i^\dagger a_i) \qquad i = s, t \tag{5.3.21}$$

where a_i stands for the source and target cavity modes. As an example, for the weak intra-cavity coupling regime, the evolution of the expectation value of the cavity photon number as a function of pump rate Γ_s^p is plotted in Fig.5.3.1 The occupation probability of the photon decrease when the incoherent pumping strength increases. This is true for the source as well as for all the cases in the target cavity. The mechanism behind this decline can be understood through the noise terms with rates Γ_s^p (incoherent pumping strength) and $\sqrt{\kappa_s\gamma_t}$ (the coupling strength to the waveguide). These terms play a double-edged sword role. At the same time increase the probability to produce a photon by exciting emitters and also cause the loss of photons through coupling to the bath or waveguide. The corresponding formalism can be seen in the master equation (5.3.19) where the minus part and plus part plays as a protagonist in this paradoxical behavior. For larger pumping strength, the pumping mechanism adiabatically introduces dephasing which eliminates the emitter dynamics and the output field ends up in a thermal state [99, 101, 102].

This is a different process from the so called self-quenching where the photon number decreases as a function of pumping strength. In self-quenching phenomena, the physical process that causes this decline is the destruction of coherence between the TLS and the cavity modes by incoherent or electrical pumping [103, 104]. The important mechanism here is the mediator role of the target cavity modes between the TLSs. As there is no direct interaction between TLSs the only way that these systems exchange energy is through the cavity modes.

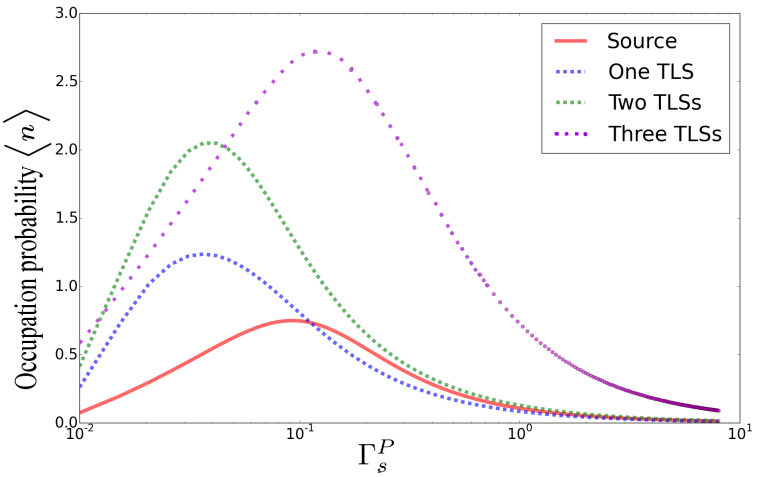

Figure 5.3.1: The evolution of photon number as a function of the source cavity incoherent pumping rate.

Another interesting pattern is that the probability of observing photons has a positive correlation with the number of emitters, i.e., if one increase the number of emitters in the target cavity the probability of finding photons in the target cavity also increases.

Another key observable of the system is the second-order correlation function which in its customary form can be presented as [76]

$$g^{(2)}_{\text{stat}}(\tau) = \lim_{t\to\infty} \frac{\left\langle a_i^\dagger(t) a_i^\dagger(t+\tau) a_i(t+\tau) a_i(t) \right\rangle}{\left\langle a_i^\dagger(t) a_i(t) \right\rangle^2}, \tag{5.3.22}$$

herein, the zero time delay $\tau = 0$, coincidence rates of two photon emission, is considered. Then, in this limit, the correlation function $g^2(\tau)$ can be reformulated as [105]

$$g^{(2)}(0) = \frac{\sum_{n=0}^{\infty} n(n-1)P(n)}{\left(\sum_{n=0}^{\infty} n\, P(n)\right)^2} \tag{5.3.23}$$

where n is the photon number and the probability of finding $n$photon is $P(n)$. Numerical evaluation of $g^{(2)}(0)$ for different incoherent pumping strength Γ_s^P is illustrated in Fig. 5.3.2.

One can see that in the antibunching regime, $g^{(2)} < 1$, for incoherently driving strengths of $\Gamma_s^P < g_s$, the source cavity acts as a single photon source.

The intra-cavity coupling of the source is not strong enough to produce more than one photon. Before the production of the second photon, the cavity dissipation forces the first photon to leave. This antibunching dynamics continues for a wide range of parameters until it starts to have a coherent behavior for pumping strengths $\Gamma_s^P > g_s$.

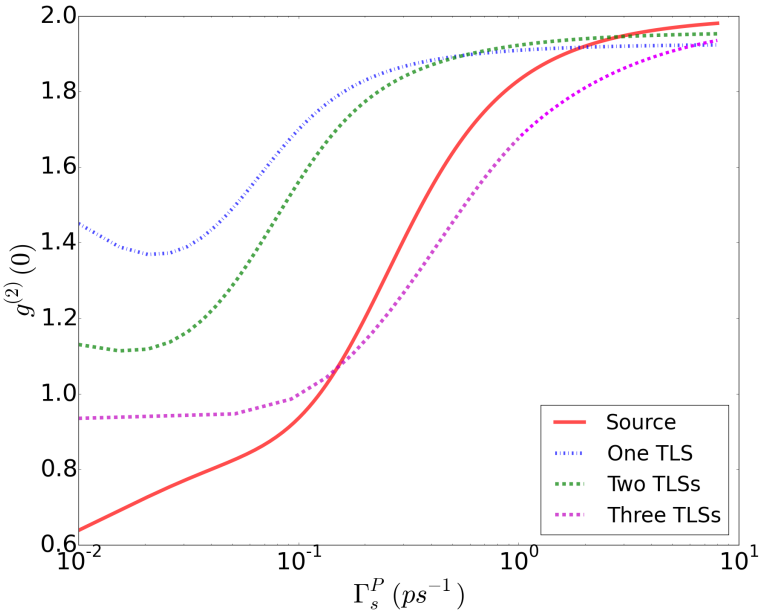

Figure 5.3.2: Second order correlation function $g^{(2)}(0)$ of the target cavity in the stationary state for the source and the target cavity. For low pump rates increasing the number of emitters produces more strongly antibunched light. When increasing the pump strength, a transition to the thermal regime occurs.

Here, we can see that the photon statistics of the cascaded system can be modified via the pumping strength. This gives an opportunity to have an adjustable source of light which can be used to excite the quantum many-level systems in a well-regulated manner When coupling nonclassical, i.e. antibunched, light from the source into the target system with one emitter, this only exhibits marginal antibunching. By increasing the number of emitters, this effect can be increased. For the regime of low pump strengths, the statistics tend towards the nonclassical Fock statistics, while for high pumps, near-thermal statistics are observed. In our study, we are especially interested in the transition from the nonclassical to the thermal regime for intermediate pump strengths.

As an important phenomenon, the target cavity with one TLS rarely produces an antibunched light even in the very weak pumping regime (blue, dashed dotted)as well as for the case of two TLSs (green, dashed line). The mechanism behind this is the dissipative transfer between the cavities, leading to thermal mixture and loss of coherence from the source to the target. Thus, the dissipative coupling via the reservoir leads to a more classical response. As we are in the weak intra-cavity

coupling regime and at weak pumping strengths there is a modification of TLS energy levels. The incoming light excites the TLS and spontaneous emission takes place. But as the cavity dissipation rate is high the cavity loses the created photon. So there is no correlation between detection of photons. By increasing the number of TLSs in the target cavity, with a stronger quantum nonlinearity, the probability for absorption-emission of photon increases. However, even in the case of two quantum emitters the photon statistics in the target cavity is less non-classical. This situation slightly changes for the case of three TLSs, as the quantum nonlinearity is sufficient to reach some antibunched pattern for the weak pumping. Still, the second order correlation function for this case is closer to coherent light than antibunched light.
Thus, we have a possibility of stable production of a photon. In the forthcoming section, we will encounter with additional evidence for closely classical production of light by target cavity with one TLS.
If there are any quantum phenomena to be observed, it can occur in an interval of weak pumping strength. In the regime $\Gamma_s^P > g_s$, the response follows the source dynamics. This highlights the fact that the target cavity mimics the quantum behavior of the source cavity which arises once it is incoherently-weakly pumped. One can conclude that a quantum cascaded coupling does not qualitatively change the second-order photon correlation function of the target . However, we will see that in the case for higher-order photon correlation functions, which we discuss in the next section, the finger print of the source statistics is observable.

The assertion that we can control the photon statistics of the target cavity, is a motivation to investigate the light production from the target more profoundly. The general method for this is to tune the system for different physical parameters and observe the produced output light. As it was referred in section.5.1, the quasiprobability distributions can present the pattern of the output field explicitly. The Fock state distributions are calculated for the target cavity with two and three TLSs. We excluded the target system with one emitter as the output of such a configuration is merely bunched photon statistics, thermal light.Thus, the nonlinear phenomena that we are interested in is barely present. In addition, two different coupling scenarios introduced in table 5.3.2 are considered.
These Fock number distributions for the target cavity are demonstrated in Fig.5.3.3. Moreover, the influence of different intra-cavity coupling strengths on these quasiprobability distributions are shown. For the target cavity with two TLSs, the first phenomenon to be observed is the flat distribution for the case.2 of intra-cavity coupling strength shown in Fig.5.3.3(a). This occurs exactly in the transition regime of $g^{(2)}(0)$ shown in Fig.5.3.2 . One can see that this setup shows a rather nontrivial photon distribution which does not match any light statistics Fig.5.3.3(c). We will elaborate on this case later. By decreasing the cooperativity of the source, target cavity with two emitters,the weak coherence produced in the source mostly is depleted in the bath and the target cavity produces thermal light. Nonetheless, one can still observe the quantum signature of the source as the distribution is not monotonously decreasing(the probability of finding one photon is still high) which is different from a pure thermal light.

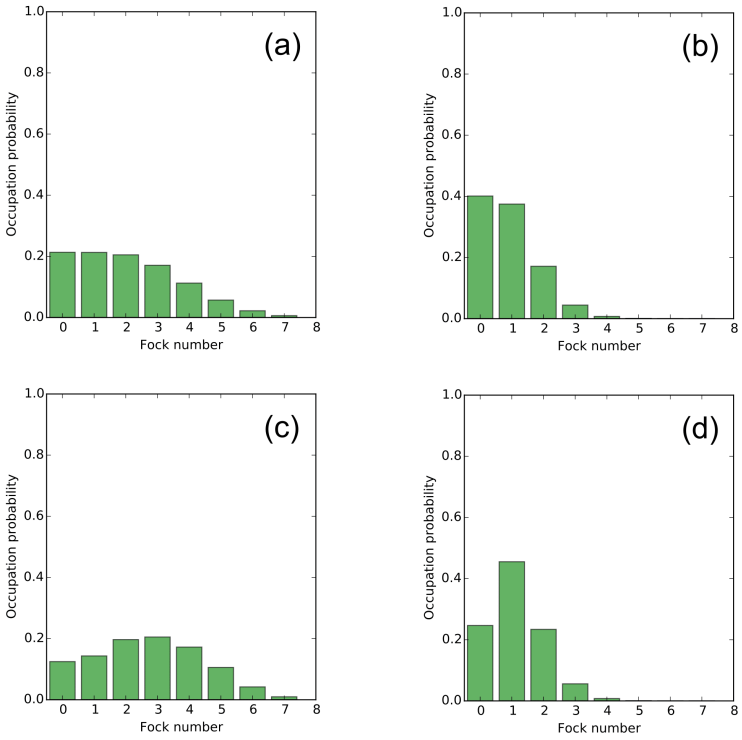

Figure 5.3.3: Fock state distribution for different configurations of the target system. These two distributions for the two and three TLSs in the target cavity are shown from top to bottom. The first column (a, c) presents the results for the cooperativity values of Case.2 in table 5.3.2. For Case.1 in this table the result is presented in the second column (b,d).

Additionally, the case for the target cavity with three TLSs are illustrated in Fig.5.3.4(c-d). In the moderate intra-cavity coupling intervals (Case.2 in the table 5.3.2), target system output behaves as a mixture of coherent and antibunched light, though the maximum of the Fock state distribution is at $n = 3$. Whereas for the Case.1 scenario the target system's properties resembles the mixture of coherent and thermal light.

Despite this, two cases show odd photon distribution in the Case.1 scenario, Fig.5.3.3(b-d). For the target cavity with two TLS, the vacuum and one photon states have similar occupation probabilities Fig.5.3.3(b). The three TLSs scenario is closely related to the production of Fock states but still has some coherent state features Fig.5.3.3 (d). Similarly to the incoherently pumped TLS case in a cavity, one can see that the weak and moderate coupling regime, in addition to weak pumping strength, are the criteria for the observation of quantum phenomena in quantum cascaded system. The odd behavior of target cavity system in the moderate coupling regime with weak pump is related to the mediator role of the cavity modes and the dissipative

nature of the bath. The stronger intra-cavity coupling regime leads to more exchange of energy between the TLSs and cavity modes. Therefore, the communication of energy between the TLSs takes place. Furthermore, The increase in the number of TLSs leads to more exchange of energy between the TLSs and consequently creates modified probability of finding more than one photon as many TLSs are excited at the same time.

All of the Fock state distributions presented in Fig.5.3.3 are matter of interest, as they deviate from the typical photon distribution. However, we will concentrate on the most interesting case where we observed a flat distribution and investigate its properties. The next step here is to have a more profound understanding about the odd quasiprobability distributions that we observed above. For that, investigation of $g^{(n)}(0)$ is proposed in the next section.

5.3.3 Higher order correlation functions

A more ostensible understanding of the cascaded systems can be achieved through the manifold of $g^{(n)}(0)$ function. In experimental physics, higher-order photon-correlations have become feasible [106]. These correlation functions open a possibility to characterize the quantum light field more precisely in photon detection setups. For example, a $g^{(2)}(0) \approx 1$ is often taken to be an indicator for a coherent light field (in the Glauber state). Another example is a Fock state which has a large photon number

$$g^{(2)}_{\text{Fock}}(0) = 1 - 1/N \to 1 \tag{5.3.24}$$

for $N = \langle a^\dagger a \rangle \gg 1$. Although, the second order correlation function is a powerful tool, for a more explicit characterization of the light field one can consider higher order correlation functions. For zero time delay $\tau = 0$ and steady-state they are defined in their customary form as

$$g^{(n)}_{\text{stat}}(0) = \frac{\left\langle a_i^{\dagger n} {a_i}^n \right\rangle}{\left\langle a_i^\dagger a_i \right\rangle^n}, \tag{5.3.25}$$

where $i = s, t$ for the source and the target cavity. The $g^{(n)}(0)$ gives clear distinction of the type of light that the source cavity is producing. In Fig.5.3.5 such a plot for the source cavity is shown for different incoherent pumping strength. By increasing theΓ_P source cavity shifts from sub-Fock emission to the sub-thermal radiation.

The behavior of the source in the manifold of $g^{(n)}(0)$is sufficient indication that, by the incoherent pumping mechanism, we have a control over the type of light that we can produce from the source cavity.
The $g^{(n)}(0)$ as a function of n for two (and three) TLSs are computed here. Even for a case when the $g^{(2)}(0)$ function values are equal, one still can measure such higher-order

correlations to distinguish the output fields. For three typical types of light statistics, we can characterize the behavior of $g^{(n)}(0)$. The Fock state higher-order correlation functions are formulated as

$$g^{(n)}_{\mathrm{Fock}}(0) = N!/[N^n(N-n)!], \tag{5.3.26}$$

where $n < N = \langle a^\dagger a \rangle$. This implies that $g^{(n)}_{\mathrm{Fock}}(0) > g^{(n+1)}_{\mathrm{Fock}}(0)$. This is in contrast to a coherent distribution, where we have $g^{(n)}_{\mathrm{coh}}(0) = g^{(n+1)}_{\mathrm{coh}}(0) = 1$. For a thermal light field where $\bar{n}$ is the mean photon number, the unnormalized form of the higher-order correlation functions read $\langle a^{\dagger n} a^n \rangle = n!(\bar{n})^n$ and computed as

$$p_n = (\bar{n})^n/(1+\bar{n})^{n+1}. \tag{5.3.27}$$

Subsequently, the correlation function follows the relation: $g^{(n)}_{\mathrm{therm}}(0) < g^{(n+1)}_{\mathrm{therm}}(0) = (n+1)!$. By applying these three limiting cases, one can visualize the output of the quantum cascade driving setup.

The higher-order correlation functions are numerically evaluated and plotted in Fig.5.3.4.The source cavity (red, solid) and the target cavity with one (blue, dashed dotted) and two (green, dashed) TLSs are distinguished. The same physical parameters for the calculation of quasiprobability distribution are allocated here. To illustrate different states of light,the $g^{(n)}(0)$ of pure thermal light, coherent light and quantum light are plotted. Additionally, we colored each area to differentiate between these states(super-thermal and sub-thermal fields, and super- and sub-Fock states). Considering the Fock state limits , we set the number of Fock photons equal to the order of the correlation function $N = n$.

The corresponding correlations of the source $g^{(n)}_s(0)$ and target system $g^{(n)}_t(0)$ are presented for a fixed value of $\Gamma^P_s = 0.1\mathrm{ps}^{-1} = g$. The output field from the source cavity shows a monotonic behavior in the sub-Poissonian state i.e. $g^{(n)}_s > g^{(m)}$ for all $n < m < 10$. Comparing to the vast shaded area(light blue), it is very characteristic for a non-classical output field to be that close to the pure antibunched light. It is interesting to notice that the non-classical nature of the source cavity was hardly detectable in the quasiprobablity distributions presented in Fig.5.1.2
Similar to the source, for the case of one TLS in the target cavity, we also see a monotonic behavior, but this time with increasing distribution $g^{(n)}_s < g^{(m)}$ for all $n < m < 10$. As we expected, apparently, the target cavity with a single TLS is far from entering the quantum regime. Conversely, the output field of the target cavity with two TLSs does not display such a monotonous behavior, e.g. $g^{(2)}_t(0) < g^{(3)}_t$ but $g^{(2)}_t(0) > g^{(6)}_t$. As an unorthodox type of distribution, its trajectory starts from the sub-thermal states and after passing a maximum enters to the sub-Poissonian area. This output corresponds to the Fock state distribution which is shown in Fig.5.3.3 (c). In the light of this difference, it appears that the target dynamics is not purely

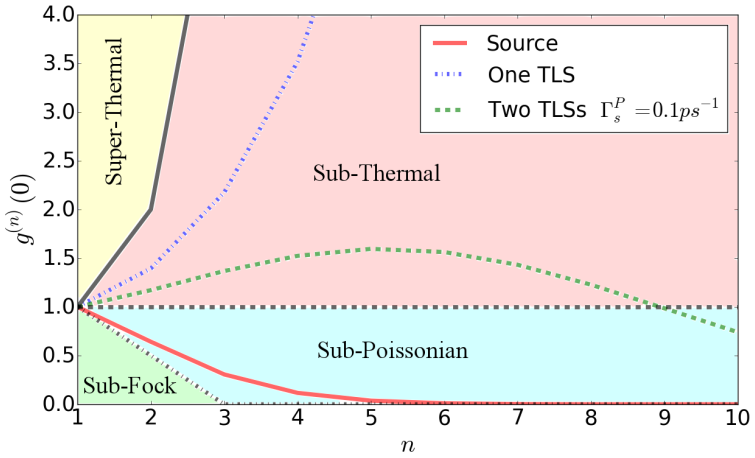

Figure 5.3.4: Higher Correlation functions in the steady state, when the pump strength is equal to the cavity coupling ($\Gamma_s^P = g$) for source (red, solid) and target with two TLSs (green, dashed) and a single TLS (blue, dashed dotted). The solid, dashed and dash dotted gray lines present thermal, coherent and pure quantum light. The source is antibunched and in the subpoissonian regime for all orders in the correlation function. The target with a single TLS exhibits thermal light. However, the target cavity when containing two TLSs shows a transitional behavior, where it starts out in the sub-thermal regime but goes to the sub-Poissonian regime for higher orders.

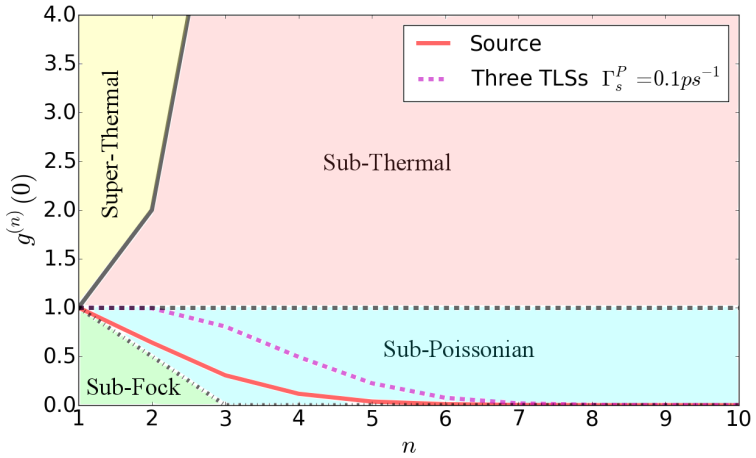

Figure 5.3.5: Stationary higher order correlation function of the target cavity with three emitters up to the tenth order.

imprinted from the simple image of the source. The previously discussed, dissipative degradation which takes place in the source-target transfer is not solely responsible for the source and target deviation and cannot only be traced back to this process.

In target cavity with three TLSs, for the moderate intra-cavity coupling and the weak pumping strength $\Gamma_p = 0.1$, the output field resembles coherent light for $n < 4$. However, for higher photon number it strays and enters the sub-Poissonian photon statistics (magenta line in Fig.5.3.5).We can see that in the cascaded setup with three emitters in the target, the source state is not straight forwardly mapped to the target system and quantum statistics of the target is remarkably much closer to a coherent driving setup, although it is of purely dissipative nature.
In the rest of this section, we will only focus on the case of a target with two TLSs, as we have found exciting photon probability distributions for this case. Also, since the target system with one emitter does not exhibit non-monotonic behavior and the case for three emitters mostly resembles the coherent distribution in parameter regime, we concentrate on the two emitters scenario. This scenario for quantum cascade coupling prevents drastically a straightforward imprinting of the source statistics on the target quantum dynamics as it is visible in $g_t^{(n)}(0)$ distribution.

In Fig. 5.3.6 we investigated the influence of incoherent pumping mechanism on the higher order correlation functions. The corresponding correlation functions of the source and target system $g_t^{(n)}(0)$ are plotted for different incoherent pumping strengths of the source system Γ_s^P. As a compelling result, one can see that the response from the target system deviate drastically from the source quantum statistics. The source system,for all pumping strengths, behaves monotonically, always decreasing: $g_s^{(n)}(0) > g_s^{(m)}(0)$ for all $n < m \leq 10$. Moreover, for high orders of photon

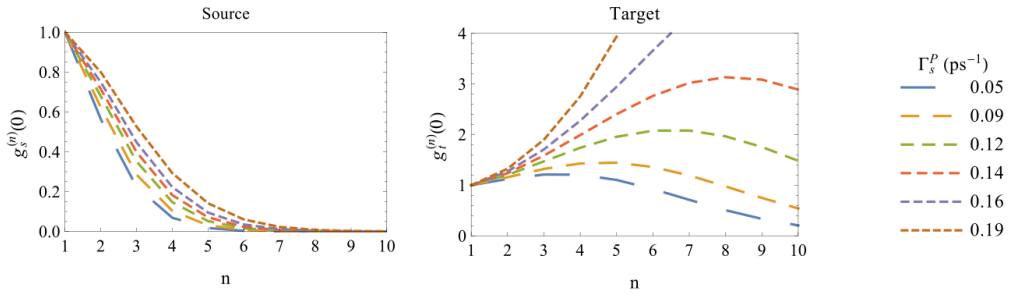

Figure 5.3.6: Higher-order correlation functions of the source $g_s^{(n)}(0)$ and target system with two TLSs $g_t^{(n)}(0)$ for different incoherent pumping strength of the source system Γ_s^P. Remarkably, the target system exhibits a different behavior than the source system.

number $n > 5$, the quantum statistics converges to lower values and finally reaches very small values close to zero . This behavior is due to the fact that the incoherent driving and the cooperativity [107] $C_s = g_s^2/(\Gamma_R \kappa_s)$ restricts the obtainable photon manifold, i.e. there will be always a cut-off number n_c with corresponding $p_{n_c} = 0$ and therefore the relevance of higher-order correlations decreases: $g_s^{(n)}(0) \to 0$ for $(n - n_c) \to 0$.

In contrast to the source, the target system arrive first at a maximum point for a certain m with $g_t^{(m)}(0) \geq g_t^{(n)}(0)$ for all n. This maximum shifts for higher pumping strength towards larger m. This phenomena is expected, since the maximum number of photons also shifts to larger values. After the target passes its maximum, the $g_t^{(n)}(0)$ distribution follows the same fashion as of the source system and inclines towards the lower values. This behavior is stabilized for a wide interval of pumping strength values. As a result of a cut-off number presence in the source photon manifold n_c, the target quantum distributions will follow the same faith and eventually merge to zero. However, This process only occurs for large n, wherein, the target system follows the source quantum statistics, always after passing a maximum point. The maximum point, however, can increase to the higher values until it suddenly shifts to very large orders in correlation, particularly from a certain pumping strength on: $\Gamma_s^P = 0.2\text{ps}^{-1}$ (blue, dashed line). Thus, we consider a certain transition point for the maximum of target system $g_t^{(n)}(0)$ distributions.

Moreover, a qualitative transition of the target system in the correlation functions $g^{(n)}(0)$ is revealed in Fig. 5.3.6. In the case of the target cavity, for low incoherent pump strengths, the correlation curve is turning downwards. Then , for a certain pumping strengths, there is a transition point where the curve turns upwards and resembles the thermal statistics . We quantify the transition process by the

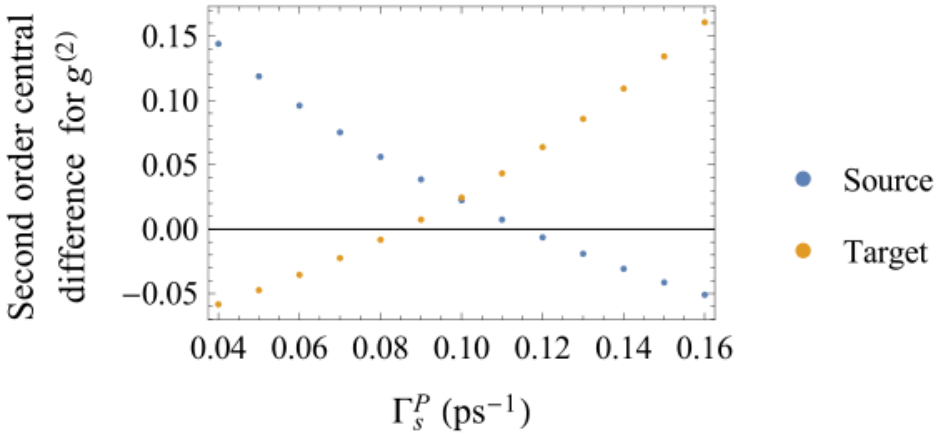

Figure 5.3.7: The transition observed in the system illustrated by the second order finite difference at the $g^{(2)}$-function. While the source correlations cross from an upwards to a downwards turning point, the target correlations exhibit the opposing behavior. The curves cross at the coupling strength $g = 0.1\text{ps}^{-1}$ common to source and target.

second order central difference written as

$$g^{(n)\prime\prime} = \frac{g^{(n+1)} - 2g^{(n)} + g^{(n-1)}}{(n+1-n)(n-(n-1))}. \tag{5.3.28}$$

In the course of transition from coherent to thermal light, the nth order correlation function of the target system flips up. Wherein, the source behavior stays in about the same regime of light. To characterize this transition mechanism in the target, we implement the second order difference at the $g^{(2)}$-function. That will show the flipping process, where the curve here points upwards. In Fig. 5.3.7 we illustrate this transition for the second order central difference. One can observe that the target system proceed from a downwards to an upwards turning point. In contrast, simultaneously, the source system exhibits a totally different pattern, a transition from an upwards to a downwards turning point. The crossing point for the corresponding curves are at the coupling strength $g = 0.1\text{ps}^{-1}$. Thus, albeit it is not trivial how the source influences the target, we can still illustrate the transition in the target system by a reciprocal transition in the source system.

5.3.4 Characterization of quantum cascaded driving

To have a better view of the properties of the quantum cascade, one can compare the higher-order correlation g^n and Fock state distribution with a target system which is not cascaded to the source but is coherently or incoherently driven. One can decouple the source and target cavities by switching the output of the source cavity off, setting $\kappa_s = 0$. As a milestone, here also we concentrate on the case of two TLSs in the target system. In the master equation formalism we will adopt two distinct

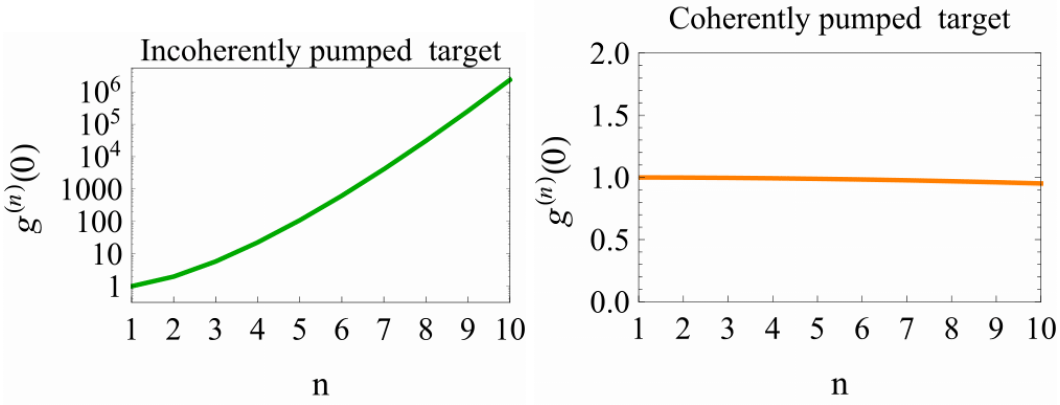

Figure 5.3.8: Higher-order correlation functions of the target system with no quantum source pumping $\kappa_t = \Gamma_s^P = 0$. Instead the target is directly pumped incoherently (left) and coherently (right) with $\Gamma_t^P = \sqrt{\gamma_t \kappa_s}$. Note the logarithmic scale for incoherent pumping, and the monotonous increase, which is in contrast to the coherent driving induced maximum in the $g^{(n)}(0)$ distribution. The incoherent driving exhibits thermal statistics, while the coherent driving is close to coherent statistics for a wide range of pump parameters.

scenarios. Firstly, the coherent driving of the target system is considered and included by displacing of the target cavity's photon operator as $a_t^\dagger \to a_t^\dagger + \Gamma_t^P/g_t$. Secondly, for the scheme where the target system is driven directly with incoherent light, one can alternate the incoherent pumping operators from $\mathcal{D}[\sqrt{\Gamma_s^P}\sigma_s^+]\rho \to \mathcal{D}[\sqrt{\Gamma_t^P}\sigma_t^+]\rho$. We have evaluated numerically these two scenarios for higher order correlation function $g^n(0)$ which is depicted in Fig. 5.3.8. The comparison for the case of incoherent pumping (left panel, green line) and coherent pumping (right panel, orange line) of the target system is illustrated. All the physical parameters of the target system are kept the same which allows one to compare these two scenarios with the quantum cascaded case.

A recognizable qualitative behavior of $g^n(0)$ in the cascaded setup (cf. Fig. 5.3.6), with the incoherently and the coherently pumped cases is observed. While, in the case of cascaded setup, $g^n(0)$ exhibits a maximum in the correlation functions and then passes the sub-thermal and sub-Poassonian boundary, the incoherently driven target exhibits thermal statistics, increasing monotonously. For the case of coherently driven target system, $g^n(0)$ exhibits a closely related statistics to coherent light. Thus, one can conclude that the form of accessible photon statistics for the cascaded system is drastically different from the other excitation scenarios. This is due to the fact that some parts of the composed Hilbert space of stationary cascaded system is now accessible from the target system, that would not be available by other means of excitation [27].

This result is at first glance surprising, as the the output field of the source is

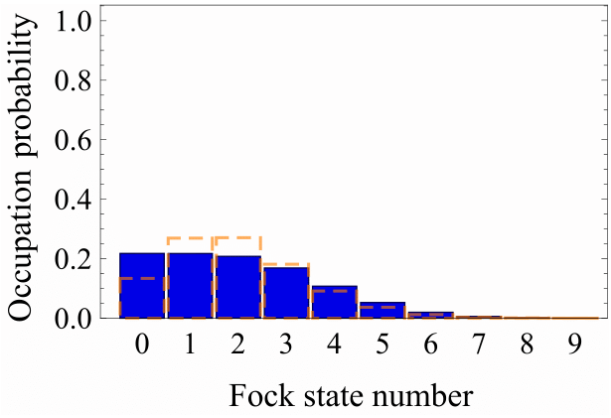

Figure 5.3.9: Occupation probability of the Fock states for $\Gamma_s^P = 0.1\text{ps}^{-1}$ corresponding to the photon statistics shown in Fig. 5.3.3 (solid, blue). Due to the cascaded coupling the photon number distribution is exceptionally flat. This illustrates the photon statistics that deviate from the prototypical cases. For reference (dashed, orange), the coherent distribution is shown.

clearly in the antibunching regime, and the coupling mechanism is mediated due to dissipative processes. By inspecting the coupling terms, one can have some physical intuition for the observed result, . While the cascaded coupling is derived using an intermediate bath and thus constitutes a dissipative coupling, the coupling preserves some properties of the source statistics in certain regimes. However, investigating the quantum cascade coupling in the master equation Eq. (5.3.19), it can be written in terms of anti-commutators.

If one exchanges $\sqrt{\gamma_t \kappa_s} \to -\sqrt{\gamma_t \kappa_s}$, the system dynamics and results remain unchanged, as it is the same with $H_{t/s} \to -H_{t/s}$.

This can give an explanation for the part of the target cavity dynamics that preserves the source cavity photon statistics in the low pump strengths interval. This behavior is not expected from a dissipative coupling as the standard Lindblad form is independent of a change in the sign. In the weak incoherent pumping interval, quantum coherences can be constructed and those quantum processes (produced and came out) from the source cavity are mediated via $a_s^\dagger$ to the coherences of the target cavity system σ_t^+. In this limit, the coherent coupling dominates and leads to a characteristic maximum in the $g^{(n)}(0)$ distribution, comparable to the peak in the Poissonian distribution. However, for strong incoherent pumping, the emitter dynamics follows the population dynamics adiabatically, since the incoherent pumping destroys any quantum coherences. In this limit, the target emitters are driven by the population, which enforces a dissipative, thermal behavior without inherent quantum coherences. Nonetheless, in the intermediate coupling regime a transition takes place. This allows one to obtain rather specific photon distributions by only partially feeding

the source cavity photon statistics into the target which is visible in the high-order correlation functions.
Herein, we compare the Fock state distribution presented in Fig.5.3.3(a) , corresponding to the statistics of $g^{(n)}(0)$ function observed in Fig. 5.3.4 , with a coherently pumped target. The differences between these two distribution are illustrated in Fig. 5.3.9. One can observe a flat distribution of photons, where the probabilities for the first few photon number states are similar(solid,blue) and its deviation from the coherent distribution, with a maximum and then thermal distribution, (dashed,orange)

To conclude, higher-order photon correlations show that the quantum cascaded driving leads to a very unexpected behavior and creates an interesting regularization of the quantum output, i.e. the target quantum statistics is dissipatively driven with a non-classical light and exhibits an intriguing mixture of coherent, thermal and anti-bunching correlation functions. We can drive a system via a quantum cascaded setup into a mixture of different quantum statistics and there exists a critical incoherent pumping strength for the source system, above which the target's response changes without a qualitative change in the source quantum statistics. The quantum cascaded system shows a promising route to combine a super-Poissonian in a sub-Poissonian field to Poissonian one . This is an interesting regime to create a mixture of quantum statistics within a single target system by the mixture of Hamiltonian and decoherence processes, mediated by the cascaded setup.

5.4 Indirect coupling to the target emitter(s)

In the case of indirect coupling the modes of two cavities couple to each other and through this coupling the photon statistics is transferred from the source to the target system. The formalism for this case is similar to the case of indirect coupling discussed in section 5.2. The only difference here is the target cavity coupling rate to the waveguide which is set to be the cavity photon decay rate, $\gamma_t \to \kappa_t$. Thus , following the formalism in Eq.(5.3.19) the general master equation for this case takes the form

$$\begin{aligned}\frac{d\rho}{dt} &= \frac{1}{i\hbar}[H_0 + H_s + H_t, \rho] \\ &+ \mathcal{D}[\sqrt{\Gamma_s^P}\sigma_s^+]\rho + \mathcal{D}[\sqrt{\gamma_s}\sigma_s^-]\rho + \mathcal{D}[\sqrt{\kappa_s}a_s]\rho \\ &+ \mathcal{D}[\sqrt{\kappa_t}a_t]\rho + \sum_{i=1,2}\mathcal{D}[\sqrt{\gamma_t}\sigma_{t,i}^-]\rho \\ &- \sqrt{\kappa_s\kappa_t}\sum_{i=1,2}\Big([a_{t,i}^+, a_s\rho] + [\rho a_s^\dagger, a_{t,i}]\Big). \end{aligned} \tag{5.4.1}$$

Herein, we consider one or two emitters inside the target cavity. The cavities couple to the unidirectional waveguide through the cavity dissipation rates κ_i for $i = s, t$.

The simple sketch of the considered setup is presented in Fig.5.4.1. The master equation for such a system can be evaluated numerically for both cases. However, in the following we concentrate on the case that target system contains only one emitter. This is due to the fact that the characteristic futures, that we are interested in, are observed to be similar for both cases. Latter in the study of the control of entropy we will consider two TLSs in the target system. For the direct coupling scenario,

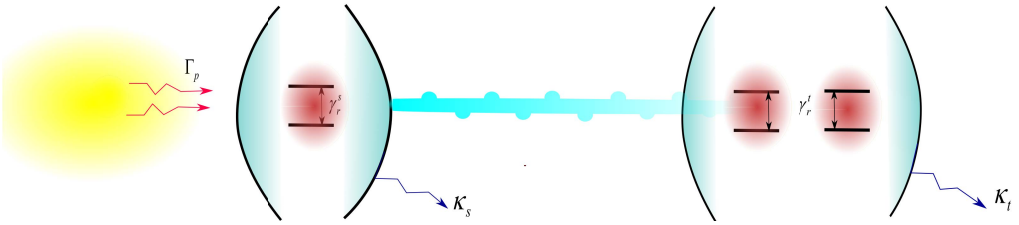

Figure 5.4.1: Schematic depiction of the studied setup. The source cavity, which contains a TLS, is pumped incoherently with rate Γ_p. The emission of the source cavity is fed into the target system which excites indirectly the emitters contained in the target cavity.

presented in section 5.2, we have fixed all the parameters of the target system and only changed the source cavity incoherent pumping strength. In addition, we have changed the source cavity cooperativity to examine how such changes in the source effects the whole cascade dynamics.
Here we propose another approach in which we change the physical parameters of the target system and examine their influence on the quantum statistics of the cascaded system . To have a better understanding of the influence of these parameters in statistical distribution, we change one parameter each time and see how the photon statistics of the target system changes. All the parameters are chosen in according to table 5.3.1.

5.4.1 Control of photon statistics of target cavity

Firstly, we numerically evaluated the evolution of the photon number of the source and target. This evolution is illustrated in Fig.5.4.2 for different values of g_t and γ_t. The parameters of the source cavity are fixed here and we only change one of the parameters of the target which changes the intra-cavity dynamics . One can see that, by increasing cooperativity, C_t, through the increase of its nominator g_t, the probability of producing photon decreases.

For the second order correlation function $g^2(0)$, the increase in C_t shifts the output light of the target cavity from antibunched(dashed dotted line) to highly bunched light(dashed line). This shift in the quality of the produced light is illustrated in Fig.5.4.3.

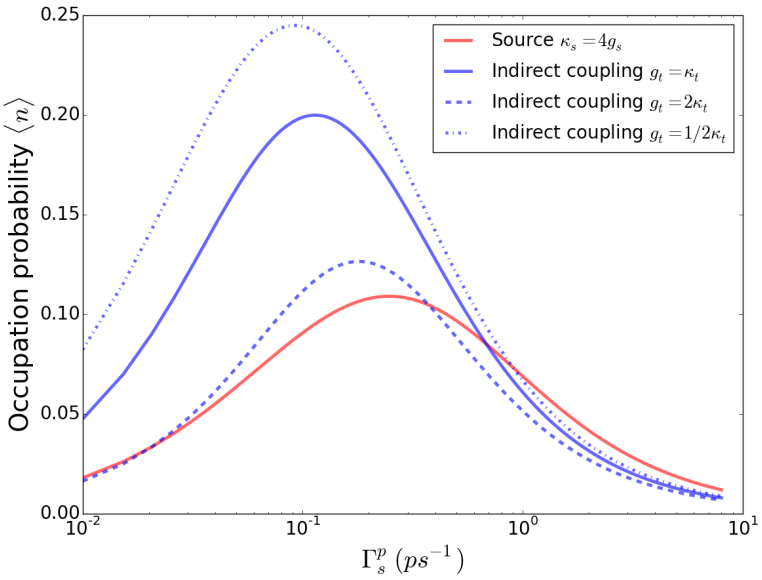

Figure 5.4.2: The manifold of occupation probability of photons evolving for the target cavity in respect to pumping strength. Different inter-cavity coupling strengths are echoed here.

To describe this result, one can argue that the incoming light from the source cavity first couples to the target cavity bosonic modes. Afterward, through the target cavity modes, the TLS interacts with the imposed excitation. It can be seen that the influence of the coupling strength is exceptional. This is due to the fact that the TLS exchange of energy with the cavity modes depends on g_t.
To clarify this process, we can analyze the role of g_t in the cascaded formalism. Firstly, the atomic operator and cavity modes exchange energy only via the interaction(Jaynes–Cummings) Hamiltonian, H_t. One should notice that, in the case of indirect coupling, fermionic operators communicate to the incoming field through the target cavity mode operator a_t. The rate of this communication is determined by g_t. Metaphorically, we use the term communication where the components of quantum system exchange quanta of energy through the Hamiltonian operator. Thus, we can interpret the situation as follows: in the case of indirect coupling, the communication between incoming photons and the atom inside the cavity takes place through a meditator, namely the cavity bosonic field. These cavity modes exchange energy with the single photon source and simultaneously communicate to the atoms . As it can be seen from Eq.(5.4.1), for the case of direct coupling to the target cavity emitters a different process occurs.

For a better understanding of the target cavity dynamics, this time after fixing all parameters of the target, we change the denominator of C_t, namely the atomic

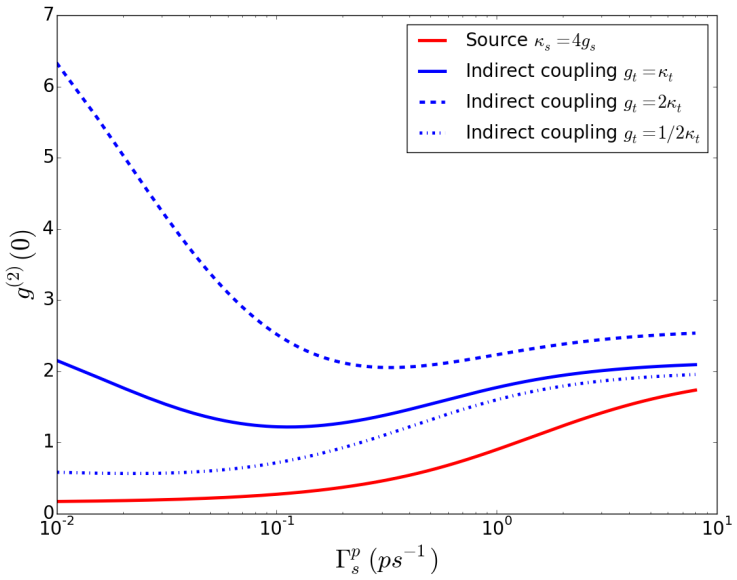

Figure 5.4.3: Second order correlation function, $g^2(0)$, diagrams for the source cavity and the target cavity with one TLS. The ratio of g_t is changed in respect to the cavity dissipation rate κ_t . Different incoherent pumping strengths are considered here.

dissipation rate γ_t. Similarly to the case above for g_t, the photon number expectation value and the second order correlation function are considered. In Fig.5.4.4 the behavior of these two observables for different γ_t are illustrated. The increase in atomic dissipation rate leads to the increase in cooperaitivity of the target cavity. Thus, a similar behavior is deserved to the case with changing the intra-cavity coupling strength g_t. This behavior can be explained by desynchronization of coupled cavities when the intra-cavity dynamics of the target dominates, there is an increase in C_t, and coherence get lost in a transformation process from the source to the target by dissipative environment. That describes the thermal nature of the output light from the target cavity. By decreasing the rate of C_t the source and target synchronize again and the target system mimics the photon statistics of the source, behaves antibunched for weak pumping regime Γ_s^P. To understand the desynchronization we evaluate the second order correlation function for different g_t which is shown in Fig.5.4.5.

The target system desynchronize from the source when the inter-cavity coupling strength is bigger than the mean coupling rate to waveguide, $g_t \succeq \kappa_t$. After passing this point the system approaches the thermal regime, as no input field enters the cavity and the remaining photons also naturally leave the target system. As a matter of importance for the control mechanism of cascaded system, we can propose a protocol for synchronization of the two coupled cavities: by changing the target

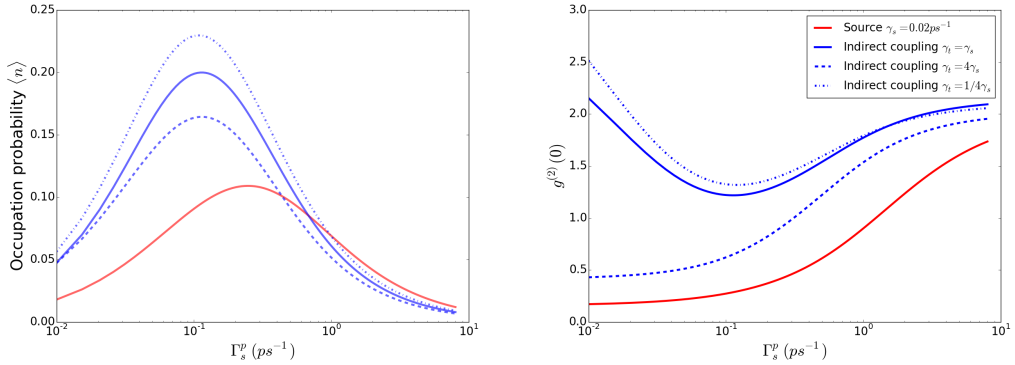

Figure 5.4.4: The manifold of photon number and $g^2(0)$ function evolution for the target cavity with one emitter in respect to the pumping strength Γ_s^P. Different atomic dissipation rateγ_t are considered. The atomic dissipation rate of TLS in the source γ_s is fixed and in respect to that, the γ_t is varied.

system internal dynamics one can synchronize (or desynchronize) the target cavity from the cascaded setup.

5.4.2 Control of entanglement between two emitters in the target cavity

One of the most important property of bipartite quantum systems is the concept of entanglement. For this purpose, we assume now that the target system contains two emitters and examine the entanglement between these two TLSs. One of the measures of entanglement is the relative entropy which is based on the Von Neumann entropy. Von-Neumann entropy is the quantum counterpart of entropy in classical information theory. For a density matrix of two emitters with reduced bipartite density matrix ρ_b the Von Neumann entropy is defined as [108]

$$S(\rho_b) = -Tr(\rho_b ln \rho_b) \tag{5.4.2}$$

where S is changed to an interval $0 \leq S \leq lnN$ where the zero value is for pure states and lnN for maximally mixed states. N represent the dimension of the composed Hilbert space of the bipartite quantum system.
Considering the steady state limit for the cascaded system, we evaluate $S(\rho_b)$ numerically. Additionally, we fix κ_t and change the intra-cavity dynamics of the target by changing the coupling ratio g_t between emitters and the target cavity. The values of $S(\rho_b)$ versus the incoherent pumping strength of source cavity is illustrated in Fig.5.4.6. In the case of moderate intra-cavity coupling $g_t = \kappa_t$ (solid line) the trajectory of S is on top of other intra-cavity coupling scenarios. As we increase the incoherent pumping strength, for all cases, the quantum coherence between two emitters is destroyed and the entropy tend to zero. Also, following the same line of reasoning, the maximum entropy can be obtained for moderate intra-cavity coupling

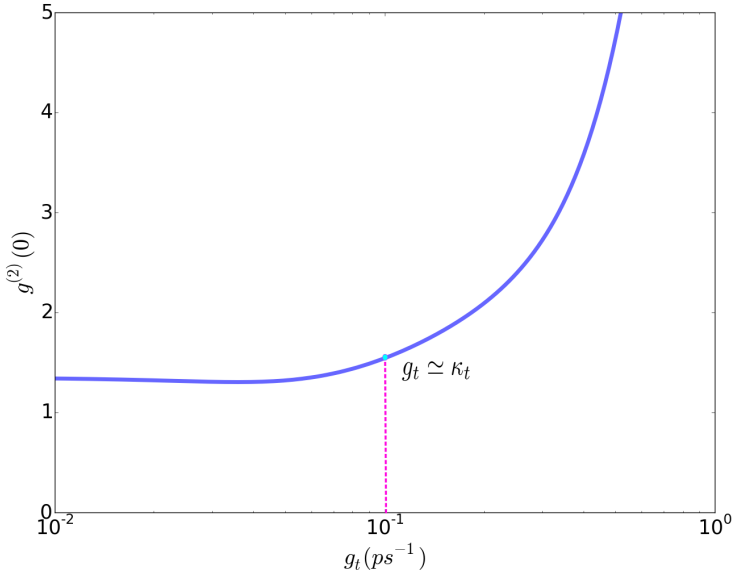

Figure 5.4.5: The manifold of $g^2(0)$ function evolution for the source cavity in respect to the target cavity coupling strength g_t.

and a rather weak incoherent pumping strength, $\Gamma_s^P \approx 10^{-1}$.
In addition, for a bigger cooperativity C_t(dashed line) the entropy is minimal which suggests that by increasing the coupling ratio between emitters and target cavity we decrease the entanglement between the two emitters. Another important aspect is the shift in the maximums of each line. The maximum for smaller cooperativity takes a place for weaker Γ_s^P and by increasing C_t the maximums shift to stronger Γ_s^P.

5.5 Conclusion

Herein, a quantum cascaded system, in which an incoherently pumped source system drives a target system with its quantum output field, is investigated. As an important observables, we went beyond second-order correlation functions and focused on higher-order photon- correlations $g^{(n)}(0)$. Interestingly, for the case of direct coupling to the waveguide, we find that the response of the target system differs strongly for different values of the incoherent pump parameters. When the incoherent pumping strength has a lower values than the coupling constant of the target system $\Gamma_s^P < g_t$, the quantum statistics of the source system are imprinted on the target system. For larger values of Γ_s^P the target system's output field resembles an incoherently driven quantum system. However, the interesting phenomenon happen in an intermediate regime. A mixture of coherent and incoherent processes due to the coupling mechanism occurs leading to quantum statistics differing from the prototypical coherent and thermal shapes and giving rise to the possibility of producing flat photon distributions.

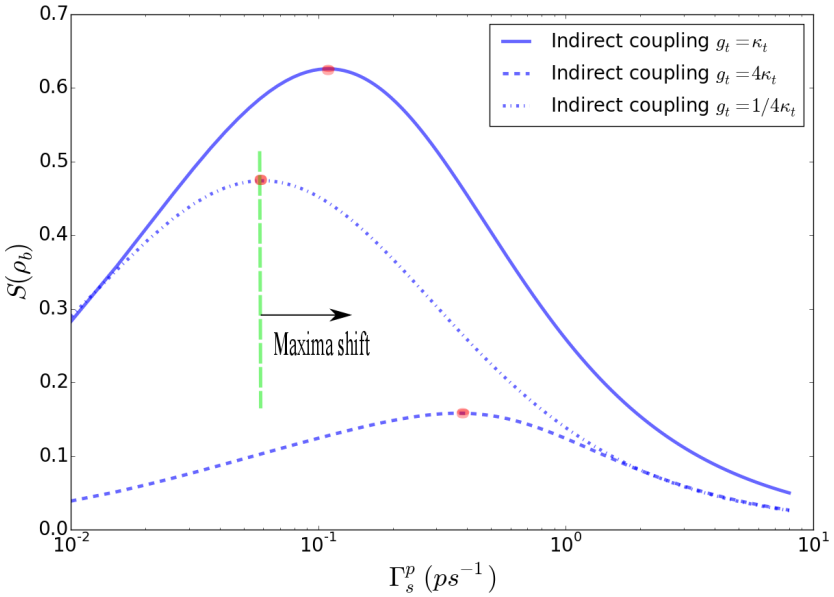

Figure 5.4.6: The manifold of $S(\rho_b)$ evolution for two emitters in the target cavity in respect to incoherent pumping strength Γ_s^P. Different inter-cavity coupling ratios, g_t, are presented. The maxima of the S shifts to the right by increasing g_t

For the case of indirect coupling, the deviation of source into target is more visible in low pumping intervals, $\Gamma_s^P < g_t$. It is suggestive that the internal dynamics of target system is dominant in this regime but by increasing the pumping strength and entering into the intermediate regime again the quantum statistics of the source is imprinted to the target.

6 Dynamical Casimir effect: A source for two photon production

In this chapter we introduce different methods for two photon production sources. Two photon emission takes place when a transition between atomic levels by simultaneous production of two photons takes place[109]. This makes the process a second order optical process which conventionally occurs in the realm of nonlinear optics. There are many important implications in quantum information science and atomic physics for such a source of quantum light [110, 111, 112, 113, 114]. For example, the pairs of photon has implication in quantum key distribution [115], quantum teleportation [116] and quantum repeaters [117].
In the first part, we provide an overview of the spontaneous parametric down conversion(SPDC) which is the major source for the production of the entangled photons in nonlinear optics. Secondly, we introduce an example for such a source of two photon emission in nonlinear optics. This example shows that the dynamical Casimir effect which we briefly introduced in chapter 4 can be implemented for a rather efficient production of two entangled photons. The main idea behind this example, is the consideration of the emission of photon pairs by metal-dielectric interface or waveguide excited by normally falling plane wave. The excitation causes temporal oscillations of the phase velocities of surface plasmon polaritons. This eventually leads to the dynamical Casimir effect - the generation of pairs of polariton quanta, which transfer to photons outside of the interface. The emitted pairs of photons are in the polarization entangled state.
A part of this chapter has been published in Applied physics A, Physics letters A and OSA proceeding [118, 119, 120].

6.1 Two photon emission processes in nonlinear optics

Spontaneous emission of photon(s) is an aspect of nonlinear optical processes [121, 24, 25]. We shortly present an overview of the most important processes that account for two photon emission, i.e, the parametric down conversion. Another process for the spontaneous emission of two photons is the four waves mixing that we excluded here. For more information on the latter process we refer the reader to the related literature on this topic [122, 123, 124].

Spontaneous parametric down conversion,SPDC
SPDC is a process in which a pair of photons is created by a laser beam incidence to a nonlinear crystal with defects. The reason for such a photon generation are the

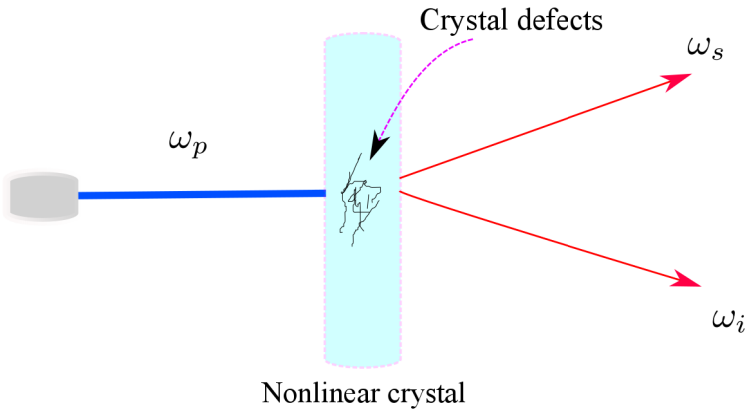

Figure 6.1.1: Production of two photons by spontaneous parametric down conversion. The laser beam is illuminating to the nonlinear crystal and the output is a pair of photons. The blue color for the laser beam indicates the higher frequency, ω_p, while the red color for the generated pair of photons shows the lower output frequencies, ω_s and ω_i.

crystal defects which are for example noncentrosymmetric. These defects make the second order susceptibility nonzero, $\chi^{(2)} \neq 0$. The nonlinear interaction of a intense laser beam with these defects results in the annihilation of a laser photon and the creation of pair of photons which are called signal and idler. The sketch of such a process is shown in Fig.6.1.1. The frequency of each of these photons are smaller than the laser frequency. This can be seen as a coherent process between three photons [125] where they traditionally follow the phase matching condition [126]

$$\omega_p = \omega_s + \omega_i \ , \qquad k_p = k_s + k_i. \tag{6.1.1}$$

This process can be explained as the intensive laser beam drive the oscillations of the electrons in the crystal defect to behave in a nonlinear fashion. In this regime we have a second order interaction occurs which results in the annihilation of laser photon and the creation of two down-converted photons. The photon pairs created in SPDC are entangled both in the wave number and the frequency. This shows that we have an entanglement in space as well as in time between two produced photons, signal and idler. There are two types of SPDC regarding to the polarization between these photons. If both photons have a similar polarization then we have type-I SPDC. The type-II SPDC arises when signal and idler photons have orthogonal polarization.

6.2 Example: Plasmon-enhanced emission of polarization entangled photons

Herein, we consider the spontaneous emission of entangled photon pairs by a metal-dielectric interface or waveguide exposed into strong laser waves with the wavefront parallel to the interface. This wave, due to the nonlinear interaction of light with matter, evokes periodical oscillations in time of the optical length of the surface plasmon polaritons (SPPs) - the electromagnetic excitations of the interface. This oscillation causes periodical perturbation in time of the zero-point state of the excitations resulting in the two-photon emission. Thus, the emission is fully analogous to the dynamical Casimir effect: the generation of pairs of photons in a resonator with changing its optical length in time [127, 128, 129, 83, 130, 131]. As it was discussed in chapter 4, we need to oscillate the mirror(s) of the resonator with the relativistic velocity for the observation of the dynamical Casimir effect [25]. This is a condition that is very difficult to fulfill by the current technologies. Thus, if one carries out this type of experiment, the intensity of the corresponding emission is extremely hard to observe. However, if one uses a superconducting circuit consisting of a coplanar transmission line, then one can achieve for microwaves a rather strong changing in time of the electrical length. In a recent experiment, the dynamical Casimir effect was observed in the range of 10 GHz [132].

In the realm of visible light, the dynamical Casimir effect may be also enhanced if one uses a strong laser excitation. However, due to very small field association with the corresponding zero point fluctuations one needs to use very strong laser excitation to observe this effect [133]. A suggestive possibility for overcoming this difficulty is to create plasmon polaritons: The required intensity of the laser excitation may be strongly reduced if one uses a metal-dielectric interface as a transformer of laser photons to photon pairs. The electromagnetic excitations of the metal-dielectric interface – SPPs, have a much smaller group velocity in the visible spectrum than the light velocity. Therefore, the electric field associated with one SPP quantum is strongly enhanced as compared to that of a photon in free space or in an usual dielectric. The goal of introducing this setup is to consider the effect of this enhancement on the generation of pairs of quanta of electromagnetic excitations. We will show that in this way one indeed can strongly enhance the dynamical Casimir effect.The yield of the two-photon emission in this process may strongly exceed the yield of two-photon emission in dielectrics in case of renown nonlinear optical process, spontaneous parametric down conversion [134, 133].

6.2.1 Physical setup

We consider a lengthy interface between metal and vacuum or a dielectric with small refractive index and suppose that mutually parallel mirrors are placed on the ends of the interface. The interface is exposed to strong laser waves through a high refractive index medium falling normally to the interface. In this case the wave front of the

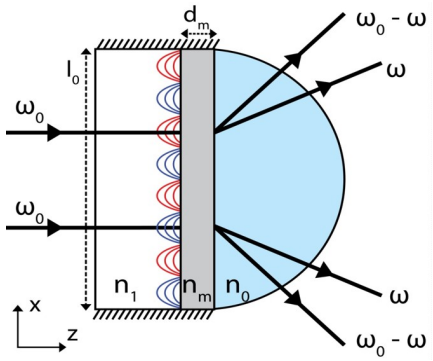

Figure 6.2.1: Production of two photons by excited metal-dielectric interface. The source of excitation comes from laser with falling plane wave and frequency ω_0. There are three different refractive indices in this setup. n_0 for the prism, n_m for the metal and n_1 for the dielectric. The SPPs created here with frequencies ω and $\omega_0 - \omega$ leave the system as pairs of photons going through prism.

excitation is parallel to the interface. The latter wave causes periodical oscillations of the refractive index (mode index)in time of a SPPs at the interface, which have the same for all coordinates x of the interface. These oscillations cause the periodic variation in the optical length of SPPs at the interface resulting in the generation of pairs of their quanta. The generated SPPs can leave the interface as photons to direction

$$\varphi_0 = \arccos(\frac{n}{n_0}) \tag{6.2.1}$$

corresponding to the Kretschmann configuration. In this direction the wave vector of a SPP coincides with the x- component of the wave vector of a photon with the same frequency in the dielectric. The scheme for such an experiment is given in Fig.6.2.1. Two-photon emissions due to dynamical Casimir effect in the dielectric-metal-vacuum (dielectric) interface with refractive indexes satisfying the condition $n_1 < n_m < n_0$ where n_i are three different refractive indices of dielectric, metal and the prism.

What is presented here holds for surface plasmon polaritons (SPPs) in metal-dielectric interfaces, for guided 2D-waves propagating along a thin dielectric slab with a high refractive index surrounded by dielectrics with smaller refractive indexes (guided dielectric waves (GDWs)) [135, 136] and for D'yakonov waves (DWs) existing in the interface of dielectrics of different symmetry [137] (recently observed in [138]. The enhancement factor η for such a variety of setups is illustrated in Fig. 6.2.2.

6.2.2 Theoretical model

The efficiency rate of the emission of photons due to the dynamical Casimir effect is determined by the dimensionless parameter

$$v = \frac{\pi a_0}{\lambda_0} = \frac{V}{c} \tag{6.2.2}$$

where $a_0/2$ is the amplitude of oscillations of the optical length, $\lambda_0 = 2\pi c/\omega_0$, with ω_0 being the laser frequency and V is the maximum velocity of the oscillations of the optical length corresponding to the resonator for generated photons.Further, c is the speed of light. In the visible spectrum one can use laser light to call up the periodical oscillations in time of the refractive index and the optical length of a dielectric placed in the resonator. However, the parameter ν in this case is usually very small due to the fact that the nonlinear interaction of light with matter is very weak. In this case the rate of emission of photons due to DCE is also very weak. Nevertheless, in the microwaves frequency, by means of a superconducting circuit, one can achieve a rather strong change of the electrical length in time to observe DCE [139, 132]. The time-dependent part, δn_t, of the refractive index of SPPs in the case under consideration is described by the equation

$$\delta n_t = \chi^{(2)} E_0 \cos(\omega_0 t). \tag{6.2.3}$$

Here $E_0 = \sqrt{Z_0 I_0}$ is the amplitude of the electric field of the laser wave, $Z_0 = 376.7\Omega$ is the impedance of free space, I_0 is the intensity of the laser light, ω_0 is its frequency, $\chi^{(2)}$ is the second order nonlinear susceptibility. Furthermore, it is assumed that $|\delta n_t| \ll 1$. This gives rise to $a_0 \sim \left|\chi^{(2)}\right| E_0$ and consequently

$$v \sim \left|\chi^{(2)}\right| \frac{E_0 l_0}{\lambda_0} \tag{6.2.4}$$

where l_0 is the length of the resonator. In a usual dielectrics where $\left|\chi^{(2)}\right| \sim 10^{-12}\mathrm{m/V}$ and $c = c_0/n$, it is supposed that $l_0 \lesssim l_\Delta$, where l_Δ is the propagating distance of the surface excitations. The length (in x direction) and the width of the interface, respectively, are l_0 and l_1; the optical length of a SPP is $L = n_m l_0$. The generation of pairs of SPPs quanta takes place due to time modulation of this length by the laser light. We suppose that one of the ends of the interface is situated at the coordinate $x = 0$ and the other at $x = L_0$. Due to the oscillations in the refractive index of SPPs the optical length of the interface L_t changes periodically in time

$$L_t = L + a\cos(\omega_0 t). \tag{6.2.5}$$

Here $L = L_0 n$, with n being the refractive index of the SPP under consideration, Furthermore, $a = l_0 \delta n_0$ is the amplitude of the oscillations in the optical length and l_0 ($\ll L$) is the length of the excited area. It is supposed that this length does not exceed the coherence length l_{SPP} of the SPP which is determined by the imaginary part of its refractive index: $l_{SPP} \sim c/\left(\omega \,\mathrm{Im}[n]\right)$). Let us now consider SPPs outside

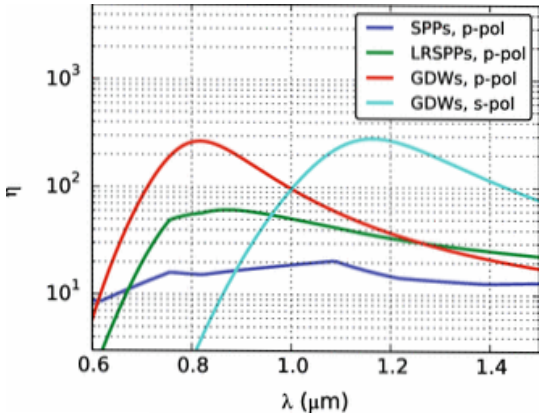

Figure 6.2.2: The illustration of the enhancement factors, η, for surface plasmon polaritons (SPPs), for long-range surface plasmon polaritons (LPSPPs) and for guided dielectric waves (GDWs).

the excited area at the interface.
If the rate of generation of the pairs $\dot{N}$ is sufficiently small, we find:

$$\dot{N} \ll \frac{c}{\lambda} \sim 10^{15} \ \text{sec}^{-1} \tag{6.2.6}$$

then we are in the regime of spontaneous emission of pairs of quanta.Thus, before the next pair of quanta is created the generated identical quanta leave the interface which makes our setup an exact source of two photon generation. This process differs from DCE of the microwaves in an optical cavity wherein we have a stimulated emission and the number of created quanta increases exponentially.

Consider now the generation of pairs of quanta in a 2D-waves limit and the wave vectors $\vec{\kappa}$ and $\vec{\kappa}'$ which have the components

$$\kappa_x = \frac{\pi\kappa}{L} \ , \ \kappa_y = \frac{\pi q}{l_1} \ \text{ and } \ \kappa'_x = \frac{\pi\kappa'}{L} \ , \ \kappa'_y = -\kappa'_y \tag{6.2.7}$$

These wave vector also follow the relation

$$\frac{|\vec{\kappa}|}{n} + \frac{|\vec{\kappa}'|}{n'} = \frac{\omega_0}{c_0} \tag{6.2.8}$$

, where $k, k', q = 0, 1, 2, ...$ In the following we calculate the number of created quanta $N_{k,q}$ with the mode (k, q) using the large-time asymptotic function of the field correlation.
We use the Bogoljubov transformation of the field operators to find the number of generated photons [139]

$$\hat{b}^{(1)}_{k,q} = \mu_{k,q}\hat{b}_{k,q} + \nu_{k,q}\hat{b}^{\dagger}_{k,q} \tag{6.2.9}$$

where $\hat{b}_k$ and $\hat{b}_k^{(1)}$ are the annihilation operators of the mode (k,q) for a small and a large time scale. Herein, $\mu_{k,q}$ and $\nu_{k,q}$ are the complex parameters satisfying the condition $|\mu_{k,q}|^2 = 1 + |\nu_{k,q}|^2$. The number of created photons is obtained from

$$N_{k,q} = |\nu_{k,q}|^2 . \tag{6.2.10}$$

Here we use another, although similar way to find N_k based on the calculation of the large time asymptotic of the pair correlation function $d_{k,q}(t,\tau)$ of the field operator $\hat{A}_{k,q}$ which can be written as [140]

$$\hat{A}_{k,q}(t) = \sqrt{\frac{\hbar}{2\omega_{k,q}}}\hat{b}_{k,q}^{(1)} e^{-i\omega_{k,q}t}. \tag{6.2.11}$$

where $\omega_{k,q}$ is the frequency of the mode (k,q)

$$\omega_{k,q} = c\sqrt{(\frac{\pi k}{L})^2 + (\frac{\pi q}{l_1})^2} \tag{6.2.12}$$

Then, in the large time scale we have for the correlation function $d_{k,q}(t,\tau)$

$$d_{k,q}(t,\tau) = \langle 0|\hat{A}_{k,q}^{\dagger}(t+\tau)\hat{A}_{k,q}(t)|0\rangle = (\frac{\hbar}{2\omega_{k,q}})N_k e^{i\omega_{k,q}\tau} \tag{6.2.13}$$

with $|0\rangle$ being the initial zero-point state. Thus, $N_{k,q}$ can be reformulated as

$$N_{k,q} = (\frac{2\omega_{k,q}}{\hbar})e^{-i\omega_{k,q}\tau}\langle 0|\hat{A}_{k,q}^{\dagger}(t+\tau)\hat{A}_{k,q}(t)|0\rangle, \text{ for } t \to \infty. \tag{6.2.14}$$

In the situation where there are no laser excitations then the operator of the mode (k,q) is given by equation

$$\hat{A}_{k,\vec{q}}^{(0)}(t) = \sqrt{\frac{\hbar}{2\omega_{k,q}}}\left(\hat{a}_{k,\vec{q}}e^{-i\omega_{k,q}t} + \hat{a}_{k,\vec{q}}^{+}e^{i\omega_{k,q}t}\right) \tag{6.2.15}$$

where $\hat{a}_{k,\vec{q}}$ stands for the destruction operator of the undisturbed field. The field operator $\hat{A}$ of SPPs in this area satisfies the Klein-Gordon wave equation in 2D

$$\ddot{\hat{A}} + c^2(\frac{\partial^2\hat{A}}{\partial x^2} + \frac{\partial^2\hat{A}}{\partial y^2}) = 0. \tag{6.2.16}$$

As boundary conditions we consider here $\hat{A}(x=0,t) = 0$ and $\hat{A}(x=L_t,t) = 0$. Here c is the phase velocity of the SPP under consideration and we neglect its dependence on frequency. Therefore the x and y dependence of this operator can be presented as the linear combination of the plane wave operators. We take

$$\hat{A}(x,y,t) = \sum_{k,q}\hat{A}_{k,q}e^{iqy}\sin(\frac{\pi kx}{L_t}) \tag{6.2.17}$$

By inserting this operator into the Eq. (6.2.16) in the large L/λ limit we obtain the following equation:

$$\sum_{k=-\infty}^{\infty}\left[\left(\ddot{\hat{A}}_{k,q}+\omega_{k,q}^2\hat{A}_{k,q}\right)\sin(\pi kxL_t^{-1})-k\pi xL_t^{-2}(2\dot{L}_t\dot{\hat{A}}_{k,\vec{q}}+\ddot{L}_t\hat{A}_{k,q})\cos(\pi kxL_t^{-1})\right]=0 \tag{6.2.18}$$

Thereby, the terms $\propto L_t^{-m}$ with $m \gg 3$ are neglected. We now make use of the equation for the Fourier series of the saw-tooth wave

$$x=-\sum_{j\neq 0}(-1)^j j^{-1}\sin(jx), \quad x-\pi\in 2\pi n \text{ for } (n=\pm 1,\pm 2,...) \tag{6.2.19}$$

which allow us to reformulate the Eq.(two before) for $\hat{A}_{k,q}=(-1)^k\hat{A}_{k,q}$ as

$$\ddot{\hat{A}}_k+\omega_k^2\hat{A}_k=\omega_k\hat{B}_k \tag{6.2.20}$$

where the frequency of the modes is $\omega_k=\pi ck/L$, and the operator $\hat{B}_{k,q}$ is written as:

$$\hat{B}_{k,q}=\sum_{j\neq k}\frac{j(2\dot{L}_t\dot{\hat{A}}_{j,q}+\ddot{L}_t\hat{A}_{j,q})}{\pi c(j^2-k^2)} \tag{6.2.21}$$

The operator $\hat{B}_k$ stands for the effect of oscillations of the optical length and for dynamical Casimir effect in the case considering the emission due to oscillations of optical length. To find $d_{k,q}(\tau)$ and $N_{k,q}$ we write Eq. (6.2.20) in its integral form

$$\hat{A}_{k,q}(t)=\hat{A}_{k,q}^{(0)}(t)-\int_{-\infty}^{t}\sin(\omega_{k,q}(t-t'))\hat{B}_{k,q}(t')dt' \tag{6.2.22}$$

where $\hat{A}_{k,q}^{(0)}(t)$ represents the operator of the undisturbed field. Consequently,one can use the theory presented above to find the intensity and the spectrum of the emission . In the case of steady oscillations of the optical length, one may consider the limit of large time ($t\to\infty$). Due to the nonzero contribution to the integral in Eq. (6.2.22) this limit comes from the terms proportional to $e^{\pm i(\omega_0-\omega_{k,q}-\omega_{j,q})t}$ with $\omega_{j,q}+\omega_{k,q}=\omega_0$. This means that we can take

$$2\dot{L}_t\dot{\hat{A}}_j+\ddot{L}_t\hat{A}_j\cong a\left(\frac{\pi c_0}{L}\right)^2(j^2-k^2)\cos(\omega_0 t)\hat{A}_{j,q} \tag{6.2.23}$$

Correspondingly, the denominator (j^2-k^2) in the equation for $\hat{B}_{k,q}$ cancels and we can approximate $\hat{B}_{k,q}\cong\hat{B}_q$ we then have

$$\hat{B}_q=2a\cos(\omega_0 t)\hat{Q}_q \tag{6.2.24}$$

where the operator $\hat{Q}_q$ is written as

$$\hat{Q}_q=L^{-1}\sum_{j=1}^{\infty}\omega_j\hat{A}_{j,q}(t) \tag{6.2.25}$$

with $\omega_j = \pi cj/L$. Inserting Eq. (6.2.22) and Eq. (6.2.24) into Eq. (6.2.14) and also taking into account that the negative frequency term proportional to $e^{i\omega_{k,q}\tau}$ in the correlation function $d_k(\tau)$ follows from the $\sin(\omega_k(t+\tau-t'))$ in Eq. (6.2.22), we can reformulate it as

$$N_{k,q}(t) \simeq \frac{a^2\omega_{k,q}}{2\hbar L}\int_{-\infty}^{t} dt_1 \int_{-\infty}^{t} dt_1' e^{i(\omega_0-\omega_{k,q})(t_1-t_1')} D_q(t_1,t_1') \tag{6.2.26}$$

with $\omega_k = \pi ck/L$. The correlation function of the field perturbation $D_q(t_1,t_1')$ is defined by:

$$D_q(t_1,t_1') = L\langle 0|\hat{Q}_q^\dagger(t_1)\hat{Q}_q(t_1')|0\rangle \tag{6.2.27}$$

Taking now into account that in the limit $t_1, t_1' \to \infty$ the pair-correlation function only depends on the time difference meaning $D_q(t_1,t_1') = D_q(t_1-t_1')$ we can formulate the following equation for the emission rate

$$\dot{N}_{k,q} = \left(\frac{a^2}{2\hbar L}\right)\omega_{k,q} D_q(\omega_0-\omega_{k,q}) \tag{6.2.28}$$

where $D_q(\omega)$ is the Fourier transform of $D_q(t)$. In the limit $L \to \infty$ the discrete quantities k and ω_k can be replaced by the continuous variables k and ω. This gives rise to a more simple version of the equation for the spectral density of the emission rate

$$\dot{N}_q(\omega) \equiv \frac{dN_q(\omega)}{dt} = \left(\frac{a^2}{2\pi c\hbar}\right)\omega\, D_q\left(\omega_0-\omega_q\right) \tag{6.2.29}$$

where $D_q(\omega) = \int_{-\infty}^{\infty} dt e^{i\omega t} D_q(t)$ is the spectral function.
To find the rate of emission we need to calculate the spectral function $D_q(\omega_0-\omega_{k,q})$

$$D_q(\omega_0-\omega_{k,q}) = \int_{-\infty}^{\infty} d\tau e^{(i\omega_0-\omega_{k,q})\tau} D_q(\tau). \tag{6.2.30}$$

One can observe from Eq. (6.2.20) and Eq. (6.2.24) that the DCE takes place due to the quantum modes of perturbation in time. As a matter of fact, $\hat{B}_q(t)$ stands for this perturbation which is k independent. Consequently, $\hat{B}_q(t)$ has a localization in the direction of x and comes from the mirrors. This makes mirrors the center for generation of radiation, wherein, the emitted quanta fill the space between the mirrors and then leave the resonator through an optical prism.
From this point the solution of D_q depends on the approximation that we make. First, we show the solution for the case where the amplitude of the oscillation in the optical length is much smaller than the wavelength of SPP, where one needs to use the perturbation theory. Second, after presenting that specific solution, we give a general way of treating this problem without limitations for dimensionless parameter v.

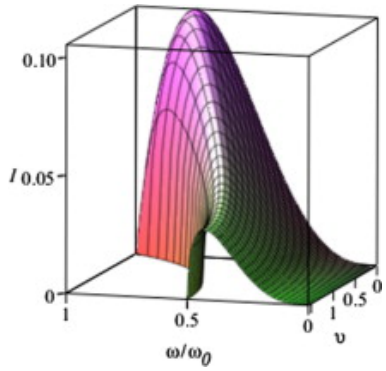

Figure 6.2.3: Dependence of the rate of emission on spectral and angular parameters ϑ, ω/ω_0.

6.2.3 Solution for $v \ll 1$

Here we discuss the case of small amplitudes of oscillations of the optical length compared to the wave length $\lambda = 2\pi/\omega$ of the SPP: $a \ll \lambda$. In this case the velocity $V = a\omega$ of oscillations of the optical length is small compared to the phase velocity: $V \ll c$. This implies for the dimensionless parameter: $v \ll 1$. The case $V \sim c$ was considered in [141, 142]. Then one can take

$$\hat{Q}(t) \approx \hat{Q}^{(0)}(t) = L^{-1} \sum_{j=1}^{\infty} \omega_j \hat{A}_j^{(0)}(t) \tag{6.2.31}$$

in Eq. (6.2.27), which results in

$$D_q(\tau) \approx D_q^{(0)}(\tau) = \frac{\hbar}{2L} \sum_{j=1}^{\infty} \frac{\omega_j^2}{\omega_{j,q}} e^{-i\omega_{j,q}\tau}. \tag{6.2.32}$$

Again for the limit of large length L/λ we can substitute the discrite sum over j by a continuous integral over $\omega' = \pi cj/L$. Additionally, we take relation $dj = Ld\omega'/\pi c$ into account. By doing so we arrive at less complicated equation for D_q

$$D_q(\omega - \omega_{k,q}) = \hbar c^{-1} \sqrt{(\omega_0 - \omega_{k,q})^2 - \omega_q^2} \tag{6.2.33}$$

where $\omega_q = \pi cq/L$. By substituting D_q in Eq. (6.2.29) we obtain the SPP rate of generation:

$$\dot{N}_{k,q} \approx \frac{a^2 \omega_{k,q}}{2Lc} \sqrt{(\omega_0 - \omega_{k,q})^2 - \omega_q^2} \tag{6.2.34}$$

For the limitation that $v \ll 1$ we have the number of corresponding modes $\omega_0^2 L l_1/(4\pi c^2)$.This makes the SPP rate of emission linearly dependent on l_1 and in the L, l_1 limits the summation over modes can be replaced by an integral. The integral has the form of

$\int ...dkdq$ where $dkdq = \omega L l_1 d\omega dv/(\pi c^2)$ with the angle of emission $\vartheta = \arcsin(k_y/k_c)$. By solving this integral we get

$$\dot{N}_{k,q} = \frac{4\pi^2 a^2 l_1}{\lambda_0^3}(\frac{\omega}{\omega_0})^3 \sqrt{[(1-\frac{\omega}{\omega_0})^2 - (\frac{\omega}{\omega_0})^2 \sin^2(\vartheta)]}. \tag{6.2.35}$$

One should keep in mind that $I = \dot{N}(\omega, \vartheta)$ is a dimensionless quantity and has a dependence on the spectral and the angular parameters. This dependence is shown in Fig.3. It is also possible to compute the total rate of emission of pairs of photons over the angular and the spectral domain as

$$\dot{N} = 2\int_0^{\vartheta} d\vartheta \int_0^{\omega_0/(1+sin\vartheta)} d\omega \dot{N}(\omega, \vartheta) \approx 2\alpha_{\vartheta_0} a^2 l_1 \omega_0/\lambda_0^3 \tag{6.2.36}$$

wherein, $\vartheta_0 = \arctan(l_1/l)$. The parameter α_{ϑ_0} is of order 1.

6.2.4 Solution for the case of general v

The amplitude of the oscillations in time of the refractive index n in the order of magnitude is obtained from Eq. (6.2.3). Analogously, one may get an enhancement of the dimensionless parameters v for GDWs and DWs. For SPPs the enhancement factor η may reach 30 with $l_\Delta \sim 1$ mm. For long-range SPPs one can achieve even significantly larger η and l_Δ. Even for GDWs and for DWs one gets η and l_Δ due to small losses in dielectrics. In these cases one can get $v \gtrsim 1$ already for rather moderate excitations $I_0 \lesssim 10^5$ W/m^2. In such a case the working nonlinear interaction is not weak anymore and Eqs. (6.2.4) is not applicable. To find the rate of emission of photons due to DCE one needs to develop a more general theory. It appears that there exists a characteristic interaction corresponding to v when the emission is strongly enhanced.
For the general calculation of the rate of emission one needs to find the spectral function. To this end we use Eqs. (6.2.21) and (6.2.22) which give

$$\hat{Q}_q(t) = \hat{Q}_q^{(0)}(t) - 2v\int_{-\infty}^{\infty} dt_1 G(t-t_1)\cos(\omega_0 t_1)\hat{Q}_q(t_1) \tag{6.2.37}$$

where $v = a\omega_0/c$ is the maximum dimensionless velocity of the oscillations of the optical length. The two functions $\hat{Q}_q^{(0)}$ and $G(t)$ can be calculated as

$$\hat{Q}_q^{(0)} = L^{-1}\sum_j \omega_j \hat{A}_{j,q}^{(0)} \tag{6.2.38a}$$

$$G(t) = \Theta(t)\,(c/\omega_0 L)\sum_{k=1}^{k_m}\left(\omega_k^2/\omega_{k,q}\right)\sin(\omega_{k,q}t) \tag{6.2.38b}$$

where $\Theta(t)$ is the Heaviside step-function. Now one gets the following equation for $D_q(t-t')$

$$D_q(t-t') \simeq D_{0,q}(t-t') + v^2 \int_{-\infty}^{\infty} dt_1 \int_{\infty}^{\infty} dt_2 G(t-t_1)G(t_1-t_2)e^{i\omega_0(t_1-t_2)}D_q(t_1,t_2) \tag{6.2.39}$$

where

$$D_{0,q}(t-t') = L\langle 0|\hat{Q}_q^{(0)}(t)\hat{Q}_q(t')|0\rangle, \;\; t,t' \to \infty \tag{6.2.40}$$

The function $D^*_{0,q}(t-t')$ also satisfies Eq. (6.2.40) but with $D_q^{(0)}(t-t') = L\langle 0|\hat{Q}_q^{(0)}(t)\hat{Q}_q^{(0)}(t')|0\rangle$ instead of $D_{0,q}(t-t')$. Performing a Fourier transformation of Eq. (6.2.29) and replacing the sum over k by the integral over the frequency $\omega = \pi ck/L$ one gets

$$D_q(\omega) = D_{0,q}(\omega) + v^2 G(\omega)G^*(\omega_0-\omega)D_q(\omega)$$

where $\vartheta = \arcsin(cq/\omega)$. The functions $D_q^{(0)}$ and $G(\omega)$ are written as:

$$D_q^{(0)}(\omega_0-\omega) = (\hbar/2\pi c)\sqrt{(\omega_0-\omega)^2 - \omega^2\sin^2\vartheta} \tag{6.2.41a}$$

$$G(\omega) = \pi^{-1}\cos\vartheta\left[1 - \frac{\omega}{\omega_0}\sin\vartheta + \frac{\omega}{2\omega_0}\ln[\frac{(\omega_0-\omega)(1+\sin\vartheta)}{(\omega_0+\omega)(1-\sin\vartheta)} + \frac{i\pi\omega}{2\omega_0}]\right] \tag{6.2.41b}$$

One also can obtain an analogues equation for $D^*_{0,q}(\omega)$. Solving these equations we find

$$D_q(\omega) = D_q^{(0)}(\omega)\Big/\left|1 - v^2G(\omega)G^*(\omega_0-\omega)\right|^2. \tag{6.2.42}$$

Let us find now the spectral density of the rate of emission. In the limit $L, l_1 \gg \lambda_0$ the sum $\Sigma_{k,\vec{q}}$ can be replaced by the integral $(Ll_1/2\pi c)\int\int \omega d\omega d\vartheta$ which results in the following spectral and angular density of the rate of emission

$$I(\omega,\vartheta) = \frac{v^2 l_1\omega^2\cos\vartheta\sqrt{(\omega_0-\omega)^2 - \omega^2\sin^2\vartheta}}{2\pi\lambda_0\omega_0^3\left|1 - v^2G_\vartheta(\omega)G^*_\vartheta(\omega_0-\omega)\right|^2} \tag{6.2.43}$$

The total rate of emission of photon pairs is determined by the integral

$$I_T \simeq 2\int_0^{\vartheta_0} d\vartheta \int_0^{\omega_0/(1+\sin\vartheta)} d\omega\, I(\omega,\vartheta) \tag{6.2.44}$$

where $\vartheta_0 = \arctan(l_1/l_0)$ is the maximum angle of emission. Herein, we can also consider previous limitation of this setup where the dimensionless parameter is $v \ll 1$. From Eq. (6.2.43) it follows that for $v \ll 1$ the spectral rate of emission equals

$$I(\omega,\vartheta) \approx I^{(0)}(\omega,\vartheta) \approx \left(\frac{v^2 l_1}{2\pi\lambda_0\omega_0^3}\right)\omega^2\cos\vartheta\sqrt{(\omega_0-\omega)^2 - \omega^2\sin^2\vartheta} \tag{6.2.45}$$

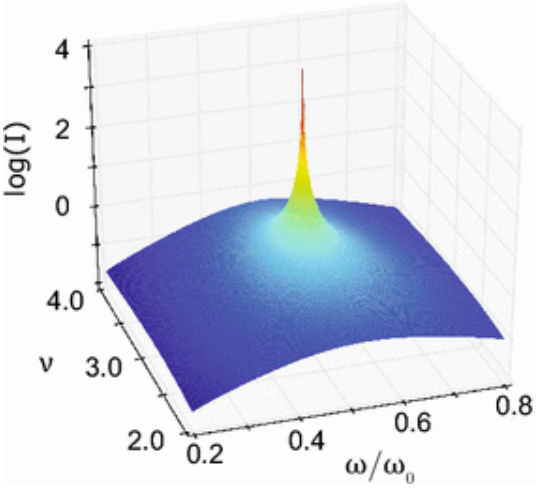

Figure 6.2.4: The relation between the intensity of forward emission ($\nu = 0$) on frequency and $v \approx |\chi^{(2)}|E_0$.

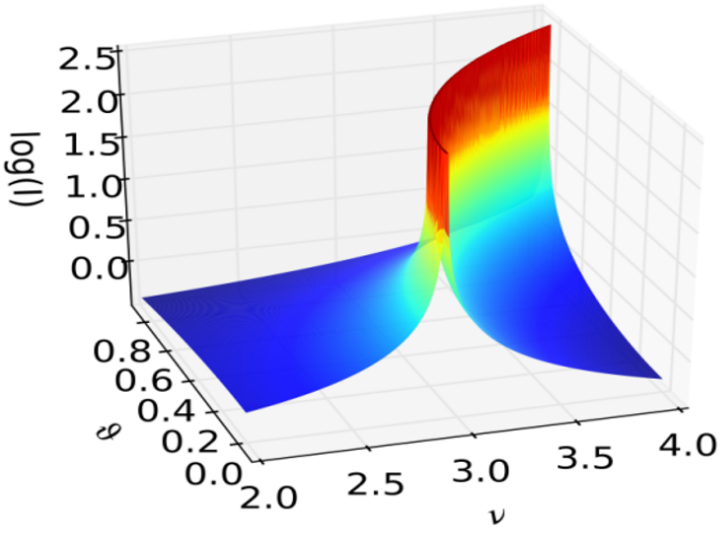

Figure 6.2.5: The relation of the spectral density of emission due to DCE on v and the emission angle ϑ. The red color emphasize the increase of intensity.

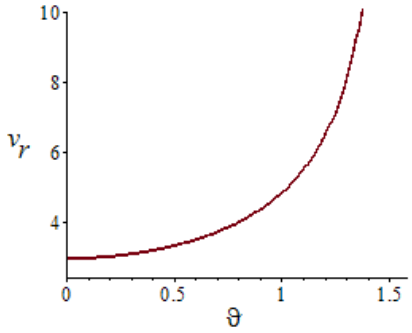

Figure 6.2.6: The correlation between v_r and the angle of emission ϑ.

The spectrum of emission is continuous. The total rate of the emission of the quanta integrated over all frequencies is

$$I_T^{(0)} \approx \frac{0.01\alpha_{\vartheta_0}\omega_0 v^2 l_1}{2\lambda_0} \tag{6.2.46}$$

where for $\vartheta_0 \sim 1$ (i.e. for $l_1 \sim l_0$) the dimensionless parameter $\alpha_{\vartheta_0} \sim 1$. e.g. $\alpha_{0.2\pi} \approx 1.1$ ($\vartheta_0 = 36^o$),$\alpha_{0.3\pi} \approx 1.3$ ($\vartheta_0 = 54^o$), and $\alpha_{0.3\pi} \approx 1.4$ ($\vartheta_0 = 72^o$). Taking into account that the rate of falling of photons of excitation to the area $l_0 l_1$ equals $I_0 l_0 l_1/\hbar\omega_0$, one gets the yield of emission in the order of magnitude which is given by Eq. (6.2.46).

If $v \geq 2.939$ then the yield of the emission is resonantly enhanced at the frequency $\omega = \omega_0/2$. The corresponding value of v equals to $v_r = 1/|G(1/2)|$ (see Fig. 6.2.7). The dependence of the resonant value v_r on the angle of emission ϑ is given in Fig. 6.2.6.

The main contribution to the rate of emission of quanta for $v \geq 2.9$ is given by a small frequency $\bar{\omega} = \omega - \omega_0/2$. Expanding the G-functions over $\bar{\omega}$ up to terms proportional to $\bar{\omega}^2$ included and considering that the integral

$$\int_{-\infty}^{\infty} \frac{dx}{((a^2 - b^2x^2)^2 + x^2)} = \frac{\pi}{|a|} \tag{6.2.47}$$

does not depend on b and one gets after the integration over $\bar{\omega}$ the following equation for the dependence of the rate of the emission on v and ϑ

$$I(v,\vartheta) \approx \frac{l_1\omega_0/\lambda_0 C_\vartheta}{\left|1 - (v/\pi)^2 \cos^2\vartheta \left(C_\vartheta^2 + \pi^2/16\right)\right|} \tag{6.2.48}$$

where C_ϑ is an angular dependent constant given by

$$C_\vartheta = \left|1 - \frac{1}{2}\sin\vartheta - \frac{1}{4}\left(\ln(3) + \ln\left(\frac{1-\sin\vartheta}{1+\sin\vartheta}\right)\right)\right|. \tag{6.2.49}$$

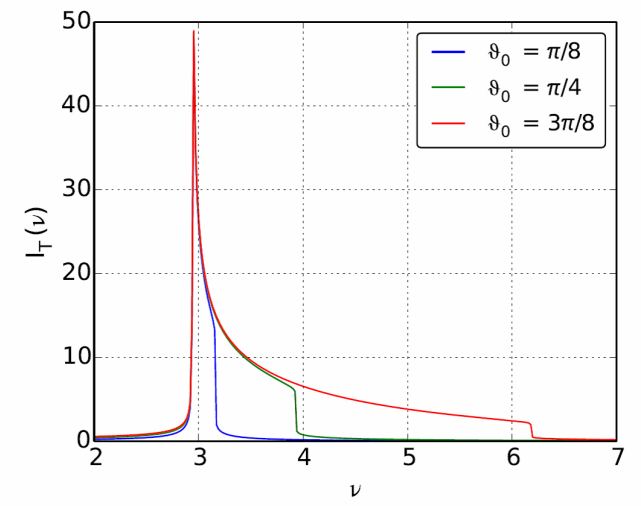

Figure 6.2.7: Dependence of the total intensity of emission $I_T = \int_0^{\vartheta_0} I(\vartheta)d\vartheta$ on v . Different values of the maximum angle of the emission $\vartheta_0 = \arctan(l_1/l_0)$.

The rate of emission integrated over angle then becomes

$$I_T(v) = 2\int_0^{\vartheta_0} d\vartheta I(v,\vartheta) \tag{6.2.50}$$

which has a sharp peak at $v \approx 2.94$ (see Fig. 7) and a smoothly diminishing tail at larger v.

6.2.5 Concluding remarks on production of pairs of entangled photons

In the case of $v \ll 1$, the main effect of the SPPs is a strong reduction of their group velocity leading to the enhancement of the field and by that, to the enhancement of the nonlinear interactions of the excitation. This enhancement can be described by the enhancement factor $P \sim \left(\eta_0(\omega_0)\eta^2(\omega_0/2)\right)^2$, where $\eta_0(\omega_0)$ is the renormalization of the laser field with frequency ω_0 at the interface in the case of normal incidence, $\eta(\omega_0/2)$ is the enhancement of the field of the SPPs with the frequency $\omega_0/2$.

Note that, according to [141, 142] one can expect to enlarge the yield additionally if one uses a sufficiently strong laser excitation. According to our considerations the dynamical Casimir effect at a metal-dielectric interface may allow one to prepare a source of entangled photons with a good yield of the order of $\kappa \sim 10^{-4}$ or even more.

From the consideration that $\vartheta > 1$, it follows that for the observation of the emission due to DCE there exists an optimal intensity of excitation, corresponding to $v_0 \approx 3$. The latter value of v is close to π which means that the enhancement takes place if $a_0 \approx \lambda_0$, i.e. if the full amplitude of the oscillations of the optical length

coincides with the wavelength of excitation and with the half of wavelength of emission. This phenomenon can be considered as a kind of parametric resonance describing a sharply enlarged response of the system (here the spontaneous two-photon emission) at a specific value of the external parameter (here the intensity of laser excitation $I_0 = I_r = 0.22\lambda_0^2/l_0^2\eta^4 Z_0 \left|\chi^{(2)}\right|^2$). For long-range SPPs, one may achieve $\eta \sim 10^2$ and $(\lambda_0/l_0)^2 \sim 10^9$. Taking $\left|\chi^{(2)}\right| \sim 10^{-12}$m/V one gets $I_r \sim 10^4$ W/m^2 which is a rather moderate intensity of the laser excitation.

If the intensity of the excitation is below I_r then the spectrum of emission due to DCE and the angular dependence of it are broad. However, the spectrum of emission becomes monochromatic when I_0 approaches the resonant value: both quanta have the same frequency $\omega = \omega_0/2$. The directions of the emission also become fixed: for $I = I_r$ the emission takes place along the resonator; with increasing I the emitted quanta propagate along two directions with an angle of $2\,|\vartheta|$ between them; the latter increases with increasing I.

Reaching the point of the resonance the yield of emission may two (or even more) orders of magnitude. Therefore, for the resonant case one can take

$$\zeta \sim \zeta_r \sim \eta^4 \hbar\omega_0^2 l_0 \left|\chi^{(2)}\right|^2 \frac{Z_0}{2\lambda_0^3}. \tag{6.2.51}$$

For SPPs one may have $\eta \sim 30$, $l_0 \sim l_\Delta \sim 10^{-3}$ m which gives for $\lambda = 2, \lambda_0 = 10^{-6}$ m and $\left|\chi^{(2)}\right| \sim 1$ pm/V the yield $\zeta \sim 10^{-3}$. One may achieve an even larger yield for the long-range SPPs, guided dielectric waves and D'yakonov waves. The resonance considered here may even allow one to get a full conversion of photons of the laser to photon pairs with the half frequency using DCE.

It is interesting to compare the two-photon spontaneous emission due to DCE discussed here and the spontaneous parametric down conversion (SPDC). Note that for both processes the emitted photon pairs are entangled. If the excitation is weak ,then, up to a dimensionless parameter of the order of 10^{-2} the equations for the yields of these processes differ only by the power of the ratio l_0/λ_0: $\zeta_{SPDC} \propto (l_0/\lambda_0)^2$ [143, 123], $\zeta_{DCE} \propto l_0/\lambda_0$ [119]. This means that in the case of weak excitation and ceteris paribus the SPDC is several orders of magnitudes more efficient. The spectrum of DCE is bi-chromatic and the emission is well directed. However, to get SPDC one needs to fulfill the phase-matching condition. In the case of the emission due to DCE, there is no phase matching condition, which essentially simplifies the experiment. Besides, in case of strong excitation (which, in fact may be not too strong at all) one can highly enhance the yield of the DCE-emission if it is applied to laser excitation with resonant intensity I_r. (At present it is not known, whether an analogous enhancement may exist for SPDC.). In this case the DCE-emission becomes monochromatic and well directed; for $I_0 > I_r$ the photons of a photon pair are emitted under a definite angle, the larger the bigger is the difference $I_0 - I_r$.
It is important to note that for such a setup one can generate polarization entangled photons. Indeed at the interface the mirror symmetry in z-direction is absent. Therefore the components $\chi^{(2)}_{y,yz}$ and $\chi^{(2)}_{y,zy}$ of the second-order nonlinear susceptibility

tensor describing generation of pairs of photons in x direction differ from zero (here the first index corresponds to polarization of the excitation, while last two indices correspond to the polarization of emitted quanta). This means that one of the generated SPPs has an y-polarization and another has a z-polarization. Due to the identity of both emitted SPPs their wave function must be a linear combination of the wave functions with both polarizations

$$|\psi\rangle_{yz} = \frac{1}{2}\left(|\psi_{1z}\rangle|\psi_{2y}\rangle + |\psi_{2z}\rangle|\psi_{1y}\rangle\right) \tag{6.2.52}$$

where $|\psi_{n\alpha_0}\rangle$ is the wave function of a photon number $n = 1, 2$ with polarization index $\alpha_0 = z, y$. This wave function of the pair of generated SPPs describes the basic for the quantum informatics Bell-type state. This state cannot be written as a product of two one-photon states. otherwise there will be a possibility to find both photons with the same polarization which is impossible here. This means that the generated pairs of surface plasmon polaritons and also the pairs of photons emitted by the interface are in the polarization entangled state. At that one of emitted photons will have y-polarization and another the orthogonal to y-polarization z'. Note that photons with different frequency are emitted in different directions. If to choose the polarization of one of them (signal) to be, e.g. y, then the polarization of another photon (idler) will be z'. However, if to choose polarization of the signal photon to be z' then the idler photon will be polarized in y-direction. It is just what one needs for using the polarization entangled photons for quantum cryptography [20].

7 Cascaded system 2: excitation via coherently and incoherently pumped biexciton

An example for the spontaneous emission of two photons in nonlinear optics is already discussed in chapter 6. The randomness and the low efficiency of the production of entangled photon[144] are downsides of these sources of two photon emission. The pair statistics of these sources are also in a Poissonian distribution that results in insubordinate many photon production [145]. Here, we introduce another quantum optical system which also can produce two entangled photons, namely biexciton. The richness of quantum phenomena that can be observed in biexciton system, makes them a desirable candidate for the exploitation to cascade quantum systems.
In the current chapter we first explore the possibilities and aspects that a biexciton offers for two photon emission. Then, we consider a cascaded system consisting of two coupled biexcitons. By applying the cascaded formalism for such coupled systems, we derive the full Lindblad master equations for the density matrix of the combined systems. We evaluate this master numerically equation for the case , wherein the source biexciton is excited by incoherent pumping. Our choice for the pumping mechanism is based on the fact that the strong coherent driving may destroy the biexciton structure which is a restriction for the biexciton two photons generation[146, 147]. While for the incoherent driving, we have no limits for the pumping strength. Finally, we present some results for an incoherently pumped source biexcition which is coupled to the target system and show that environment affects on the statistical mapping between two biexcitons.

7.1 Biexciton: a source for two photons emission

The physics of biexcitons , as a source for the non-classical light and two entangled photons, has been a matter of interests in the recent years[145, 148]. Biexcitons can be considered as a single quantum dot emitter in solid state physics[144]. The bunched and anti-bunched photon pairs as well as the polarization entanglement between the two emitted photons are the important aspects that make biexcitons an attractive candidate as a source of two photon emission. This stimulating features are based on the fact that biexcitons construct the coherent superposition of two quantum states. The typical example for that structure is a dot in the ground state $|00\rangle$. After the excitation we will have polarized exitonic states $|01\rangle$ and $|10\rangle$. Finally,

the coherence between these two states produces a biexciton state $|11\rangle$ which consist of two opposite spin excitons as result of the Coulomb coupling [149].
However there are different possible ways to excite a biexciton: here we restrict ourselves to the continues type of pumping, which is assumed to be either coherent(laser like) or incoherent. This varieties in the pumping scenario opens new possibilities to explore the dynamical behavior of biexciton(s). The schematics of the biexcition with different pumping scenarios is represented in Fig.7.1.1.

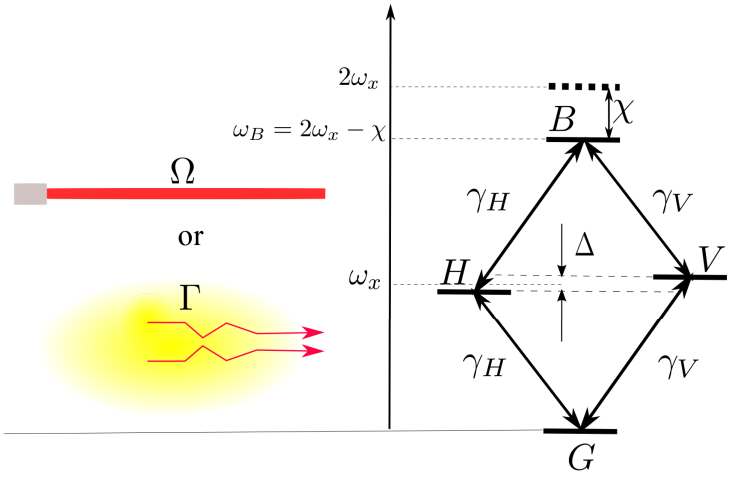

Figure 7.1.1: Representation of the pumped biexciton. The fine structure spliting Δ creates two polarized channels for two photon emission.

Typically, the transition from the ground state to the biexcition state is forbidden. Each transiton from biexciton to exciton(vertical or horizontal) and from exciton to ground state produces a photon. But there is also the possibility of what is the so called Leapfrog process, which is a direct transition from biexciton to ground state producing two photons. One can pump such system by using a laser(coherent light) with controllable intensity Ω or by incoherent light with pumping rate Γ. The biexciton frequency is two times of the average exciton frequency ω_x minus the biexciton binding energy χ.

7.2 Cascaded formalism for the coupled biexcitons

7.2.1 Hamiltonian of the coupled systems

First, we can define the general Hamiltonian as a sum of the system Hamiltonian plus the coupling Hamiltonian such that : $H = H_{sys} + H_c$. To compute the master equation for the coupling between two cascaded systems we concentrate on the coupling Hamiltonian H_c. Later in section 7.2.4 we treat the systems Hamiltonian,H_{sys},

respectively. For such a physical system the coupling Hamiltonian is given through

$$H_c = H_{XXs} + H_{XXt} + H_{int} + H_B \tag{7.2.1}$$

where the first two terms correspond to the free part of the Hamiltonian.The Hamiltonian of the source and the target which contributes in coupling dynamics are H_{XXs} and H_{XXt}. Each part can be written explicitly as

$$H_{XXs} = \hbar \sum_i \omega_i c_i^\dagger c_i \tag{7.2.2a}$$

$$H_{XXt} = \hbar \sum_j \omega_j P_j^\dagger P_j \tag{7.2.2b}$$

where we write the source and target systems Hamiltonian in the form of transition operators c_i, P_j. Naturally,at the same time, they can be written in a form of pseudo Pauli operators

$$H_{t/s} = \hbar(\omega_B \sigma_{BB}^m + \omega_H \sigma_{HH}^m + \omega_V \sigma_{VV}^m) \ . \tag{7.2.3}$$

The other parts of coupling Hamiltonian are defined as

$$H_B = \hbar \int d\omega \, \omega \, b_{\omega,H}^\dagger b_{\omega,H} + \hbar \int d\omega \, \omega \, b_{\omega,V}^\dagger b_{\omega,V} \tag{7.2.4a}$$

$$\begin{aligned} H_{int} = \hbar \int d\omega \, [\sum_{i=1}^{2} g_s^H(\omega)(c_{i,H}^\dagger b_{\omega,H} + h.c) + \sum_{j=1}^{2} g_t^H(\omega)(P_{j,H}^\dagger b_{\omega,H} e^{i\omega\tau'} + h.c)] \\ + \hbar \int d\omega \, [\sum_{i=1}^{2} g_s^V(\omega)(c_{i,V}^\dagger b_{\omega,V} + h.c) + \sum_{j=1}^{2} g_t^V(\omega)(P_{j,V}^\dagger b_{\omega,V} e^{i\omega\tau'} + h.c)] \end{aligned} \tag{7.2.4b}$$

where H_B and H_{int} are Hamiltonian of the bath and interaction. Moreover, $b_\omega^\dagger$ is a waveguide operator and, according to the Jordan–Wigner like transformation

$$c_{i,X} = \begin{cases} \sigma_{GX}^s \\ \sigma_{XB}^s \end{cases} \qquad P_{j,X} = \begin{cases} \sigma_{GX}^t \\ \sigma_{XB}^t \end{cases} \tag{7.2.5}$$

Additionally, the time delay between the source and target is taken to be τ'. Also we should keep in mind that the the time delay is assumed to be the same for the both horizontally and vertically polarized channels. Then we can write H_c as

$$\frac{H_c}{\hbar} = \int d\omega\, \omega\, b^\dagger_{\omega,H} b_{\omega,H} + \int d\omega\, \omega\, b^\dagger_{\omega,V} b_{\omega,V} + \sum_{j=1}^{2} \omega_j P_j^\dagger P_j + \sum_{i=1}^{2} \omega_i c_i^\dagger c_i$$
$$+ \int d\omega\, [\sum_{i=1}^{2} g_s^H(\omega)(c^\dagger_{i,H} b_{\omega,H} + h.c) + \sum_{j=1}^{2} g_t^H(\omega)(P^\dagger_{j,H} b_{\omega,H} e^{i\omega\tau'} + h.c)]$$
$$+ \int d\omega\, [\sum_{i=1}^{2} g_s^V(\omega)(c^\dagger_{i,V} b_{\omega,V} + h.c) + \sum_{j=1}^{2} g_t^V(\omega)(P^\dagger_{j,V} b_{\omega,V} e^{i\omega\tau'}] + h.c)]. \quad (7.2.6)$$

By moving to the interaction picture the coupling Hamiltonian is expressed as

$$\frac{H_c}{\hbar} = \sum_{i=1}^{2} \int d\omega g_s^H(\omega)(c^\dagger_{i,H} e^{i\omega_i t} b_{\omega,H} e^{-i\omega t} + c_{i,H} e^{-i\omega_i t} b^\dagger_{\omega,H} e^{i\omega t})$$
$$+ \sum_{j=1}^{2} \int d\omega\, g_t^H(\omega)(P^\dagger_{j,H} e^{i\omega_j t} b_{\omega,H} e^{-i\omega t} e^{i\omega\tau'} + P_{j,H} e^{-i\omega_j t} b^\dagger_{\omega,H} e^{i\omega t} e^{-i\omega\tau'})$$
$$+ \sum_{i=1}^{2} \int d\omega g_s^V(\omega)(c^\dagger_{i,V} e^{i\omega_i t} b_{\omega,V} e^{-i\omega t} + c_{i,V} e^{-i\omega_i t} b^\dagger_{\omega,V} e^{i\omega t})$$
$$+ \sum_{j=1}^{2} \int d\omega\, g_t^V(\omega)(P^\dagger_{j,V} e^{i\omega_j t} b_{\omega,V} e^{-i\omega t} e^{i\omega\tau'} + P_{j,V} e^{-i\omega_j t} b^\dagger_{\omega,V} e^{i\omega t} e^{-i\omega\tau'}) \quad (7.2.7)$$

where $\sigma_{mn} = |m\rangle\langle n|$ is defined as pseudo Pauli operators and stands for vertical or horizontal excitons, $X = H$ or V.

By defining $\Gamma_m^H(t) = \int d\omega g_i^H(\omega) e^{-i\omega t} b_\omega e^{i\omega\tau'}$ and $\Gamma_m^V(t) = \int d\omega g_i^V(\omega) e^{-i\omega t} b_\omega e^{i\omega\tau'}$ $(m = s, t)$ where we inserted $e^{i\omega\tau'}$ into the definition of $\Gamma_i(t)$ in the way that $\tau' = 0$ for the $m = s$, there is no time delay between the source and itself. We can write the above equation in form of

$$H_c/\hbar = \sum_{i=1}^{2} (c^\dagger_{i,H} e^{i\omega_i t} \Gamma_s^H(t) + c_{i,H} e^{-i\omega_i t} \Gamma_s^{\dagger H}(t))$$
$$+ \sum_{j=1}^{2} (P^\dagger_{j,H} e^{i\omega_j t} \Gamma_t^H(t) + P_{j,H} e^{-i\omega_j t} \Gamma_t^{\dagger H}(t))$$
$$+ \sum_{i=1}^{2} (c^\dagger_{i,V} e^{i\omega_i t} \Gamma_s^V(t) + c_{i,V} e^{-i\omega_i t} \Gamma_s^{\dagger V}(t))$$
$$+ \sum_{j=1}^{2} (P^\dagger_{j,V} e^{i\omega_j t} \Gamma_t^V(t) + P_{j,V} e^{-i\omega_j t} \Gamma_t^{\dagger V}(t)) \quad (7.2.8)$$

7.2.2 General derivation of master equation

From the Born approximation, $\rho_{tot} \approx \rho(t) \otimes \rho_B$, the evolution of density matrix is written as

$$\frac{\partial \rho}{\partial t} = -\frac{1}{\hbar^2} \int ds\, tr_B \left\{ [H_c(t), [H_c(s), \rho(s)\rho_B]] \right\}. \tag{7.2.9}$$

Transforming the coupling Hamiltonian to a summation formula

$$\frac{H_c(t)}{\hbar} = \sum_{X=H,V} \sum_{l} f_{l,X} \Gamma_l^X \tag{7.2.10}$$

which can be red for $X = H, V$. Each components of summation can be defined as

$$f_{1,X}(t) = c_{i,X}^{\dagger} e^{i\omega_i t} \quad f_{2,X}(t) = c_{i,X} e^{-i\omega_i t} \quad f_{3,X}(t) = P_{j,X}^{\dagger} e^{i\omega_j t} \quad f_{4,X}(t) = P_{j,X} e^{-i\omega_j t}. \tag{7.2.11}$$

$$\Gamma_1^X = \Gamma_s^X(t) \quad \Gamma_2^X = \Gamma_s^{\dagger X}(t) \quad \Gamma_3^X = \Gamma_t^X(t) \quad \Gamma_4^X = \Gamma_t^{\dagger X}(t) \tag{7.2.12}$$

Thus, the Eq. 7.2.9 can be written as

$$\frac{\partial \rho}{\partial t} = -\frac{1}{\hbar^2} \sum_{X=H,V} \sum_{l.k} \int_0^t dstr_B \{ [f_{l,X}(t)\Gamma_l^X(t), [f_{k,X}(s)\Gamma_k^X(s), \rho(s)\rho_B]] \}. \tag{7.2.13}$$

One should notice that the Hamiltonian $H_c(t)$differs from$H_c(s)$and we separate them respectively in our abbreviation $l \to k$ and in the transition operators as$i \to i'$and $j \to j'$.

To simplify the master equation, we firstly analyze the correlation functions of the bath $\langle \Gamma_l(t)\Gamma_k(s) \rangle_B$ and $\langle \Gamma_k(s)\Gamma_l(t) \rangle_B$. In the beginning the$\Gamma_l$'s are defined as

$$\begin{cases} \Gamma_s^X(t) = \int d\omega\, g_s^X(\omega)\, e^{-i\omega t} b_{\omega,X} \\ \Gamma_s^{\dagger X}(t) = \int d\omega\, g_s^X(\omega)\, e^{i\omega t} b_{\omega,X}^{\dagger} \end{cases} \quad \begin{cases} \Gamma_t^X(t) = \int d\omega\, g_t^X(\omega)\, e^{-i\omega t} b_{\omega,X} e^{i\omega\tau'} \\ \Gamma_t^{\dagger X}(t) = \int d\omega\, g_t^X(\omega)\, e^{i\omega t} b_{\omega,X}^{\dagger} e^{-i\omega\tau'} \end{cases} \tag{7.2.14}$$

As a part of the Markovian master equation one can assume that $\langle \Gamma_i(t)\Gamma_k(s) \rangle_B \approx \delta(t-s)$ which results from the that many correlation function of bath with tend to zero.In addition , one should keep in mind that the bath correlation functions between vertical and horizontal polarization channels are zero. Consequently, herein, we tend to find the non-zero correlation functions of the bath. It can be proven that the only remaining non-zero correlation functions are:

$$\left\langle \Gamma_s^H(t)\Gamma_s^{\dagger H}(s) \right\rangle_B \neq 0, \left\langle \Gamma_t^H(t)\Gamma_t^{\dagger H}(s) \right\rangle_B \neq 0, \left\langle \Gamma_s^H(t)\Gamma_t^{\dagger H}(s) \right\rangle_B \neq 0$$
$$\left\langle \Gamma_t^H(t)\Gamma_s^{\dagger H}(s) \right\rangle_B \neq 0 \tag{7.2.15a}$$

$$\left\langle \Gamma_s^V(t)\Gamma_s^{\dagger V}(s) \right\rangle_B \neq 0, \left\langle \Gamma_t^V(t)\Gamma_t^{\dagger V}(s) \right\rangle_B \neq 0, \left\langle \Gamma_s^V(t)\Gamma_t^{\dagger V}(s) \right\rangle_B \neq 0$$
$$\left\langle \Gamma_t^V(t)\Gamma_s^{\dagger V}(s) \right\rangle_B \neq 0 \tag{7.2.15b}$$

The corresponding non-zero correlation functions in Eq. (7.2.13) are

$$\left\langle \Gamma_1^H(t)\Gamma_2^H(s)\right\rangle_B \neq 0, \left\langle \Gamma_1^H(t)\Gamma_4^H(s)\right\rangle_B \neq 0, \left\langle \Gamma_3^H(t)\Gamma_4^H(s)\right\rangle_B \neq 0, \left\langle \Gamma_3^H(t)\Gamma_2^H(s)\right\rangle_B \neq 0 \tag{7.2.16a}$$

$$\left\langle \Gamma_1^V(t)\Gamma_2^V(s)\right\rangle_B \neq 0, \left\langle \Gamma_1^V(t)\Gamma_4^V(s)\right\rangle_B \neq 0, \left\langle \Gamma_3^V(t)\Gamma_4^V(s)\right\rangle_B \neq 0, \left\langle \Gamma_3^V(t)\Gamma_2^V(s)\right\rangle_B \neq 0 \tag{7.2.16b}$$

Rewriting the Eq. (7.2.13) with the remaining correlation functions respectively we have

$$\begin{aligned}\frac{\partial\rho}{\partial t} = -\frac{1}{\hbar^2}\sum_{X=H,V}\int_0^t ds\Big\{&[[f_{1,X}(t)f_{2,X}(s)\rho(s) - f_{2,X}(s)\rho(s)f_{1,X}(t)]\\ &\left\langle \Gamma_1^X(t)\Gamma_2^X(s)\right\rangle_B + h.c]\\ &+ [[f_{3,X}(t)f_{4,X}(s)\rho(s) - f_{4,X}(s)\rho(s)f_{3,X}(t)]\left\langle \Gamma_3^X(t)\Gamma_4^X(s)\right\rangle_B + h.c]\\ &+ [[f_{1,X}(t)f_{4,X}(s)\rho(s) - f_{4,X}(s)\rho(s)f_{1,X}(t)]\left\langle \Gamma_1^X(t)\Gamma_4^X(s)\right\rangle_B + h.c]\\ &+ [[f_{3,X}(t)f_{2,X}(s)\rho(s) - f_{2,X}(s)\rho(s)f_{3,X}(t)]\left\langle \Gamma_3^X(t)\Gamma_2^X(s)\right\rangle_B + h.c]\Big\}.\end{aligned} \tag{7.2.17}$$

We can write the functions with their definitions in Eq. 7.2.11 and by a careful adjustment of summation process we arrive at

$$\begin{aligned}\frac{\partial\rho}{\partial t} = -\frac{1}{\hbar^2}\sum_{X=H,V}\int_0^t ds\Big\{&\sum_{i=1}^{2}\sum_{i'=1}^{2}[[c_{i,X}^\dagger e^{i\omega_i t}c_{i',X}e^{-i\omega_{i'}s}\rho(s) - c_{i',X}e^{-i\omega_{i'}s}\rho(s)c_{i,X}^\dagger e^{i\omega_i t}]\\ &\left\langle \Gamma_s^X(t)\Gamma_s^{\dagger X}\right\rangle_B + h.c]\\ &+\sum_{j=1}^{2}\sum_{j'=1}^{2}[[P_{j,X}^\dagger e^{i\omega_j t}\rho(s)P_{j',X}e^{-i\omega_{j'}s} - P_{j',X}e^{-i\omega_{j'}s}\rho(s)P_{j,X}^\dagger e^{i\omega_j t}]\left\langle \Gamma_t^X(t)\Gamma_t^{\dagger X}(s)\right\rangle_B + h.c]\\ &+\sum_{i=1}^{2}\sum_{j=1}^{2}[[c_{i,X}^\dagger e^{i\omega_i t}P_{j,X}e^{-i\omega_j s}\rho(s) - P_{j,X}e^{-i\omega_j s}\rho(s)c_{i,X}^\dagger e^{i\omega_i t}]\left\langle \Gamma_s^X(t)\Gamma_t^{\dagger X}(s)\right\rangle_B + h.c]\\ &+\sum_{i=1}^{2}\sum_{j=1}^{2}[[P_{j,X}^\dagger e^{i\omega_j s}c_{i,X}e^{-i\omega_i t}\rho(s) - c_{i,X}e^{-i\omega_i t}\rho(s)P_{j,X}^\dagger e^{i\omega_j s}]\left\langle \Gamma_t^X(t)\Gamma_s^{\dagger X}(s)\right\rangle_B + h.c]\Big\}\end{aligned} \tag{7.2.18}$$

Defining $\tau = t - s$ we can rearrange the above equation in the form of

$$\frac{\partial\rho}{\partial t} = -\frac{1}{\hbar^2}\sum_{X=H,V}\int_0^t d\tau\Big\{\sum_{i=1}^{2}\sum_{i'=1}^{2}[[c^\dagger_{i,X}c_{i',X}\rho(t-\tau) - c_{i',X}\rho(t-\tau)c^\dagger_{i,X}]e^{i\omega_i t - i\omega_{i'}t + i\omega_{i'}\tau}$$
$$\left\langle\Gamma^X_s(t)\Gamma^{\dagger X}_s(t-\tau)\right\rangle_B + h.c]$$
$$+\sum_{j=1}^{2}\sum_{j'=1}^{2}[[P^\dagger_{j,X}P_{j',X}\rho(t-\tau) - P_{j',X}\rho(t-\tau)P^\dagger_{j,X}]e^{i\omega_j t - i\omega_{j'}t + i\omega_{j'}\tau}\left\langle\Gamma^X_t(t)\Gamma^\dagger_t(t-\tau)\right\rangle_B + h.c]$$
$$+\sum_{i=1}^{2}\sum_{j=1}^{2}[[c^\dagger_{i,X}P_{j,X}\rho(t-\tau) - P_{j,X}\rho(t-\tau)c^\dagger_{i,X}]e^{i\omega_i t - i\omega_j t + i\omega_j\tau}\left\langle\Gamma^X_s(t)\Gamma^{\dagger X}_t(t-\tau)\right\rangle_B + h.c]$$
$$+\sum_{i=1}^{2}\sum_{j=1}^{2}[[P^\dagger_{j,X}c_{i,X}\rho(t-\tau) - c_{i,X}\rho(t-\tau)P^\dagger_{j,X}]e^{-i\omega_i t + i\omega_j t - i\omega_j\tau}\left\langle\Gamma^X_t(t)\Gamma^{\dagger X}_s(t-\tau)\right\rangle_B + h.c]\Big\} \tag{7.2.19}$$

Now we can evaluate the correlation function of the bath properties. We assume $\bar{n}(\omega,T) = 0 \to [\bar{n}(\omega,T)+1] = 1$. This means that we have zero mean photon number for the bath harmonic oscillators(at temperature $T$for the thermal equilibrium). There are other assumptions to be made. First, we assume that the bath is in the vacuum field and the density of state which determines the numbers of frequencies of the oscillators in bath is one , $G(\omega) = 1$. This is due to the fact that we presumed all harmonic oscillators to communicate with system in one frequency namely frequency of the system.
Secondly, as apart of the Markovian approximation we presume that the coupling strength to the bath is the frequency independent so again for a compact form $X = H, V$ we will have:

$$g^X_s(\omega) = g^X_s = \sqrt{\frac{\gamma^X_s}{2\pi}} \qquad g^X_t(\omega) = g^X_t = \sqrt{\frac{\gamma^X_t}{2\pi}} \tag{7.2.20}$$

Then the integrals in the frequency domain reads

$$\left\langle \Gamma_s^X(t)\Gamma_s^{\dagger X}(t-\tau)\right\rangle_B = \int_0^\infty \left|g_s^X\right|^2 e^{-i\omega\tau} tr_B\left[B_0 b_{\omega,X} b_{\omega,X}^\dagger\right] d\omega$$
$$= \int_{-\infty}^{+\infty} \left|g_s^X\right|^2 e^{-i\omega\tau} G(\omega) d\omega = \gamma_s^X \delta(-\tau) \quad (7.2.21a)$$

$$\left\langle \Gamma_t^X(t)\Gamma_t^{\dagger X}(t-\tau)\right\rangle_B = \int_0^\infty \left|g_t^X\right|^2 e^{-i\omega\tau} tr_B\left[B_0 b_{\omega,X} b_{\omega,X}^\dagger\right] d\omega$$
$$= \int_{-\infty}^{+\infty} \left|g_t^X\right|^2 e^{-i\omega\tau} G(\omega) d\omega = \gamma_t^X \delta(-\tau) \quad (7.2.21b)$$

$$\left\langle \Gamma_s^X(t)\Gamma_t^{\dagger X}(t-\tau)\right\rangle_B = \int_0^\infty g_s^X g_t^X e^{-i\omega\tau} e^{-i\omega\tau'} tr_B\left[B_0 b_{\omega,X} b_{\omega,X}^\dagger\right] d\omega$$
$$= \int_{-\infty}^{+\infty} g_s^X g_t^X e^{i\omega(-\tau-\tau')} G(\omega) d\omega = \sqrt{\gamma_s^X \gamma_t}\,\delta(-\tau-\tau') \quad (7.2.21c)$$

$$\left\langle \Gamma_t(t)\Gamma_s^\dagger(t-\tau)\right\rangle_B = \int_0^\infty g_t g_s e^{-i\omega\tau} e^{i\omega\tau'} tr_B\left[B_0 b_\omega b_\omega^\dagger\right] d\omega$$
$$= \int_{-\infty}^{+\infty} g_t g_s e^{i\omega(-\tau+\tau')} G(\omega) d\omega = \sqrt{\gamma_t \gamma_s}\,\delta(-\tau+\tau') \quad (7.2.21d)$$

where we used the relation:

$$\int_{-\infty}^{+\infty} e^{i\omega(-\tau\pm\tau')} = 2\pi\delta(-\tau\pm\tau') \quad (7.2.22)$$

Also for the Eq.(20a-b) we have the term $e^{i\omega\tau'}e^{-i\omega\tau'}$ which will vanishe.

7.2.3 Lindblad form of master equation

To have a Lindblad form of the master equation one needs to make what is so called a secular approximation. In the secular approximation the frequencies are $\omega_i = \omega_{i'}, \omega_j = \omega_{j'}and\omega_i = \omega_j$. Thus, Eq. (7.2.19) can be written as:

$$\frac{\partial\rho}{\partial t} = -\frac{1}{\hbar^2}\sum_{X=H,V}\int_0^t d\tau\{\sum_{i=1}^{2}[[c_{i,X}^\dagger c_{i,X}\rho(t-\tau) - c_{i,X}\rho(t-\tau)c_{i,X}^\dagger]\gamma_s^X\delta(-\tau) + h.c]$$
$$+\sum_{j=1}^{2}[P_{j,X}^\dagger P_{j,X}\rho(t-\tau) - P_{j,X}\rho(t-\tau)P_{j,X}^\dagger]\gamma_t^X\delta(-\tau) + h.c]$$
$$+\sum_{i=1}^{2}\sum_{j=1}^{2}[[c_{i,X}^\dagger P_{j,X}\rho(t-\tau) - P_{j,X}\rho(t-\tau)c_{i,X}^\dagger]\sqrt{\gamma_s^X\gamma_t^X}\,\delta(-\tau-\tau') + h.c]$$
$$+\sum_{i=1}^{2}\sum_{j=1}^{2}[[P_{j,X}^\dagger c_{i,X}\rho(t-\tau) - c_{i,X}\rho(t-\tau)P_{j,X}^\dagger]\sqrt{\gamma_s^X\gamma_t^X}\,\delta(-\tau+\tau') + h.c] \quad (7.2.23)$$

Herein, the terms with $\delta(-\tau-\tau')$ will vanish as $-\tau'$ is beyond the limitation of the time integral.This is exactly the assumption that we have an asymmetric coupling from the source to target, unidirectionality. Also having in mind that for a function $C(s)$ we have $\int_{t_0}^{t} C(s)\delta(t-s)ds = \frac{1}{2}C(t)$one can write the Eq.21 as(for $h=1$):

$$\begin{aligned}\frac{\partial\rho}{\partial t} = \sum_{X=H,V}\Big\{&\frac{\gamma_s^X}{2}\sum_{i=1}^{2}[[c_{i,X}^{\dagger}c_{i,X}\rho(t) - c_{i,X}\rho(t)\,c_{i,X}^{\dagger}] + h.c] \\ &+ \frac{\gamma_t^X}{2}\sum_{j=1}^{2}[[P_{j,X}^{\dagger}P\rho(t) - P_{j,X}\rho(t)P_{j,X}^{\dagger}] + h.c] \\ &- \frac{\sqrt{\gamma_s^X\gamma_t^X}}{2}\sum_{i=1}^{2}\sum_{j=1}^{2}[[-P_{j,X}\rho(t)c_{i,X}^{\dagger} - c_{i,X}\rho(t)P_{j,X}^{\dagger} + \rho(t)c_{i,X}^{\dagger}P_{j,X} + P_{j,X}^{\dagger}c_{i,X}\rho(t)]]\Big\}\end{aligned} \tag{7.2.24}$$

The first two terms in the above master equation are Lindblad terms.However, we do not need any specific restrains and we can continue this procedure, for the sake of simplicity, we make an assumption here. We presuppose that the both horizontal and vertical polarization channels have the same coupling ratio to the waveguide: $\gamma_s = \gamma_s^H = \gamma_s^V$ and $\gamma_t = \gamma_t^H = \gamma_t^V$. This is naturally true for most of the cases but for future studies where we are dealing with more general situation, it can be seen as an assumption and be neglected. From now on we set $\sigma^{\dagger} = \sigma^{+}$ and $\sigma = \sigma-$. Translating the transition operators to pseudo Pauli operators we will have counterpart Lindblad terms in Eq. 7.2.24 with atomic operators as

$$\begin{aligned}&\frac{\gamma_s}{2}\sum_{X=H^s,\,V^s}\{[[\sigma_{XB}^{\dagger}\sigma_{XB}\rho(t) - \sigma_{XB}\rho(t)\,\sigma_{XB}^{\dagger}] + h.c] + [[\sigma_{GX}^{\dagger}\sigma_{GX}\rho(t) - \sigma_{GX}\rho(t)\sigma_{GX}^{\dagger}] + h.c]\} \\ &+\frac{\gamma_t}{2}\sum_{X=H^t,\,V^t}\{[[\sigma_{XB}^{\dagger}\sigma_{XB}\rho(t) - \sigma_{XB}\rho(t)\sigma_{XB}^{\dagger}] + h.c] + [[\sigma_{GX}^{\dagger}\sigma_{GX}\rho(t) - \sigma_{GX}\rho(t)\sigma_{GX}^{\dagger}] + h.c]\}\end{aligned} \tag{7.2.25}$$

.

The last part of master Eq. (7.2.24) contains 64 terms which can be compacted with the help of the abbreviations in Fig. 7.2.1. In this figure the Pesudo Pauli operators related to the coupled biexcitons are shown.

By doing so, the master equation for the coupling between two biexcitons is written as:

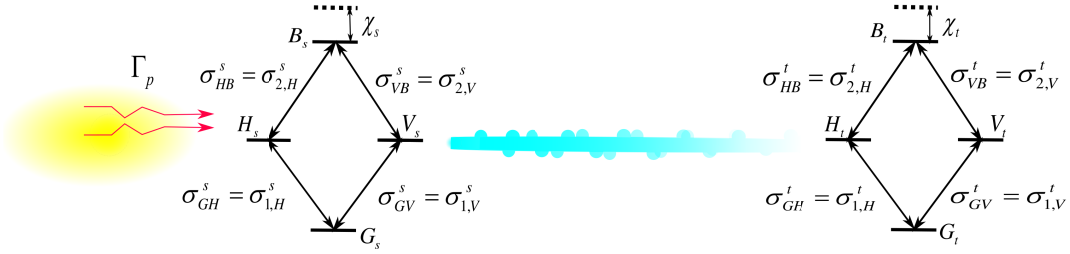

Figure 7.2.1: The unidirectional coupling between two biexcitons and their atomic operators . The fine structure spliting of the source and target are not presented(for simplicity fine structure spiting is not presented)

$$\left.\frac{\partial\rho}{\partial t}\right|_c = \frac{\gamma_s}{2}\sum_{X=H^s,\,V^s}[L(\sigma^s_{XB})+L(\sigma^s_{GX})]\rho+\frac{\gamma_t}{2}\sum_{X=H^t,\,V^t}[L(\sigma^t_{XB})+L(\sigma^t_{GX})]\rho$$
$$-\frac{\sqrt{\gamma_s\gamma_t}}{2}\sum_{i=1}^{2}\sum_{j=1}^{2}(-\sigma^t_{j,H}\rho(t)\sigma^{\dagger s}_{i,H}-\sigma^s_{i,H}\rho(t)\sigma^{\dagger t}_{j,H}+\rho(t)\sigma^{\dagger s}_{i,H}\sigma^t_{j,H}+\sigma^{\dagger t}_{j,H}\sigma^s_{i,H}\rho(t))$$
$$-\frac{\sqrt{\gamma_s\gamma_t}}{2}\sum_{i=1}^{2}\sum_{j=1}^{2}(-\sigma^t_{j,V}\rho(t)\sigma^{\dagger s}_{i,V}-\sigma^s_{i,V}\rho(t)\sigma^{\dagger t}_{j,V}+\rho(t)\sigma^{\dagger s}_{i,V}\sigma^t_{j,V}+\sigma^{\dagger t}_{j,V}\sigma^s_{i,V}\rho(t)) \tag{7.2.26}$$

Where $L(O)\rho = 2O\rho O^\dagger - O^\dagger O\rho - \rho O^\dagger O$.

7.2.4 The full Lindblad master equation for coupled biexcitons

7.2.5 Incoherently pumped source biexciton

After driving the coupling part of the master equation for the cascaded biexcition, one can move forward and analyze the other part of the master equation in its general arrangement. First, we assume that the source biexciton is incoherently pumped. The full master equation can be described as a summation of three superoperator:

$$\frac{\partial\rho}{\partial t} = L\rho = (L_s + L_c + L_t)\rho \tag{7.2.27}$$

Firstly, the system Hamiltonian of the source biexciton , by taking rotating frame at $|H\rangle \to |G\rangle$, will have the form of:

$$H_s = -\chi_s\sigma^s_{BB} + \Delta_s\sigma^s_{VV} \tag{7.2.28}$$

Where χ_s is the biexciton energy shift and Δ_s is the fine structure splitting between vertical and horizontal excitons (here it is assumed that vertical exciton has a upper

energy). If we presume that pure dephasing is neglected and the source is pumped incoherently with the pumping strengthΓ_p, then the master equation of the source reads:

$$\left.\frac{\partial\rho}{\partial t}\right|_s = -\frac{i}{\hbar}\left[H_s,\rho\right] + \Gamma_p[L_p(\sigma^s_{HB})\rho + L_p(\sigma^s_{VB})\rho + L_p(^s_{GH})\rho + L_p(\sigma^s_{GV})\rho] \quad (7.2.29)$$

Where $L_p(O)\rho = 2O^\dagger\rho O - OO^\dagger\rho - \rho OO^\dagger$. In addition, the master equation of the target biexciton has the simple form of:

$$\left.\frac{\partial\rho}{\partial t}\right|_t = -\frac{i}{\hbar}[H_t\ ,\rho] \quad (7.2.30)$$

Where the target biexciton has a similar system Hamiltonian as the source:

$$H_t = -\chi_t\sigma^t_{BB} + \Delta_t\sigma^t_{VV} \quad (7.2.31)$$

By substituting all of the Liovulian superoperator in Eq.29 one will get the full master equation of the form:

$$\begin{aligned}\frac{\partial\rho(t)}{\partial t} &= -\frac{i}{\hbar}\left[(H_s+H_t),\rho(t)\right] + \Gamma_p[L_p(\sigma^s_{HB})\rho(t) + L_p(\sigma^s_{VB})\rho(t) + L_p(\sigma^s_{GH})\rho(t) + L_p(\sigma^s_{GV})\rho(t)] \\ &+ \frac{\gamma_s}{2}\sum_{X=H^s,\,V^s}[L(\sigma^s_{XB}) + L(\sigma^s_{GX})]\rho(t) + \frac{\gamma_t}{2}\sum_{X=H^t,\,V^t}[L(\sigma^t_{XB}) + L(\sigma^t_{GX})]\rho(t) \\ &- \frac{\sqrt{\gamma_s\gamma_t}}{2}\sum_{i=1}^{2}\sum_{j=1}^{2}(-\sigma^t_{j,H}\rho(t)\sigma^{\dagger s}_{i,H} - \sigma^s_{i,H}\rho(t)\sigma^{\dagger t}_{j,H} + \rho(t)\sigma^{\dagger s}_{i,H}\sigma^t_{j,H} + \sigma^{\dagger t}_{j,H}\sigma^s_{i,H}\rho(t)) \\ &- \frac{\sqrt{\gamma_s\gamma_t}}{2}\sum_{i=1}^{2}\sum_{j=1}^{2}(-\sigma^t_{j,V}\rho(t)\sigma^{\dagger s}_{i,V} - \sigma^s_{i,V}\rho(t)\sigma^{\dagger t}_{j,V} + \rho(t)\sigma^{\dagger s}_{i,V}\sigma^t_{j,V} + \sigma^{\dagger t}_{j,V}\sigma^s_{i,V}\rho(t))\end{aligned} \quad (7.2.32)$$

7.2.6 Coherently pumped source biexciton

For the coherently pumped biexciton, the Eq. (7.2.32) should be modified. Firstly, the term corresponding to the incoherent pumping, Γ_p, will be omitted. Secondly,we will add the coherent pumping terms to the source Hamiltonian which can be reformulated as:

$$H_s = \Omega_s(\sigma^s_{VB} + \sigma^{\dagger s}_{VB}) - \chi_s\sigma^s_{BB} + \Delta_s\sigma^s_{VV} \quad (7.2.33)$$

Where Ω stands for the Rabi frequency of a single photon. By applying these two changes, the Eq. (7.2.32) is in the appropriate form for the coherently pumped cascaded system.

7.2.7 Redfield form of master equation

With respect to the secular approximation in the last section we transferred Eq. (7.2.19) to its Lindblad form given in Eq. (7.2.32). Without such an approximation the transition operators and their frequencies should be written explicitly. By separating the fast oscillating frequencies from the relaxation frequency in the exponential terms in Eq. (7.2.19), one will subsequently get the following equation

$$\begin{aligned}\frac{\partial\rho}{\partial t} = -\frac{1}{\hbar^2}\sum_{X=H,V}\int_0^t d\tau\Big\{ &\sum_{i=1}^{2}\sum_{i'=1}^{2}[[c_{i,X}^{\dagger}c_{i',X}\rho(t-\tau) - c_{i',X}\rho(t-\tau)c_{i,X}^{\dagger}]e^{i\omega_{i'}\tau}e^{i\omega_i t - i\omega_{i'}t}\\ &\left\langle\Gamma_s^X(t)\Gamma_s^{\dagger X}(t-\tau)\right\rangle_B + h.c]\\ &+\sum_{j=1}^{2}\sum_{j'=1}^{2}[[P_{j,X}^{\dagger}P_{j',X}\rho(t-\tau) - P_{j',X}\rho(t-\tau)P_{j,X}^{\dagger}]e^{i\omega_{j'}\tau}e^{i\omega_j t - i\omega_{j'}t}\left\langle\Gamma_t^X(t)\Gamma_t^{\dagger}(t-\tau)\right\rangle_B + h.c]\\ &+\sum_{i=1}^{2}\sum_{j=1}^{2}[[c_{i,X}^{\dagger}P_{j,X}\rho(t-\tau) - P_{j,X}\rho(t-\tau)c_{i,X}^{\dagger}]e^{i\omega_j\tau}e^{i\omega_i t - i\omega_j t}\left\langle\Gamma_s^X(t)\Gamma_t^{\dagger X}(t-\tau)\right\rangle_B + h.c]\\ &+\sum_{i=1}^{2}\sum_{j=1}^{2}[[P_{j,X}^{\dagger}c_{i,X}\rho(t-\tau) - c_{i,X}\rho(t-\tau)P_{j,X}^{\dagger}]e^{-i\omega_j\tau}e^{-i\omega_i t + i\omega_j t}\left\langle\Gamma_t^X(t)\Gamma_s^{\dagger X}(t-\tau)\right\rangle_B + h.c]\Big\}.\end{aligned} \tag{7.2.34}$$

One can move these non-secular exponential terms out of the commutation of the transition operators and the density matrix and Eq. (7.2.34) written in form of

$$\begin{aligned}\frac{\partial\rho}{\partial t} = -\frac{1}{\hbar^2}\sum_{X=H,V}\int_0^t d\tau\Big\{ &\sum_{i=1}^{2}\sum_{i'=1}^{2}e^{i\omega_i t - i\omega_{i'}t}[[c_{i,X}^{\dagger}c_{i',X}\rho(t-\tau) - c_{i',X}\rho(t-\tau)c_{i,X}^{\dagger}]e^{i\omega_{i'}\tau}\\ &\left\langle\Gamma_s^X(t)\Gamma_s^{\dagger X}(t-\tau)\right\rangle_B + h.c]\\ &+\sum_{j=1}^{2}\sum_{j'=1}^{2}e^{i\omega_j t - i\omega_{j'}t}[[P_{j,X}^{\dagger}P_{j',X}\rho(t-\tau) - P_{j',X}\rho(t-\tau)P_{j,X}^{\dagger}]e^{i\omega_{j'}\tau}\left\langle\Gamma_t^X(t)\Gamma_t^{\dagger}(t-\tau)\right\rangle_B + h.c]\\ &+\sum_{i=1}^{2}\sum_{j=1}^{2}e^{i\omega_i t - i\omega_j t}[[c_{i,X}^{\dagger}P_{j,X}\rho(t-\tau) - P_{j,X}\rho(t-\tau)c_{i,X}^{\dagger}]e^{i\omega_j\tau}\left\langle\Gamma_s^X(t)\Gamma_t^{\dagger X}(t-\tau)\right\rangle_B + h.c]\\ &+\sum_{i=1}^{2}\sum_{j=1}^{2}e^{-i\omega_i t + i\omega_j t}[[P_{j,X}^{\dagger}c_{i,X}\rho(t-\tau) - c_{i,X}\rho(t-\tau)P_{j,X}^{\dagger}]e^{-i\omega_j\tau}\left\langle\Gamma_t^X(t)\Gamma_s^{\dagger X}(t-\tau)\right\rangle_B + h.c]\Big\}.\end{aligned} \tag{7.2.35}$$

By moving the integral inside the summation one will have

$$\frac{\partial\rho}{\partial t} = -\frac{1}{\hbar^2}\sum_{X=H,V}\Big\{\sum_{i=1}^{2}\sum_{i'=1}^{2} e^{i\omega_i t - i\omega_{i'}t}\int_0^t d\tau[[c_{i,X}^\dagger c_{i',X}\rho(t-\tau) - c_{i',X}\rho(t-\tau)c_{i,X}^\dagger]e^{i\omega_{i'}\tau}$$
$$\Big\langle\Gamma_s^X(t)\Gamma_s^{\dagger X}(t-\tau)\Big\rangle_B + h.c]$$
$$+\sum_{j=1}^{2}\sum_{j'=1}^{2} e^{i\omega_j t - i\omega_{j'}t}\int_0^t d\tau[[P_{j,X}^\dagger P_{j',X}\rho(t-\tau) - P_{j',X}\rho(t-\tau)P_{j,X}^\dagger]e^{i\omega_{j'}\tau}\Big\langle\Gamma_t^X(t)\Gamma_t^\dagger(t-\tau)\Big\rangle_B + h.c]$$
$$+\sum_{i=1}^{2}\sum_{j=1}^{2} e^{i\omega_i t - i\omega_j t}\int_0^t d\tau[[c_{i,X}^\dagger P_{j,X}\rho(t-\tau) - P_{j,X}\rho(t-\tau)c_{i,X}^\dagger]e^{i\omega_j\tau}\Big\langle\Gamma_s^X(t)\Gamma_t^{\dagger X}(t-\tau)\Big\rangle_B + h.c]$$
$$+\sum_{i=1}^{2}\sum_{j=1}^{2} e^{-i\omega_i t + i\omega_j t}\int_0^t d\tau[[P_{j,X}^\dagger c_{i,X}\rho(t-\tau) - c_{i,X}\rho(t-\tau)P_{j,X}^\dagger]e^{-i\omega_j\tau}\Big\langle\Gamma_t^X(t)\Gamma_s^{\dagger X}(t-\tau)\Big\rangle_B + h.c]\Big\}. \tag{7.2.36}$$

If one follows the unidirectionality principle of cascaded quantum system, the transition operators responsible for the source influenced back by the target will be omitted. Also, each of the bath correlation functions can be evaluated in the same way as before in subsection 7.2.2. By doing so, one will get the more simplified version of Eq. (7.2.36)

$$\frac{\partial\rho}{\partial t} = \sum_{X=H,V}\Big\{\sum_{i'=1}^{2}\sum_{i=1}^{2} e^{i\omega_i t - i\omega_{i'}t}\frac{\gamma_s}{2}[[c_{i,X}^\dagger c_{i',X}\rho(t) - c_{i',X}\rho(t)c_{i,X}^\dagger] + h.c]$$
$$+\sum_{j'=1}^{2}\sum_{j=1}^{2} e^{i\omega_j t - i\omega_{j'}t}\frac{\gamma_t}{2}[[P_j^\dagger P_{j',X}\rho(t) - P_{j',X}\rho(t)P_{j,X}^\dagger] + h.c]$$
$$+\sum_{i=1}^{2}\sum_{j=1}^{2} e^{i\omega_i t - i\omega_j t}\frac{\sqrt{\gamma_s\gamma_t}}{2}[-P_{j,X}\rho(t)c_{i,X}^\dagger - c_{i,X}\rho(t)P_{j,X}^\dagger]$$
$$+\sum_{i=1}^{2}\sum_{j=1}^{2} e^{-i\omega_i t + i\omega_j t}\frac{\sqrt{\gamma_s\gamma_t}}{2}[P_{j,X}^\dagger c_{i,X}\rho(t) + \rho(t)P_{j,X}c_{i,X}^\dagger]\Big\}. \tag{7.2.37}$$

The above equation also can be translated to the algebra of pseudo Pauli operators explicitly.
First, we define different frequencies $\omega_i$and $\omega_{i'}$for the evaluation of the Eq.34.

$$\omega_1^s = \omega_B^s - \omega_H^s \quad \omega_2^s = \omega_B^s - \omega_V^s \quad \omega_3^s = \omega_V^s - \omega_G^s \quad \omega_4^s = \omega_H^s - \omega_G^s \quad \omega_5^s = \Delta_s \tag{7.2.38}$$

Where $\Delta_s$is the fine structure splitting. Taking the ground state as the zero point energy we will have $\omega_G^s = 0$. Then by translating the transition master equation to

the atomic operators we will have the full master equation. Herein, as we have many terms in the explicit form of the master equation, we separate these terms to three parts. These three parts are Lindblad superoperator for the source, the target and finally the coupling between two systems:

$$\frac{\partial \rho}{\partial t}\,|_c = L_c\rho = (L_{c1} + L_{c2} + L_{c3})\rho \tag{7.2.39}$$

L_{c1} andL_{c2} are the Lindblad superoperators for the source and target biexcitons, while L_{c3}stands for coupling between the source and target. As $L_{c1}$and $L_{c2}$are just dependent on the properties of the each system (source or target), it is possible to drive one of them and another one will be similar. Then we can write down the first line of Eq. (7.2.37) in the following way

$$\begin{aligned} L_{c1}\rho = \frac{\gamma_s}{2}\ \Big\{ & [[\sigma^{\dagger s}_{GH}\sigma^s_{GH}\rho(t) - \sigma^s_{GH}\rho(t)\sigma^{\dagger s}_{GH}] + h.c]e^{i(\omega^s_4-\omega^s_4)t} \\ & + [[-\sigma^s_{HB}\rho(t)\sigma^{\dagger s}_{GH}] + h.c]e^{i(\omega^s_4-\omega^s_1)t} \\ & + [[\sigma^{\dagger s}_{GV}\sigma^s_{GV}\rho(t) - \sigma^s_{GV}\rho(t)\sigma^{\dagger s}_{GV}] + h.c]e^{i(\omega^s_3-\omega^s_3)t} \\ & + [[-\sigma^s_{VB}\rho(t)\sigma^{\dagger s}_{GV}] + h.c]e^{i(\omega^s_3-\omega^s_2)t} \\ & + [[\sigma^{\dagger s}_{HB}\sigma^s_{HB}\rho(t) - \sigma^s_{HB}\rho(t)\sigma^{\dagger s}_{HB}] + h.c]e^{i(\omega^s_1-\omega^s_1)t} \\ & + [[-\sigma^s_{GH}\rho(t)\sigma^{\dagger s}_{HB}] + h.c]e^{i(\omega^s_1-\omega^s_4)t} \\ & + [[\sigma^{\dagger s}_{VB}\sigma^s_{VB}\rho(t) - \sigma^s_{VB}\rho(t)\sigma^{\dagger s}_{VB}] + h.c]e^{i(\omega^s_2-\omega^s_2)t} \\ & + [[-\sigma^s_{GV}\rho(t)\sigma^{\dagger s}_{VB}] + h.c]e^{i(\omega^s_2-\omega^s_3)t}\Big\}. \end{aligned} \tag{7.2.40}$$

If we assume that the vertically polarized exciton has a higher energy (frequency) then the fine structure splitting it can be written as $\Delta_s = \omega_V - \omega_H$ and the biexciton energy shift is $\chi_s = 2\omega_V - \omega_B$. These two relations give us the possibility to evaluate the frequency differences which appears in Eq. (7.2.40)

$$\omega^s_4 - \omega^s_1 = (2\omega^s_H - \omega^s_B) = 2(\omega^s_V - \Delta_s) - \omega^s_B = 2\omega^s_V - \omega^s_B - 2\Delta_s = \chi_s - 2\Delta_s \tag{7.2.41a}$$

$$\omega^s_3 - \omega^s_2 = 2\omega^s_V - \omega^s_B = \chi_s \tag{7.2.41b}$$

By doing so, the Eq. (7.2.40) is written as

$$\begin{aligned}
L_{c1}\rho = \frac{\gamma_s}{2}\Big\{&[[\sigma^{\dagger s}_{GH}\sigma^{s}_{GH}\rho(t) - \sigma^{s}_{GH}\rho(t)\sigma^{\dagger s}_{GH}] + h.c] \\
&+ [[-\sigma^{s}_{HB}\rho(t)\sigma^{\dagger s}_{GH}] + h.c]e^{i(\chi_s - 2\Delta_s)t} \\
&+ [[\sigma^{\dagger s}_{GV}\sigma^{s}_{GV}\rho(t) - \sigma^{s}_{GV}\rho(t)\sigma^{\dagger s}_{GV}] + h.c] \\
&+ [[-\sigma^{s}_{VB}\rho(t)\sigma^{\dagger s}_{GV}] + h.c]e^{i(\chi_s)t} \\
&+ [[\sigma^{\dagger s}_{HB}\sigma^{s}_{HB}\rho(t) - \sigma^{s}_{HB}\rho(t)\sigma^{\dagger s}_{BH}] + h.c] \\
&+ [[-\sigma^{s}_{GH}\rho(t)\sigma^{\dagger s}_{HB}] + h.c]e^{-i(\chi_s - 2\Delta_s)t} \\
&+ [[-\sigma^{s}_{GV}\rho(t)\sigma^{\dagger s}_{VB}] + h.c]e^{-i(\chi_s)t} \\
&+ [[\sigma^{\dagger s}_{VB}\sigma^{s}_{VB}\rho(t) - \sigma^{s}_{VB}\rho(t)\sigma^{\dagger s}_{VB}] + h.c]\Big\}. \qquad (7.2.42)
\end{aligned}$$

One can note that, in addition to the population terms in Eq.41 the crossing terms, $-\sigma^{s}_{XB}\rho(t)\sigma^{\dagger s}_{GX}$ and $-\sigma^{s}_{GX}\rho(t)\sigma^{\dagger s}_{XB}$ for $X = H, V$, are preserved. This is due to the fact that we have the statistically mixed density matrix in the middle of the commutation relations.. The same procedure is implemented for the explicit form of L_{c2}. First, we need to define the frequency differences in the target biexcitons

$$\omega^t_1 = \omega^t_B - \omega^t_H \quad \omega^t_2 = \omega^t_B - \omega^t_V \quad \omega^t_3 = \omega^t_V - \omega^t_G \quad \omega^t_4 = \omega^t_H - \omega^t_G \quad \omega^t_5 = \Delta_t = \omega^t_V - \omega^t_H. \qquad (7.2.43)$$

Again for the target biexciton we set the ground state to the zero point energy. The explicit form of L_{c2} is written as

$$\begin{aligned}
L_{c2}\rho = \frac{\gamma_t}{2}\Big\{&[[\sigma^{\dagger t}_{GH}\sigma^{t}_{GH}\rho(t) - \sigma^{t}_{GH}\rho(t)\sigma^{\dagger t}_{GH}] + h.c] \\
&+ [[-\sigma^{t}_{HB}\rho(t)\sigma^{\dagger t}_{GH}] + h.c]e^{i(\chi_t - 2\Delta_t)t} \\
&+ [[\sigma^{\dagger t}_{GV}\sigma^{t}_{GV}\rho(t) - \sigma^{t}_{GV}\rho(t)\sigma^{\dagger t}_{GV}] + h.c] \\
&+ [[-\sigma^{t}_{VB}\rho(t)\sigma^{\dagger t}_{GV}] + h.c]e^{i(\chi_t)t} \\
&+ [[\sigma^{\dagger t}_{HB}\sigma^{t}_{HB}\rho(t) - \sigma^{t}_{HB}\rho(t)\sigma^{\dagger t}_{BH}] + h.c] \\
&+ [[-\sigma^{t}_{GH}\rho(t)\sigma^{\dagger t}_{HB}] + h.c]e^{-i(\chi_t - 2\Delta_t)t} \\
&+ [[-\sigma^{t}_{GV}\rho(t)\sigma^{\dagger t}_{VB}] + h.c]e^{-i(\chi_t)t} \\
&+ [[\sigma^{\dagger t}_{VB}\sigma^{t}_{VB}\rho(t) - \sigma^{t}_{VB}\rho(t)\sigma^{\dagger t}_{VB}] + h.c]\Big\}. \qquad (7.2.44)
\end{aligned}$$

The derivation of L_{c3} needs a careful analyzes. Regarding the fine structure splitting in the source and the target biexcitons, there is no need for an energy symmetry between the source and the target: we don't need to set the vertical exciton with a higher energy than horizontal one. By writing the coupling terms one will get the

following equation

$$
\begin{aligned}
L_{c3}\rho = -\frac{\sqrt{\gamma_s\gamma_t}}{2}[&-\sigma^t_{GH}\rho(t)\,\sigma^{\dagger s}_{GH} - \sigma^s_{GH}\rho(t)\,\sigma^{\dagger t}_{GH}]e^{i(\omega^s_4-\omega^t_4)t}\\
&+[\sigma^{\dagger t}_{GH}\,\sigma^s_{GH}\rho(t) + \rho(t)\,\sigma^t_{GH}\,\sigma^{\dagger s}_{GH}]e^{i(-\omega^s_4+\omega^t_4)t}\\
&+[-\sigma^t_{HB}\rho(t)\,\sigma^{\dagger s}_{GH} - \sigma^s_{GH}\,\rho(t)\,\sigma^{\dagger t}_{HB}]e^{i(\omega^s_4-\omega^t_1)t}\\
&+[\sigma^{\dagger t}_{HB}\,\sigma^s_{GH}\rho(t) + \rho(t)\,\sigma^t_{HB}\,\sigma^{\dagger s}_{GH}]e^{i(-\omega^s_4+\omega^t_1)t}\\
&+[-\sigma^t_{GH}\rho(t)\sigma^{\dagger s}_{HB} - \sigma^s_{HB}\rho(t)\sigma^{\dagger t}_{GH}]e^{i(\omega^s_1-\omega^t_4)t}\\
&+[\sigma^{\dagger t}_{GH}\sigma^s_{HB}\rho(t) + \rho(t)\sigma^t_{GH}\sigma^{\dagger s}_{HB}]e^{i(-\omega^s_1+\omega^t_4)t}\\
&+[-\sigma^t_{HB}\rho(t)\sigma^{\dagger s}_{HB} - \sigma^s_{HB}\rho(t)\sigma^{\dagger t}_{HB}]e^{i(\omega^s_1-\omega^t_1)t}\\
&+[\sigma^{\dagger t}_{HB}\sigma^s_{HB}\rho(t) + \rho(t)\sigma^t_{HB}\sigma^{\dagger s}_{HB}]e^{i(-\omega^s_1+\omega^t_1)t}\\
&+[-\sigma^t_{GV}\rho(t)\sigma^{\dagger s}_{GV} - \sigma^s_{GV}\rho(t)\sigma^{\dagger t}_{GV}]e^{i(\omega^s_3-\omega^t_3)t}\\
&+[\sigma^{\dagger t}_{GV}\sigma^s_{GV}\rho(t) + \rho(t)\sigma^t_{GV}\sigma^{\dagger t}_{GV}]e^{i(-\omega^s_3+\omega^t_3)t}\\
&+[-\sigma^t_{GV}\rho(t)\sigma^{\dagger s}_{VB} - \sigma^s_{VB}\rho(t)\sigma^{\dagger t}_{GV}]e^{i(\omega^s_2-\omega^t_3)t}\\
&+[\sigma^{\dagger t}_{GV}\sigma^s_{VB}\rho(t) + \rho(t)\sigma^t_{GV}\sigma^{\dagger s}_{VB}]e^{i(-\omega^s_2+\omega^t_3)t}\\
&+[-\sigma^t_{VB}\rho(t)\sigma^{\dagger s}_{VB} - \sigma^s_{VB}\rho(t)\sigma^{\dagger t}_{VB}]e^{i(\omega^s_2-\omega^t_2)t}\\
&+[\sigma^{\dagger t}_{VB}\sigma^s_{VB}\rho(t) + \rho(t)\sigma^t_{VB}\sigma^{\dagger s}_{VB}]e^{i(-\omega^s_2+\omega^t_2)t}. \qquad (7.2.45)
\end{aligned}
$$

7.2.8 The Redfield full master equation

Similar to the subsection 7.2.4 we can reproduce the full master equation of the coupled biexciton from Eq. 7.2.39. The only difference will be in the coupling part . As an example, the master equation for the incoherently pumped cascaded system is written as

$$
\begin{aligned}
\frac{\partial\rho}{\partial t} =& \frac{i}{\hbar}\left[(H_s+H_t),\rho(t)\right] + \Gamma_p[L_p(\sigma^s_{HB})\rho(t) + L_p(\sigma^s_{VB})\rho(t) + L_p(\sigma^s_{GH})\rho(t) + L_p(\sigma^s_{GV})\rho(t)] \\
&\frac{\gamma_s}{2}\Big\{[[\sigma^{\dagger s}_{GH}\sigma^s_{GH}\rho(t) - \sigma^s_{GH}\rho(t)\sigma^{\dagger s}_{GH}] + h.c] + [[-\sigma^s_{HB}\rho(t)\sigma^{\dagger s}_{GH}] + h.c]e^{i(\chi_s-2\Delta_s)t} \\
&+ [[\sigma^{\dagger s}_{GV}\sigma^s_{GV}\rho(t) - \sigma^s_{GV}\rho(t)\sigma^{\dagger s}_{GV}] + h.c] + [[-\sigma^s_{VB}\rho(t)\sigma^{\dagger s}_{GV}] + h.c]e^{i(\chi_s)t} \\
&+ [[\sigma^{\dagger s}_{HB}\sigma^s_{HB}\rho(t) - \sigma^s_{HB}\rho(t)\sigma^{\dagger s}_{BH}] + h.c] + [[-\sigma^s_{GH}\rho(t)\sigma^{\dagger s}_{HB}] + h.c]e^{-i(\chi_s-2\Delta_s)t} \\
&+ [[-\sigma^s_{GV}\rho(t)\sigma^{\dagger s}_{VB}] + h.c]e^{-i(\chi_s)t} + [[\sigma^{\dagger s}_{VB}\sigma^s_{VB}\rho(t) - \sigma^s_{VB}\rho(t)\sigma^{\dagger s}_{VB}] + h.c]\Big\} \\
&+\frac{\gamma_t}{2}\Big\{[[\sigma^{\dagger t}_{GH}\sigma^t_{GH}\rho(t) - \sigma^t_{GH}\rho(t)\sigma^{\dagger t}_{GH}] + h.c] + [[-\sigma^t_{HB}\rho(t)\sigma^{\dagger t}_{GH}] + h.c]e^{i(\chi_t-2\Delta_t)t} \\
&+ [[\sigma^{\dagger t}_{GV}\sigma^t_{GV}\rho(t) - \sigma^t_{GV}\rho(t)\sigma^{\dagger t}_{GV}] + h.c] + [[-\sigma^t_{VB}\rho(t)\sigma^{\dagger t}_{GV}] + h.c]e^{i(\chi_t)t} \\
&+ [[\sigma^{\dagger t}_{HB}\sigma^t_{HB}\rho(t) - \sigma^t_{HB}\rho(t)\sigma^{\dagger t}_{BH}] + h.c] + [[-\sigma^t_{GH}\rho(t)\sigma^{\dagger t}_{HB}] + h.c]e^{-i(\chi_t-2\Delta_t)t} \\
&+ [[-\sigma^t_{GV}\rho(t)\sigma^{\dagger t}_{VB}] + h.c]e^{-i(\chi_t)t} + [[\sigma^{\dagger t}_{VB}\sigma^t_{VB}\rho(t) - \sigma^t_{VB}\rho(t)\sigma^{\dagger t}_{VB}] + h.c]\Big\} \\
-\frac{\sqrt{\gamma_s\gamma_t}}{2}&\Big\{[-\sigma^t_{GH}\rho(t)\,\sigma^{\dagger s}_{GH} - \sigma^s_{GH}\rho(t)\,\sigma^{\dagger t}_{GH}]e^{i(\omega^s_4-\omega^t_4)t} + [\sigma^{\dagger t}_{GH}\,\sigma^s_{GH}\rho(t) + \rho(t)\,\sigma^t_{GH}\,\sigma^{\dagger s}_{GH}]e^{i(-\omega^s_4+\omega^t_4)t} \\
&+ [-\sigma^t_{HB}\rho(t)\,\sigma^{\dagger s}_{GH} - \sigma^s_{GH}\,\rho(t)\,\sigma^{\dagger t}_{HB}]e^{i(\omega^s_4-\omega^t_1)t} + [\sigma^{\dagger t}_{HB}\,\sigma^s_{GH}\rho(t) + \rho(t)\,\sigma^t_{HB}\,\sigma^{\dagger s}_{GH}]e^{i(-\omega^s_4+\omega^t_1)t} \\
&+ [-\sigma^t_{GH}\rho(t)\sigma^{\dagger s}_{HB} - \sigma^s_{HB}\rho(t)\sigma^{\dagger t}_{GH}]e^{i(\omega^s_1-\omega^t_4)t} + [\sigma^{\dagger t}_{GH}\sigma^s_{HB}\rho(t) + \rho(t)\sigma^t_{GH}\sigma^{\dagger s}_{HB}]e^{i(-\omega^s_1+\omega^t_4)t} \\
&+ [-\sigma^t_{HB}\rho(t)\sigma^{\dagger s}_{HB} - \sigma^s_{HB}\rho(t)\sigma^{\dagger t}_{HB}]e^{i(\omega^s_1-\omega^t_1)t} + [\sigma^{\dagger t}_{HB}\sigma^s_{HB}\rho(t) + \rho(t)\sigma^t_{HB}\sigma^{\dagger s}_{HB}]e^{i(-\omega^s_1+\omega^t_1)t} \\
&+ [-\sigma^t_{GV}\rho(t)\sigma^{\dagger s}_{GV} - \sigma^s_{GV}\rho(t)\sigma^{\dagger t}_{GV}]e^{i(\omega^s_3-\omega^t_3)t} + [\sigma^{\dagger t}_{GV}\sigma^s_{GV}\rho(t) + \rho(t)\sigma^t_{GV}\sigma^{\dagger t}_{GV}]e^{i(-\omega^s_3+\omega^t_3)t} \\
&+ [-\sigma^t_{GV}\rho(t)\sigma^{\dagger s}_{VB} - \sigma^s_{VB}\rho(t)\sigma^{\dagger t}_{GV}]e^{i(\omega^s_2-\omega^t_3)t} + [\sigma^{\dagger t}_{GV}\sigma^s_{VB}\rho(t) + \rho(t)\sigma^t_{GV}\sigma^{\dagger s}_{VB}]e^{i(-\omega^s_2+\omega^t_3)t} \\
&+ [-\sigma^t_{VB}\rho(t)\sigma^{\dagger s}_{VB} - \sigma^s_{VB}\rho(t)\sigma^{\dagger t}_{VB}]e^{i(\omega^s_2-\omega^t_2)t} + [\sigma^{\dagger t}_{VB}\sigma^s_{VB}\rho(t) + \rho(t)\sigma^t_{VB}\sigma^{\dagger s}_{VB}]e^{i(-\omega^s_2+\omega^t_2)t}\Big\}. \qquad (7.2.46)
\end{aligned}
$$

For the coherently pumped source, one can take the same procedure in subsection 7.2.6 and derive the full Redfield master equation for such a case.

7.3 Conclusion

The formalism presented in this chapter is a foundation for the future study of the two cascaded biexcitons. It is interesting to see the influence of secular approximation on the photon statistics of the coupled system.
The coupling parameter between biexcitons is determined by $\sqrt{\gamma_s \gamma_t}$ where to increase the coupling between two system we should increase γ_s while decreasingγ_t but the interval of changing these parameters is limited. As we have tow separate channels for the emitted photons, the influence of environment in the photon statistics of the separated channels is a matter of interest.

8 Conclusion and outlook

In this work, different setups for the study of quantum excitation of many level systems are presented. The conventional cascade formalism is overviewed and a new direct approach to derive a master equation for a cascaded systems is given.

Three important aspects of the cascaded coupling between quantum systems are addressed in this thesis. The first on is properties that one can observe from the excitation of a system with quantum light. As a matter of fact, the features that this type of excitation offers are stimulating for the future photonic devices in quantum information science. The quantum cascaded system can be seen as part of quantum information network wherein the photons plays as qubit to transfer information. For the first aspect, we investigated the properties of a single photon source and then we implemented it to drive another quantum system, wherein, the emitters are directly coupled to the waveguide. We observed that for the most of incoherent pumping ratios, the quantum statistics of system is mapped directly to the target. Nonetheless, there is a transition phase for intermediate pumping strength. In this transition phase, there is a combination between the coherent and incoherent processes. The methods to measure such intermixing dynamics is presented explicitly in the thesis. We did not restrict ourselves to just this type of quantum light sources. We went beyond this kind of quantum light source by introducing a nonlinear optical setup which can be used to produce a pair of polarization entangled photons. In this setup, an optimal intensity of laser excitation has been found wherein, the enhancement of DCE takes place. This gives an opportunity to produce two entangled photons with higher efficiency than other nonlinear optical processes. However this process is efficient, it is still difficult to control. Thus, we proposed a more efficient and easier to control source to produce two entangled photons , namely a biexciton quantum dot. The second question is to what extent it is possible to control a quantum system with another quantum system in cascading them. We proposed a configuration of coupled cavities wherein the emitters in target cavity are connected to the waveguide only through the cavity dissipation rate. We call this scenario the indirect coupling of cavities and the main idea is to observe the case when the intra-cavity dynamics of the target is also strong. We observed that for the weak pumping regime the intra-cavity dynamics of target is dominant. In this regime, we can control the quantum statistics of target by changing the physical parameters that governs the behavior of target cavity. When the pumping strength increases, again the source statistics is imprinted into the target in terms of adiabatic following.
The third aspect is more a fundamental question related to the concept of open

quantum systems: What is the influence of the environment on the quantum system? It is well known that the theory of open quantum system is based on the fact that the environment influences the internal dynamics of the system. Herein, we extend this question to investigate the influence of environment on the cascaded scenario where two quantum systems communicate through the environment. We can see that the environment mediates and changes the imprinting statistics of the source into the target system.

For the future study three promising directions can be considered. Firstly, one can expand the physical systems to describe the emitter more realistically. This can be done for example by using a semiconductor model to describe quantum dots. This is a way to establish and observe the effect of more complex quantum emitters on the output statistics of the cascaded system [4]. Secondly, we can consider a different type of baths to gain more insights how the transfer of photon statistics between systems may be influenced. We considered here a thermal bath but for most configurations, we need a more sophisticate treatment of the bath degrees of freedom. For some special cases like a squeezed bath [150] the formalism presented in this work is applicable. Thirdly, one can evaluate numerically the Lindblad and Redfield master equations for cascaded biexcitons. It is a matter of interest to observe a deviation between the two obtained density matrices and emphasize the limitation of secular approximation.

9 Acknowledgements

Firstly, I would like to express my gratitude to my supervisor Prof. Dr. Andreas Knorr for the continuous support through my study and specially for his patience. I also want to thank Dr. Thomas Koprucki for being the second reviewer of my thesis. I additionally thank Weierstrass Institute for the cooperation.
Besides my advisers, I would like to thank Dr. Alexander Carmele for the heated conversations and arguments about physics and beyond. I am grateful that I had an opportunity to be in his group.
Many thanks to my former office mate Nicolas L. Naumann for fruitful discussion about physics. I also thank the current office mate and friend Julian Schleibner who could survive the last months of my thesis writing. Also, I should not forget the short term office mate Tymoteusz from Poland. My sincere thanks also goes to Nikolett Nemet for her insightful comments about cascaded formalism.
I am happy that I was part of Mensa lunch group (Manuel, Leon, Judith, Nicolas, Michael, Florian, Gunnar, Malte....) which made the time at TU Berlin more relaxing.
I finally thank my family for their emotional supports especially my brother Amir whose presence made the difficulties in Berlin easier. This thesis is dedicated to my parents.

Bibliography

[1] H. Carmichael and D. Walls: "A quantum-mechanical master equation treatment of the dynamical Stark effect". *Journal of Physics B: Atomic and Molecular Physics* **9** (8) (1976), p. 1199.

[2] B. Yurke: "Use of cavities in squeezed-state generation". *Physical Review A* **29** (1) (1984), p. 408.

[3] G Rempe, R. Thompson, R. Brecha, W. Lee, and H. Kimble: "Optical bistability and photon statistics in cavity quantum electrodynamics". *Physical Review Letters* **67** (13) (1991), p. 1727.

[4] Shields Andrew J.: "Semiconductor quantum light sources". *Nat Photon* **1** (4) (2007). 10.1038/nphoton.2007.46, 215–223.

[5] N. Sim, M. F. Cheng, D. Bessarab, C. M. Jones, and L. A. Krivitsky: "Measurement of Photon Statistics with Live Photoreceptor Cells". *Phys. Rev. Lett.* **109** (11 2012), p. 113601.

[6] Munoz C. Sanchez, del Valle E., Tudela A. Gonzalez, MullerK., LichtmanneckerS., KaniberM., TejedorC., F. J., and L. P.: "Emitters of N-photon bundles". *Nat Photon* **8** (7) (2014), 550–555.

[7] Lodahl Peter, Mahmoodian Sahand, Stobbe Soren, Rauschenbeutel Arno, Schneeweiss Philipp, Volz Jürgen, Pichler Hannes, and Zoller Peter: "Chiral quantum optics". *Nature* **541** (7638) (2017), 473–480.

[8] S. Strauf and F. Jahnke: "Single quantum dot nanolaser". *Laser & Photonics Reviews* **5** (5) (2011), pp. 607–633.

[9] J. Kabuss, A. Carmele, M. Richter, and A. Knorr: "Microscopic equation-of-motion approach to the multiphonon assisted quantum emission of a semiconductor quantum dot". *Phys. Rev. B* **84** (12 2011), p. 125324.

[10] A. del Valle: "Two-photon spectra of quantum emitters". *New Journal of Physics* **15** (3) (2013), p. 033036.

[11] M. Peiris, K. Konthasinghe, and A. Muller: "Franson Interference Generated by a Two-Level System". *Phys. Rev. Lett.* **118** (3 2017), p. 030501.

[12] K. E. Dorfman, F. Schlawin, and S. Mukamel: "Nonlinear optical signals and spectroscopy with quantum light". *Rev. Mod. Phys.* **88** (4 2016), p. 045008.

[13] Kira M., Koch S. W., Smith R. P., Hunter A. E., and Cundiff S. T.: "Quantum spectroscopy with Schrodinger-cat states". *Nat Phys* **7** (10) (2011). 10.1038/nphys2091, 799–804.

[14] M. Kira and S. W. Koch: "Quantum-optical spectroscopy of semiconductors". *Phys. Rev. A* **73** (1 2006), p. 013813.

[15] Aharonovich Igor, Englund Dirk, and Toth Milos: "Solid-state single-photon emitters". *Nat Photon* **10** (10) (2016), 631–641.

[16] Gaisler V. A.: "Single-photon emitters based on semiconductor nanostructures". *Bulletin of the Russian Academy of Sciences: Physics* **73** (1) (2009), 77–79.

[17] S. Vuckovic: "Engineered quantum dot single-photon sources". *Reports on Progress in Physics* **75** (12) (2012), p. 126503.

[18] Kimble H. J.: "The quantum internet". *Nature* **453** (7198) (2008). 10.1038/nature07127, 1023–1030.

[19] Zoller P., Beth Th., Binosi D., Blatt R., Briegel H., Bruss D., Calarco T., Cirac J. I., Deutsch D., Eisert J., Ekert A., Fabre C., Gisin N., Grangiere P., Grassl M., Haroche S., Imamoglu A., Karlson A., Kempe J., Kouwenhoven L., Kröll S., Leuchs G., Lewenstein M., Loss D., Lütkenhaus N., Massar S., Mooij J. E., Plenio M. B., Polzik E., Popescu S., Rempe G., Sergienko A., Suter D., Twamley J., Wendin G., Werner R., Winter A., Wrachtrup J., and Zeilinger A.: "Quantum information processing and communication". *The European Physical Journal D - Atomic, Molecular, Optical and Plasma Physics* **36** (2) (2005), 203–228.

[20] T. Jennewein, C. Simon, G. Weihs, H. Weinfurter, and A. Zeilinger: "Quantum Cryptography with Entangled Photons". *Phys. Rev. Lett.* **84** (20 2000), pp. 4729–4732.

[21] Walmsley I. A.: "Quantum optics: Science and technology in a new light". *Science* **348** (6234) (2015), p. 525.

[22] S. Schumacher, J. Förstner, A. Zrenner, M. Florian, C. Gies, P. Gartner, and F. Jahnke: "Cavity-assisted emission of polarization-entangled photons from biexcitons in quantum dots with fine-structure splitting". *Opt. Express* **20** (5) (2012), pp. 5335–5342.

[23] A Lochmann, E Stock, O Schulz, F Hopfer, D Bimberg, V. Haisler, A. Toropov, A. Bakarov, and A. Kalagin: "Electrically driven single quantum dot polarised single photon emitter". *Electronics Letters* **42** (13) (2006), pp. 774–775.

[24] R. Boyd: *Nonlinear Optics*. Elsevier Science, 2013.

[25] D. C. Burnham and D. L. Weinberg: "Observation of simultaneity in parametric production of optical photon pairs". *Physical Review Letters* **25** (2) (1970), p. 84.

[26] J. C. López Carreño, C. Sánchez Muñoz, D. Sanvitto, E. del Valle, and F. P. Laussy: "Exciting Polaritons with Quantum Light". *Phys. Rev. Lett.* **115** (19 2015), p. 196402.

[27] J. C. L. Carreño and F. P. Laussy: "Excitation with quantum light. I. Exciting a harmonic oscillator". *Phys. Rev. A* **94** (6 2016), p. 063825.

[28] M. Richter and S. Mukamel: "Ultrafast double-quantum-coherence spectroscopy of excitons with entangled photons". *Phys. Rev. A* **82** (1 2010), p. 013820.

[29] F. Troiani: "Entanglement swapping with energy-polarization-entangled photons from quantum dot cascade decay". *Phys. Rev. B* **90** (24 2014), p. 245419.

[30] C. W. Gardiner: "Inhibition of Atomic Phase Decays by Squeezed Light: A Direct Effect of Squeezing". *Phys. Rev. Lett.* **56** (18 1986), pp. 1917–1920.

[31] M. I. Kolobov and I. V. Sokolov: "Interference of a physical radiation field and of vacuum fluctuations at a light-source output". *Optics and Spectroscopy* **67** (1 1989), pp. 68–71.

[32] M. J. Collett and C. W. Gardiner: "Squeezing of intracavity and traveling-wave light fields produced in parametric amplification". *Phys. Rev. A* **30** (3 1984), pp. 1386–1391.

[33] C. W. Gardiner and M. J. Collett: "Input and output in damped quantum systems: Quantum stochastic differential equations and the master equation". *Phys. Rev. A* **31** (6 1985), pp. 3761–3774.

[34] C. W. Gardiner: "Driving a quantum system with the output field from another driven quantum system". *Phys. Rev. Lett.* **70** (15 1993), pp. 2269–2272.

[35] H. J. Carmichael: "Quantum trajectory theory for cascaded open systems". *Phys. Rev. Lett.* **70** (15 1993), pp. 2273–2276.

[36] C. W. Gardiner and P. Zoller: *Quantum Noise*. 2nd ed. Springer, Berlin, 2000.

[37] J. C. L. Carreño, C. Sánchez Muñoz, E. del Valle, and F. P. Laussy: "Excitation with quantum light. II. Exciting a two-level system". *Phys. Rev. A* **94** (6 2016), p. 063826.

[38] M. Chaichian, I. Merches, D. Radu, and A. Tureanu: *Electrodynamics: An Intensive Course*. Springer Berlin Heidelberg, 2016.

[39] A. Zangwill: *Modern Electrodynamics*. Modern Electrodynamics. Cambridge University Press, 2013.

[40] H. Breuer and F. Petruccione: *The Theory of Open Quantum Systems*. Oxford University Press, 2002.

[41] Á. Rivas and S. Huelga: *Open Quantum Systems: An Introduction*. SpringerBriefs in Physics. Springer Berlin Heidelberg, 2011.

[42] J. Ziman: *Elements of Advanced Quantum Theory*. Cambridge University Press, 1969.

[43] W. Dittrich and M. Reuter: *Classical and Quantum Dynamics: From Classical Paths to Path Integrals*. Springer International Publishing, 2017.

[44] E. Bittner: *Quantum Dynamics: Applications in Biological and Materials Systems*. CRC Press, 2009.

[45] F. Low: *Classical Field Theory: Electromagnetism and Gravitation*. Physics textbook. Wiley, 2008.

[46] G. Arfken, H. Weber, and F. Harris: *Mathematical Methods for Physicists: A Comprehensive Guide*. Elsevier Science, 2011.

[47] D. Bleecker: *Gauge theory and variational principles*. Global analysis, pure and applied. Addison-Wesley Pub. Co., Advanced Book Program/World Science Division, 1981.

[48] Y. Nazarov and J. Danon: *Advanced Quantum Mechanics: A Practical Guide*. Advanced Quantum Mechanics: A Practical Guide. Cambridge University Press, 2013.

[49] M. Orszag: *Quantum Optics: Including Noise Reduction, Trapped Ions, Quantum Trajectories, and Decoherence*. Springer International Publishing, 2016.

[50] W. Vogel and D. Welsch: *Quantum Optics*. Wiley, 2006.

[51] J. Klauder and E. Sudarshan: *Fundamentals of Quantum Optics*. Dover books on physics. Dover Publications, 2006.

[52] C. Rovelli: *Quantum Gravity*. Cambridge Monographs on Mathematical Physics. Cambridge University Press, 2004.

[53] Ehrenfest P.: "Bemerkung über die angenäherte Gültigkeit der klassischen Mechanik innerhalb der Quantenmechanik". *Zeitschrift für Physik* **45** (7) (1927), 455–457.

[54] T. Heinosaari and M. A. Ziman: *The Mathematical Language of Quantum Theory: From Uncertainty to Entanglement*. Cambridge University Press, 2011.

[55] R. Kates and F. Schwabl: *Quantum Mechanics*. Springer Berlin Heidelberg, 2013.

[56] H. P. Breuer and F. Petruccione: *The Theory of Open Quantum Systems*. Oxford University Press, Oxford, 2002.

[57] D. Petz: *Quantum Information Theory and Quantum Statistics*. Theoretical and Mathematical Physics. Springer Berlin Heidelberg, 2007.

[58] M. Nielsen and I. Chuang: *Quantum Computation and Quantum Information: 10th Anniversary Edition*. Cambridge University Press, 2010.

[59] S. Virmani: *Entanglement Quantification and Local Discrimination*. University of London, 2001.

[60] Kossakowski A.: "On quantum statistical mechanics of non-Hamiltonian systems". *Reports on Mathematical Physics* **3** (4) (1972), 247–274.

[61] Gorini Vittorio, Kossakowski Andrzej, and Sudarshan E. C. G.: "Completely positive dynamical semigroups of N-level systems". *Journal of Mathematical Physics* **17** (5) (1976). doi: 10.1063/1.522979, 821–825.

[62] G. Lindblad: "On the generators of quantum dynamical semigroups". *Comm. Math. Phys.* **48** (2) (1976), pp. 119–130.

[63] H. Carmichael: *An Open Systems Approach to Quantum Optics: Lectures Presented at the Université Libre de Bruxelles, October 28 to November 4, 1991*. Lecture Notes in Physics Monographs. Springer Berlin Heidelberg, 2009.

[64] S. S. Schweber: *An introduction to relativistic quantum field theory*. Courier Corporation, 2011.

[65] C. Gardiner and A. Parkins: "Driving atoms with light of arbitrary statistics". *Physical Review A* **50** (2) (1994), p. 1792.

[66] H. J. Carmichael: *Statistical Methods in Quantum Optics 1*. Springer, Berlin, Heidelberg, 1999.

[67] B. Smirnov: *Physics of Atoms and Ions*. Graduate Texts in Contemporary Physics. Springer New York, 2003.

[68] M. Scully and M. Zubairy: *Quantum Optics*. Cambridge University Press, 1997.

[69] W. Demtröder: *Laser Spectroscopy: Basic Concepts and Instrumentation*. Advanced Texts in Physics. Springer Berlin Heidelberg, 2002.

[70] H. B. Casimir: "On the attraction between two perfectly conducting plates". In: *Proceedings of the KNAW*. Vol. 51. 7. 1948, pp. 793–795.

[71] M. Fox: *Quantum Optics: An Introduction*. Oxford Master Series in Physics. OUP Oxford, 2006.

[72] M. Bordag, G. Klimchitskaya, U. Mohideen, and V. Mostepanenko: *Advances in the Casimir Effect*. International Series of Monographs on Physics. OUP Oxford, 2009.

[73] B. Duplantier and V. Rivasseau: "Vacuum Energy-Renormalization". In: *Vacuum Energy-Renormalization*. 2003.

[74] V. Hizhnyakov: "Plasmon-supported emission of entangled photons and zero-point energy". *arXiv preprint arXiv:1311.6824* (2013).

[75] K. A. Milton: *The Casimir effect: physical manifestations of zero-point energy*. World Scientific, 2001.

[76] R. Loudon: *The quantum theory of light*. Clarendon Press, 1973.

[77] Plunien Günter, Müller Berndt, and Greiner Walter: "The Casimir effect". *Physics Reports* **134** (2) (1986), 87–193.

[78] S. K. Lamoreaux: "Demonstration of the Casimir force in the 0.6 to 6 μ m range". *Physical Review Letters* **78** (1) (1997), p. 5.

[79] Blocki J., Randrup J., Swiatecki W.J., and Tsang C.F.: "Proximity forces". *Annals of Physics* **105** (2) (1977), 427–462.

[80] U. Mohideen and A. Roy: "Precision Measurement of the Casimir Force from 0.1 to 0.9μm". *Phys. Rev. Lett.* **81** (21 1998), pp. 4549–4552.

[81] V. V. Dodonov: "Current status of the dynamical Casimir effect". *Physica Scripta* **82** (3) (2010), p. 038105.

[82] K. Husimi: "Miscellanea in elementary quantum mechanics, II". *Progress of Theoretical Physics* **9** (4) (1953), pp. 381–402.

[83] V. Dodonov, A. Klimov, and D. Nikonov: "Quantum phenomena in nonstationary media". *Physical Review A* **47** (5) (1993), p. 4422.

[84] M. Visser: "Some general bounds for one-dimensional scattering". *Phys. Rev. A* **59** (1 1999), pp. 427–438.

[85] G. Plunien, R. Schützhold, and G. Soff: "Dynamical Casimir effect at finite temperature". *Physical review letters* **84** (9) (2000), p. 1882.

[86] M. Crocce, D. A. Dalvit, and F. D. Mazzitelli: "Resonant photon creation in a three-dimensional oscillating cavity". *Physical Review A* **64** (1) (2001), p. 013808.

[87] W. Marshall, C. Simon, R. Penrose, and D. Bouwmeester: "Towards Quantum Superpositions of a Mirror". *Phys. Rev. Lett.* **91** (13 2003), p. 130401.

[88] A. Bassi, E. Ippoliti, and S. L. Adler: "Towards quantum superpositions of a mirror: an exact open systems analysis". *Physical review letters* **94** (3) (2005), p. 030401.

[89] J. Jaskula, G. B. Partridge, M. Bonneau, R. Lopes, J. Ruaudel, D. Boiron, and C. I. Westbrook: "Acoustic Analog to the Dynamical Casimir Effect in a Bose-Einstein Condensate". *Phys. Rev. Lett.* **109** (22 2012), p. 220401.

[90] W.-J. Kim, J. H. Brownell, and R. Onofrio: "Detectability of Dissipative Motion in Quantum Vacuum via Superradiance". *Phys. Rev. Lett.* **96** (20 2006), p. 200402.

[91] G. Rempe, F. Schmidt-Kaler, and H. Walther: "Observation of sub-Poissonian photon statistics in a micromaser". *Phys. Rev. Lett.* **64** (23 1990), pp. 2783–2786.

[92] H. Padamsee: "The science and technology of superconducting cavities for accelerators". *Superconductor science and technology* **14** (4) (2001), R28.

[93] Barton G. and Eberlein C.: "On Quantum Radiation from a Moving Body with Finite Refractive Index". *Annals of Physics* **227** (2) (1993), 222–274.

[94] S. C. Azizabadi, N. L. Naumann, M. Katzer, A. Knorr, and A. Carmele: "Quantum cascade driving: Dissipatively mediated coherences". *Phys. Rev. A* **96** (2 2017), p. 023816.

[95] K. E. Cahill and R. J. Glauber: "Density Operators and Quasiprobability Distributions". *Phys. Rev.* **177** (5 1969), pp. 1882–1902.

[96] L. Lutterbach and L Davidovich: "Method for direct measurement of the Wigner function in cavity QED and ion traps". *Physical review letters* **78** (13) (1997), p. 2547.

[97] M. Kim, G Antesberger, C. Bodendorf, and H Walther: "Scheme for direct observation of the Wigner characteristic function in cavity QED". *Physical Review A* **58** (1) (1998), R65.

[98] L. Teuber, P. Grünwald, and W. Vogel: "Nonclassical light from an incoherently pumped quantum dot in a microcavity". *Phys. Rev. A* **92** (5 2015), p. 053857.

[99] P. Gartner: "Two-level laser: Analytical results and the laser transition". *Phys. Rev. A* **84** (5 2011), p. 053804.

[100] E. del Valle and F. P. Laussy: "Mollow Triplet under Incoherent Pumping". *Phys. Rev. Lett.* **105** (23 2010), p. 233601.

[101] P. R. Rice and H. J. Carmichael: "Photon statistics of a cavity-QED laser: A comment on the laser˘phase-transition analogy". *Phys. Rev. A* **50** (5 1994), pp. 4318–4329.

[102] S. Ritter, P. Gartner, C. Gies, and F. Jahnke: "Emission properties and photon statistics of a single quantum dot laser". *Opt. Express* **18** (10) (2010), pp. 9909–9921.

[103] O. Benson and Y. Yamamoto: "Master-equation model of a single-quantum-dot microsphere laser". *Physical Review A* **59** (6) (1999), p. 4756.

[104] Y. Mu and C. M. Savage: "One-atom lasers". *Phys. Rev. A* **46** (9 1992), pp. 5944–5954.

[105] H. J. Carmichael and D. F. Walls: "A quantum-mechanical master equation treatment of the dynamical Stark effect". *Journal of Physics B: Atomic and Molecular Physics* **9** (8) (1976), p. 1199.

[106] Assmann M., Veit F., Bayer M., van der Poel M., and Hvam J. M.: "Higher-Order Photon Bunching in a Semiconductor Microcavity". *Science* **325** (5938) (2009), p. 297.

[107] D. F. Walls and G. J. Milburn: *Quantum Optics*. Springer, Berlin, Heidelberg, 1994.

[108] E. Andersson and P. Öhberg: *Quantum Information and Coherence*. Scottish Graduate Series. Springer International Publishing, 2014.

[109] Hayat Alex, Ginzburg Pavel, and Orenstein Meir: "Observation of two-photon emission from semiconductors". *Nat Photon* **2** (4) (2008). 10.1038/nphoton.2008.28, 238–241.

[110] J. Shapiro and G. Breit: "Metastability of $2s$ States of Hydrogenic Atoms". *Phys. Rev.* **113** (1 1959), pp. 179–181.

[111] D. Bouwmeester, A. Ekert, and A. Zeilinger: *The Physics of Quantum Information: Quantum Cryptography, Quantum Teleportation, Quantum Computation*. Physics and astronomy online library. Springer Berlin Heidelberg, 2000.

[112] P. Kumar, P. Kwiat, A. Migdall, S. W. Nam, J. Vuckovic, and F. N. Wong: "Photonic technologies for quantum information processing". *Quantum Information Processing* **3** (1-5) (2004), pp. 215–231.

[113] Z. D. Walton, A. F. Abouraddy, A. V. Sergienko, B. E. Saleh, and M. C. Teich: "One-way entangled-photon autocompensating quantum cryptography". *Physical Review A* **67** (6) (2003), p. 062309.

[114] J. L. O'brien, A. Furusawa, and J. Vučković: "Photonic quantum technologies". *Nature Photonics* **3** (12) (2009), pp. 687–695.

[115] D. Naik, C. Peterson, A. White, A. Berglund, and P. G. Kwiat: "Entangled state quantum cryptography: eavesdropping on the Ekert protocol". *Physical Review Letters* **84** (20) (2000), p. 4733.

[116] I Marcikic, H de Riedmatten, W Tittel, H Zbinden, and N Gisin: "Long-distance teleportation of qubits at telecommunication wavelengths". *Nature* **421** (6922) (2003), pp. 509–513.

[117] C. Simon, H. De Riedmatten, M. Afzelius, N. Sangouard, H. Zbinden, and N. Gisin: "Quantum repeaters with photon pair sources and multimode memories". *Physical review letters* **98** (19) (2007), p. 190503.

[118] S. C. Azizabadi and V. Hizhnyakov: "Plasmon-enhanced emission of polarization entangled photons". In: *Advanced Photonics*. Optical Society of America, 2014, JTu3A.45.

[119] Hizhnyakov V., Loot A., and Azizabadi S.Ch.: "Dynamical Casimir effect for surface plasmon polaritons". *Physics Letters A* **379** (5) (2015), 501–505.

[120] Hizhnyakov V., Loot A., and Azizabadi S. C.: "Enhanced dynamical Casimir effect for surface and guided waves". *Applied Physics A* **122** (4) (2016), p. 333.

[121] J.-W. Pan, Z.-B. Chen, C.-Y. Lu, H. Weinfurter, A. Zeilinger, and M. Żukowski: "Multiphoton entanglement and interferometry". *Reviews of Modern Physics* **84** (2) (2012), p. 777.

[122] S. Odulov, M. Soskin, and A. Khizhni.a.ik: *Optical Oscillators with Degenerate Four-wave Mixing (dynamic Grating Lasers)*. DYNAMIC GRATING LASERS. Harwood Academic Publishers, 1991.

[123] D. Klyshko: *Photons Nonlinear Optics*. Taylor & Francis, 1988.

[124] E. Hanamura, Y. Kawabe, and A. Yamanaka: *Quantum Nonlinear Optics*. Advanced texts in physics. Springer Berlin Heidelberg, 2007.

[125] Y. Zhang and M. Xiao: *Multi-Wave Mixing Processes: From Ultrafast Polarization Beats to Electromagnetically Induced Transparency*. Springer Berlin Heidelberg, 2009.

[126] P. Unsbo: *Phase Conjugation and Four-wave Mixing*. Trita-FYS. 1995.

[127] G. T. Moore: "Quantum Theory of the Electromagnetic Field in a Variable-Length One-Dimensional Cavity". *Journal of Mathematical Physics* **11** (9) (1970), pp. 2679–2691.

[128] A. Lobashev and V. M. Mostepanenko: "Quantum effects in nonlinear insulating materials in the presence of a nonstationary electromagnetic field". *Theoretical and Mathematical Physics* **86** (3) (1991), pp. 303–309.

[129] V. Hizhnyakov: "Quantum emission of a medium with a time-dependent refractive index". *Quantum Optics: Journal of the European Optical Society Part B* **4** (5) (1992), p. 277.

[130] H. Johnston and S. Sarkar: "Moving mirrors and time-varying dielectrics". *Physical Review A* **51** (5) (1995), p. 4109.

[131] M. Cirone, K. Rzaz-Dotewski, and J. Mostowski: "Photon generation by time-dependent dielectric: a soluble model". *Physical Review A* **55** (1) (1997), p. 62.

[132] C. Wilson, G Johansson, A Pourkabirian, M Simoen, J. Johansson, T Duty, F Nori, P Delsing, D. A. Dalvit, J. C. Lee, et al.: "Observation of the dynamical Casimir effect in a superconducting circuit". *Nature* **479** (2011), pp. 376–379.

[133] V. Hizhnyakov, H. Kaasik, and I. Tehver: "Spontaneous nonparametric down-conversion of light". *Applied Physics A* **115** (2) (2014), pp. 563–568.

[134] V. Hizhnyakov and A. Loot: "Spontaneous down conversion in metal-dielectric interface-a possible source of polarization-entangled photons". *arXiv preprint arXiv:1406.2174* (2014).

[135] D. Marcuse: "Light transmission optics" (1972).

[136] R. Sainidou, J. Renger, T. V. Teperik, M. U. González, R. Quidant, and F. J. Garcia de Abajo: "Extraordinary all-dielectric light enhancement over large volumes". *Nano letters* **10** (11) (2010), pp. 4450–4455.

[137] M. Dyakonov and V. Y. Kachorovskii: "Theory of streamer discharge in semiconductors". *Sov. Phys. JETP* **67** (5) (1988), pp. 1049–1054.

[138] O. Takayama, L. Crasovan, D. Artigas, and L. Torner: "Observation of Dyakonov surface waves". *Physical review letters* **102** (4) (2009), p. 043903.

[139] H. Saito and H. Hyuga: "The dynamical Casimir effect for an oscillating dielectric model". *Journal of the Physical Society of Japan* **65** (11) (1996), pp. 3513–3523.

[140] N. Birrell and P. Davies: *Quantum fields in curved space, volume 7 of Cambridge Monographs on Mathematical Physics*. 1982.

[141] V Hizhnyakov: "Strong two-photon emission by a medium with periodically time-dependent refractive index". *arXiv preprint quant-ph/0306095* (2003).

[142] V. Hizhnyakov and H. Kaasik: "Dynamical Casimir effect: quantum emission of a medium with time-dependent refractive index". In: *Northern Optics, 2006*. IEEE. 2006, pp. 7–11.

[143] D. Klyshko: "Coherent photon decay in a nonlinear medium". *Soviet Journal of Experimental and Theoretical Physics Letters* **6** (1967), p. 23.

[144] Y. Ota, S. Iwamoto, N. Kumagai, and Y. Arakawa: "Spontaneous two-photon emission from a single quantum dot". *Physical review letters* **107** (23) (2011), p. 233602.

[145] M. Müller, S. Bounouar, K. D. Jöns, M Glässl, and P Michler: "On-demand generation of indistinguishable polarization-entangled photon pairs". *Nature Photonics* **8** (3) (2014), pp. 224–228.

[146] C. Cohen-Tannoudji and S. Reynaud: "Dressed-atom description of resonance fluorescence and absorption spectra of a multi-level atom in an intense laser beam". *Journal of Physics B: Atomic and Molecular Physics* **10** (3) (1977), p. 345.

[147] A. Muller, W. Fang, J. Lawall, and G. S. Solomon: "Emission spectrum of a dressed exciton-biexciton complex in a semiconductor quantum dot". *Physical review letters* **101** (2) (2008), p. 027401.

[148] I. Akimov, J. Andrews, and F Henneberger: "Stimulated emission from the biexciton in a single self-assembled II-VI quantum dot". *Physical review letters* **96** (6) (2006), p. 067401.

[149] G. Chen, T. H. Stievater, E. T. Batteh, X. Li, D. G. Steel, D. Gammon, D. S. Katzer, D. Park, and L. J. Sham: "Biexciton Quantum Coherence in a Single Quantum Dot". *Phys. Rev. Lett.* **88** (11 2002), p. 117901.

[150] G. W. Drake: *Springer handbook of atomic, molecular, and optical physics*. Springer Science & Business Media, 2006.